1

Welding and Welding Processes

Welding is a process of joining two or more pieces of the same or dissimilar materials to achieve complete coalescence. This is the only method of developing monolithic structures and it is often accomplished by the use of heat and or pressure. Although in its present form it has been used since about the beginning of 20th century but it is fast replacing other joining processes like riveting and bolting. At times it may be used as an alternative to casting.

Presently welding is used extensively for fabrication of vastly different components including critical structures like boilers and pressure vessels, ships, off-shore structures, bridges, storage tanks and spheres, pipelines, railway coaches, anchor chains, missile and rocket parts, nuclear reactors, fertilizer and chemical plants, structurals, earth moving equipment, plate and box girders, automobile bodies, press frames and water turbines. Welding is also used in heavy plate fabrication industries, pipe and tube fabrication, jointing drill bits to their shanks, automobile axles to brake drums, lead wire connections to transistors and diodes, sealing of containers of explosives like nitroglycerine, welding of cluster gears, and the like.

1.1. CLASSIFICATION OF WELDING AND ALLIED PROCESSES

Although almost all materials (metals, plastics, ceramics, and composites) can be welded but not by the same process. To achieve this universality a large number of Welding and Allied Processes have been developed. Most of the industrially important processes amongst them classified depending upon the nature of heat source and its movement resulting in spot, seam or zonal welds; or on the extent of heat generation *viz.*, low heat and high heat, are shown in *Fig. 1.1*. This rather unusual type of process classification has been chosen because often these processes will be referred to accordingly in the remaining text.

Brief description and important uses of these processes are given in the following sections.

1.2. CAST-WELD PROCESSES

These processes involve large amount of molten metal resulting in properties close to that of castings. For achieving the desired joint properties such as welds are usually given normalisation treatment. Two processes in this class are Thermit Welding and Electroslag Welding.

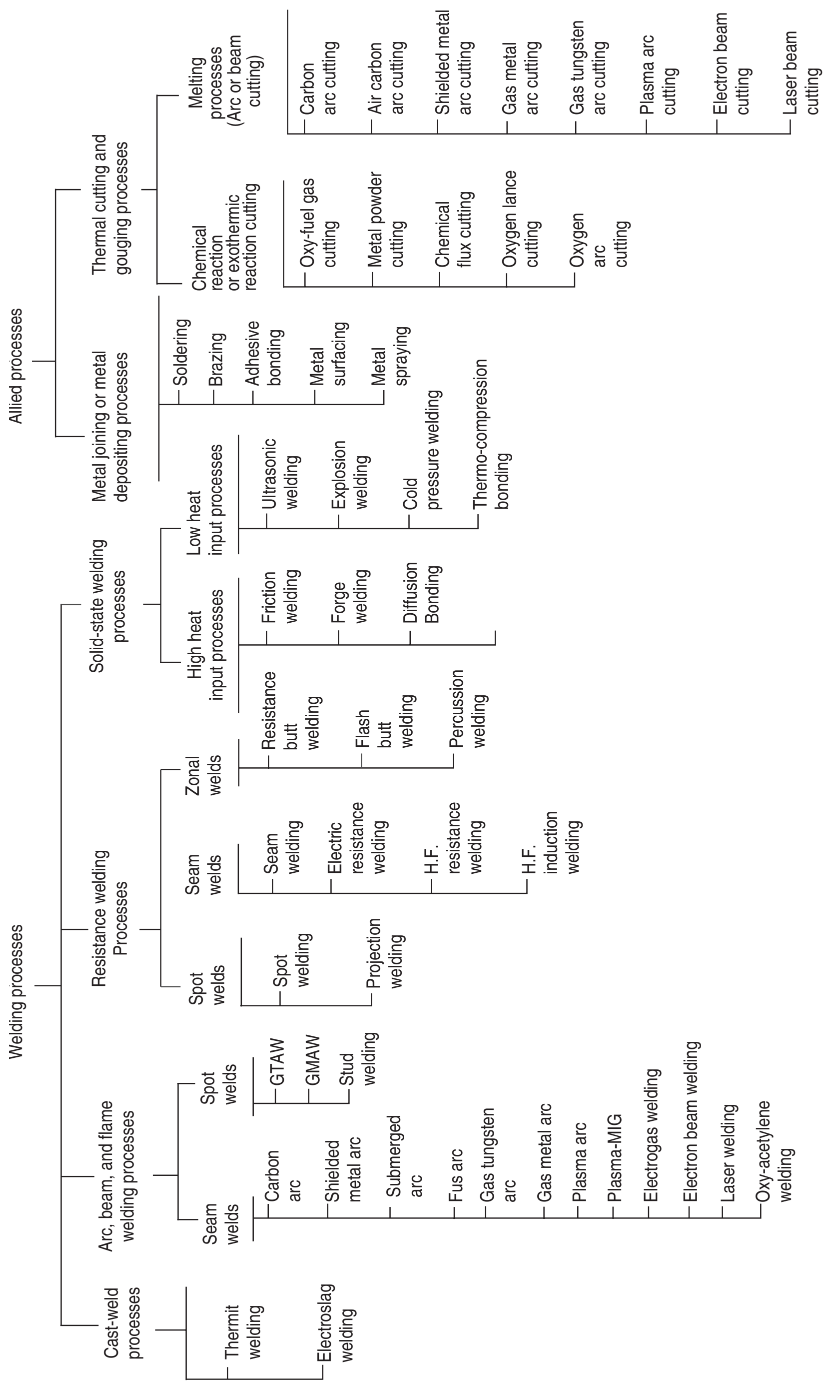

Fig. 1.1. Classification of Welding and Allied Processes.

1.2.1. Thermit Welding

Thermit is a mixture of aluminium powder and metal oxide which when ignited results in a non-explosive exothermic reaction. The heat so generated melts and reduces the metal oxide to metallic form at a high temperature. This molten metal is used for joining metal parts by pouring it between them resulting in what may be termed as a *cast-weld joint*.

One of the most used thermit mixtures is aluminium powder and ferric oxide which on ignition results in the following reaction.

$$8Al + 3Fe_3O_4 \longrightarrow 9Fe + 4Al_2O_3 + 3310 \text{ kJ/mol} \quad ...(1.1)$$

The molten metal obtained has high temperature of about 2450°C. This metal is poured into the sand mould surrounding the parts to be welded, as shown in *Fig. 1.2*. The mould is broken soon after the solidification of metal is complete and the excess metal is removed, by chisel and hammer, to give the necessary shape to the weld.

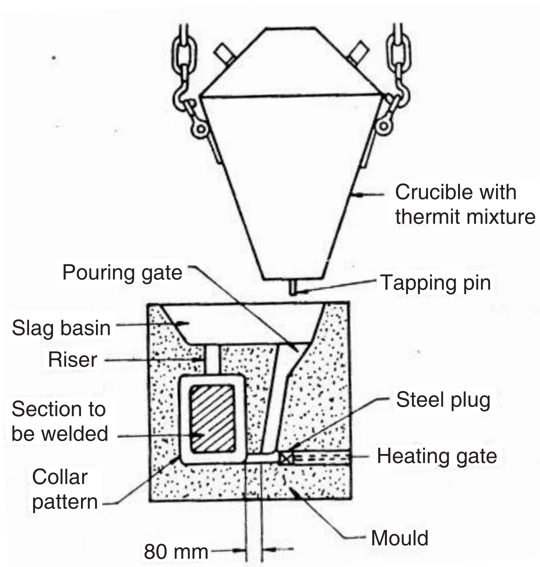

Fig. 1.2. A standard set-up for thermit welding.

Thermit welding is extensively used for joining rails at site, cable conductors, reinforcing bars for R.C.C. structures, and for heavy repairs such as those of broken necks of rollers, and ship sterns.

1.2.2. Electroslag Welding

Electroslag welding (ESW) is a fusion welding process for joining thick workpieces in a single run. This is *not* an arc welding process though most of the set-up is similar to the usual arc welding processes and arcing is required to initiate the process and may also occur subsequently when the process stability is disturbed. Apart from the conventional ESW process in which the usual electrode wire with contact tube is employed there is a popular variant of the process called Consumable Guide ESW Process; *Fig. 1.3* shows the process diagram for the latter. An essential feature of the ESW process is that the welding is done with weld joint in vertical position.

Due to high heat input the weld pool in ESW is usually quite voluminous resulting in a weld with properties resembling that of a casting which makes post weld heat treatment (PWHT) essential to achieve the desired metallurgical structure to attain the required mechanical strength.

Typically ESW is extensively used in the construction of pressure vessels, press frames, water turbines and heavy plate fabrication industries.

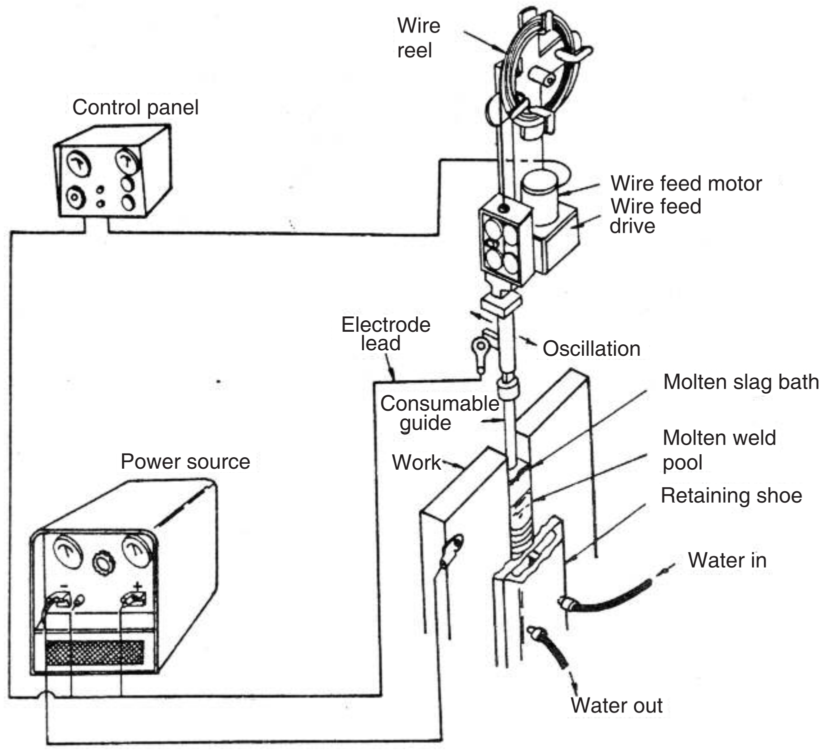

Fig. 1.3. A set-up for consumable-guide electroslag welding.

1.3. ARC AND FLAME WELDING PROCESSES

The welding processes included in this class are those which make use of an electric arc or a flame obtained by burning an oxy-fuel gas mixture. The size of the weld pool evolved depends upon the energy input per unit time, and the extent of spread of arc or flame, however the volume of the molten metal in the weld pool, at any given time, is much smaller than that obtained in electroslag welding. These processes are either used to produce welds along seams (*e.g.*, SMAW, GMAW, Oxy-fuel gas welding, etc.) or just at spots (*e.g.*, stud welding, GTAW spot welding, etc.). Brief descriptions of industrially important processes in this class follows.

1.3.1. Seam Welding Processes

These processes are mainly used for welding workpieces along straight or curved seams of desired lengths and include all well known arc and flame welding processes.

1.3.1.1. Carbon Arc Welding

In carbon arc welding, heat is produced with an arc between a carbon electrode and the work-piece, and normally no shielding gas is used. The heat from the arc melts the work material and filler wire, if required. *Fig. 1.4* shows the basic circuit for carbon arc welding.

To avoid excessive heating and consequently accelerated consumption of carbon electrode it is required to use DC (direct current) power source with electrode negative.

The weld pool produced is normally small and therefore in its manual mode carbon arc welding process can be used as an all-position welding process.

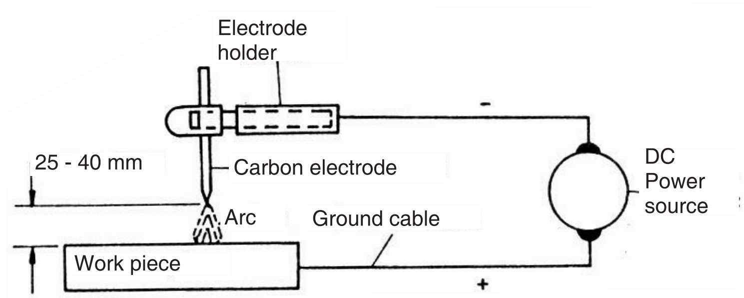

Fig. 1.4. Carbon arc welding.

Carbon arc welding can be used for welding copper since it can be used at high current to develop the high heat usually required for the purpose. It can as well be used for welding galvanized steel and repairing of steel castings.

1.3.1.2. Shielded Metal Arc Welding

This process employs coated or covered electrodes for producing an arc to act as a heat source; the covering on burning provides the necessary shield to protect the molten metal from the ill effects of oxygen and nitrogen from the surrounding atmosphere. This process is more popularly known as *Stick electrode welding* or *manual metal arc welding* and is the single most used welding process in the world. Both AC and DC power sources can be used equally effectively. *Fig. 1.5* shows the basic circuit diagram for the process.

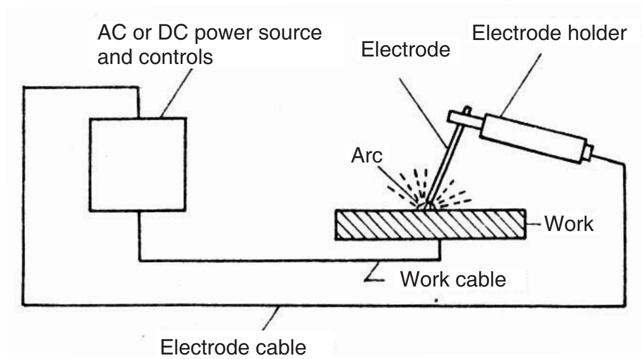

Fig. 1.5. Basic circuit for shielded metal arc welding.

The weld pool produced depends upon the size of the covered electrode and the welding current used and may vary from very small to fairly large size. Larger sized pools are used only for downhand welding. This process is an all-position welding process and is used for all types of jobs. All metals for which covered electrodes are available can be welded by this process. Because this is a very versatile process so it is still extensively used in the fabrication of ships, bridges, pressure vessels, and structurals; however it is used in its manual mode only.

1.3.1.3. Submerged Arc Welding

Submerged arc welding (SAW) is a process in which continuous copper coated spooled wire is used in conjunction with loose granulated flux poured ahead of the arc so as to provide a protective media to ward off the atmospheric gases from reacting with the molten metal pool. The electrode wire diameter may range between 2 and 10 mm. Both *AC* and *DC* power sources are used though *DC* with electrode positive (dcep) is the preferred choice.

SAW is mainly used in the downhand welding position in both automatic and semi-automatic modes. The former is a more popular mode and a set-up for the same is shown in *Fig. 1.6*.

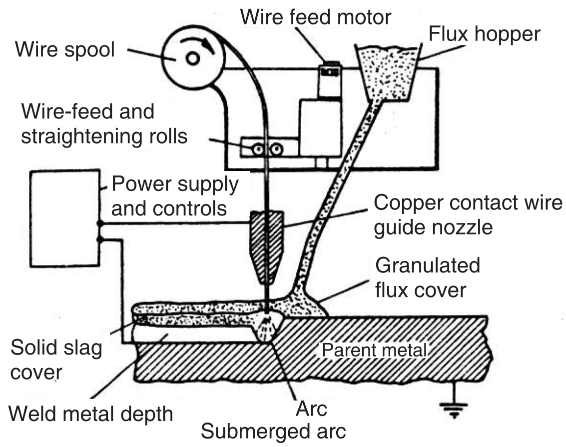

Fig. 1.6. Essential elements of an automatic submerged arc welding unit.

The weld joint produced by submerged arc welding is of very high quality and consequently this process finds extensive use in joining thick plates in long, linear seams as are encountered in ships, pressure vessels, bridges, structural work, welded pipes, and nuclear reactors.

1.3.1.4. Fusarc Welding

This process employs flux coated electrode in which the core wire is helically wrapped with both left and right handed spirals of wire shown in *Fig. 1.7*; the coating fills the spaces between the spirals. Current to the core wire flows through the contact between the contact tube and the outer wire spiral which is partly bare. Welding current from 200 A to 1000 A can be used depending upon the electrode diameter, however, the upper limit for the current is also set by the ability of the outer spiral to carry it without overheating and collapse. Long current slide is often used to overcome this difficulty. The set-up for Fusarc welding resembles the set-up used for automatic submerged arc welding excluding the flux supply and recovery system.

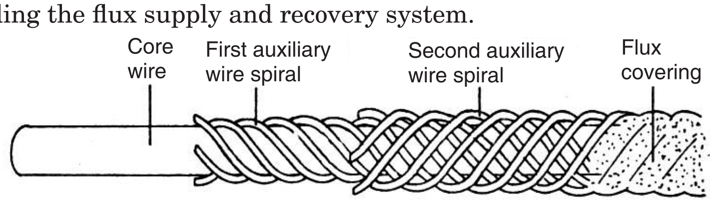

Fig. 1.7. Constructional features of a continuous covered electrode.

Fusarc welding usually employs an additional shield of CO_2 to enhance the protection of weld-pool and thereby greatly improves the weld quality.

Fusarc welding is more tolerant of joint fit-up, surface and weather conditions then other open arc processes including submerged arc welding. It, therefore, finds extensive use in shipbuilding, structural work or any long straight or circumferential seams. It also finds use for double-sided fillet welds and pressure vessel fabrication requiring sound welds and good penetration where visibility of the arc is imperative.

1.3.1.5. Gas Tungsten Arc Welding

Gas tungsten arc welding (GTAW) or tungsten inert gas (TIG) welding employs a non-consumable tungsten electrode with an envelope of inert shielding gas (Argon, helium, etc.) to protect both the electrode and the weld pool from the detrimental effects of surrounding atmospheric gases.

Both *AC* and *DC* power sources are used for GTAW. The tungsten electrode employed varies in diameter from 0.5 to 6.5 mm and the current carrying capacity varies accordingly between 5A and 650A. The welding torch used for carrying current higher than 100A is normally water cooled. The process is used mainly in its manual mode. *Fig. 1.8* shows a schematic representation of the basic elements of an *AC* GTAW unit.

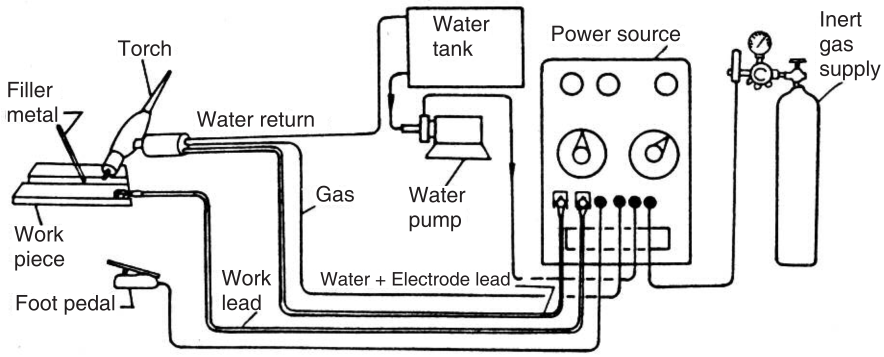

Fig. 1.8. A schematic representation of a GTAW unit.

GTAW is an all-position welding process and gives the highest quality welds amongst the commonly employed arc welding processes and is, therefore, extensively used for welding most of the industrially useful metals and alloys usually in thin grades. Aircraft industry, rocket and missile fabricators, chemical and nuclear plant fabricators are the typical user industries of this process.

1.3.1.6. Plasma Arc Welding

Plasma is a flow of ionised gas that is obtained by passing a gas through a high temperature arc which results in splitting the gas molecules to atoms and then to ions and electrons.

In plasma arc welding, the arc is created between a tungsten electrode and the workpiece, as in gas tungsten arc welding. However, the plasma arc is constricted by an outer nozzle through which the shielding gas flows.

Power source used for plasma arc welding is invariably of constant current DC type with an open circuit voltage of 70 to 80 volts and a duty cycle of 60%.

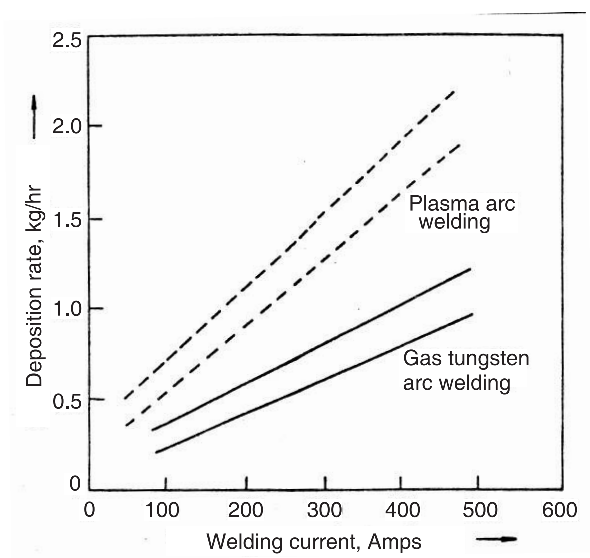

Fig. 1.9. Welding current versus deposition rate for GTAW and plasma arc welding.

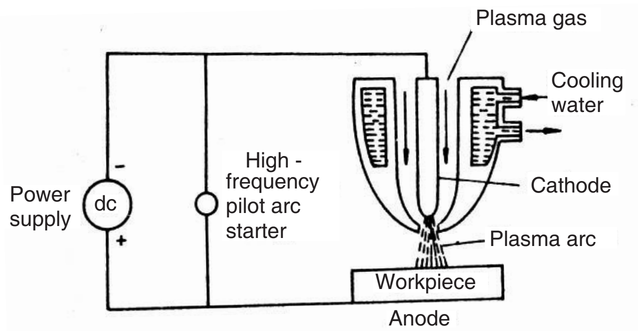

(a) Transferred arc

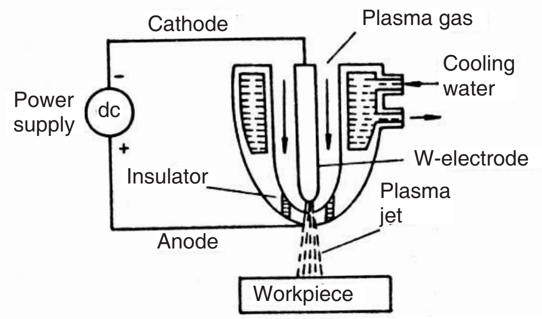

(b) Non-transferred arc

Fig. 1.10. Two modes of plasma arc welding.

There are two variants of the plasma arc welding process called non-transferred type and transferred type. In the *non-transferred type,* the tungsten electrode is the cathode and the torch tip the anode. Such a torch is very similar to oxy-acetylene torch as regards its manoeuvrability as workpiece is outside the electrical circuit. However, such a plasma arc is less intense compared with the *transferred arc* wherein the workpiece is the anode. The manoeuvrability of the transferred arc is, however, restricted. But such an arc is very intense and therefore the process results in higher thermal efficiency with consequential higher deposition rates as compared with GTAW, *Fig. 1.9* and *Fig. 1.10* shows the set-ups for two modes of the plasma welding arc.

Any gas that does not attack the tungsten electrode or the copper nozzle tip can be used for plasma welding. However, argon, and argon-hydrogen mixture are more commonly employed.

A major disadvantage of plasma arc welding process is the noise due to the operation of the plasma source. Because of this, hand-held plasma torches are used to a very limited extent. For most part, remotely operated plasma sources are employed.

Commercially, the major users of plasma welding process are the aeronautical industry and jet engine manufacturers. Typically the process is used for making piping and tubing made of stainless steels and titanium.

1.3.1.7. Gas Metal Arc Welding

In gas metal arc welding (GMAW) process, a consumable wire, of 0.8 to 2.4 mm diameter and wound in spool form, is fed at a preset speed through a welding torch wherein it is provided the electrical connection and the shielding gas. The arc which is struck by direct contact between the wire electrode and the workpiece, is maintained at a constant length by the interaction of electrical parameters. The power source used is invariably of the rectified DC type. Both, constant voltage and constant current type power sources are in use.

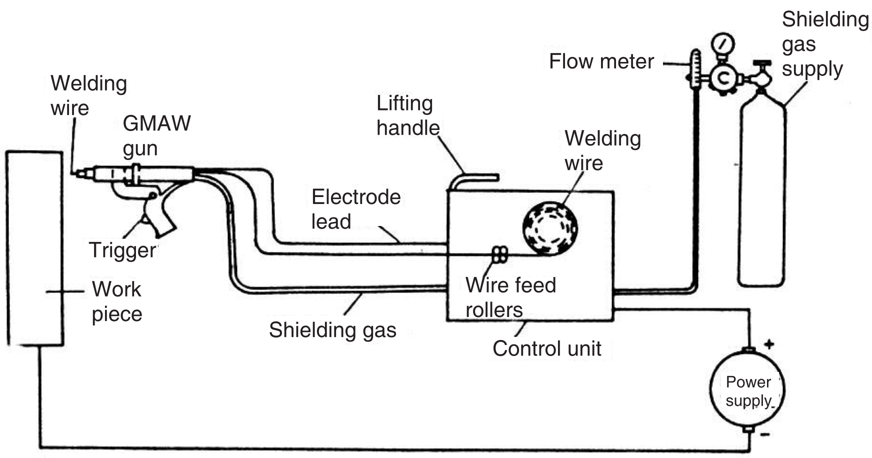

Fig. 1.11. Schematic representation of GMAW process.

Depending upon the work material, the shielding gas may be argon, helium, nitrogen, carbon dioxide, hydrogen, and their mixtures. When inert shielding gas is used the process is more popularly known as MIG (metal inert gas) welding and when CO_2 is used as the shielding gas it is referred to as CO_2 welding or MAG (metal active gas) welding.

GMAW is an all-position semi-automatic welding process though its automatic versions are also available. A set-up for semi-automatic GMAW process is shown in *Fig. 1.11.*

GMAW is a very versatile process and can be used for welding all metals for which compatible filler wires have been developed. However, its typical applications include medium-gauge fabrication such as structurals, earth moving equipment, plate and box girders, and automobile bodies. This process has great potentials for use with robotic welding systems.

1.3.1.8. Plasma-MIG Welding

This process, as the name implies, has been developed by combining the features of plasma arc welding and MIG welding processes. It has two variants; one with separate non-consumable tungsten electrode and the other uses the torch nozzle as non-consumable electrode. The essential features of torches used for these two types are shown in *Fig. 1.12.*

Essentially plasma–MIG welding process differs from the existing GMAW process in that the electrode wire is enveloped in a plasma sheath which controls heat and droplet transfer in such a way that much higher speeds and deposition rates are attained than possible with GMAW process, as is shown in *Fig. 1.13.*

This process can be used both for welding and surfacing. Most of the materials that can be welded by GMAW can as well be welded by this process and at much faster rates.

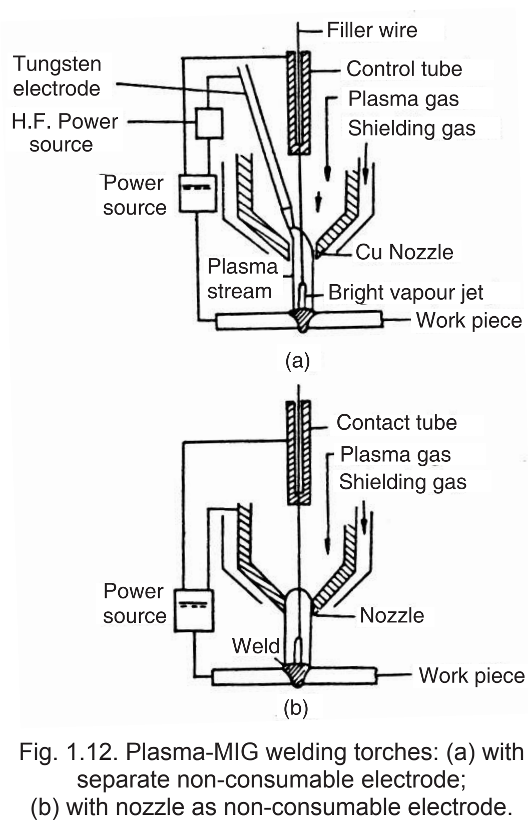

Fig. 1.12. Plasma-MIG welding torches: (a) with separate non-consumable electrode; (b) with nozzle as non-consumable electrode.

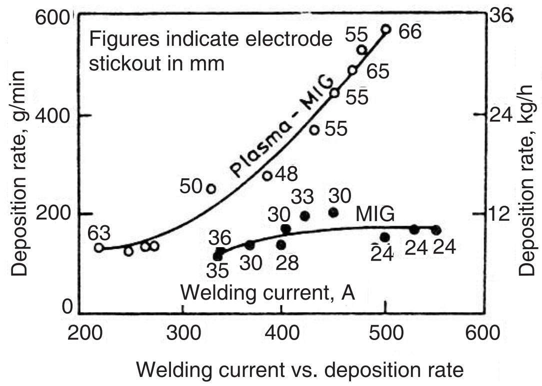

Fig. 1.13. Comparison of deposition rates for MIG and plasma-MIG welding processes.

1.3.1.9. Electrogas Welding

The equipment used for Electrogas Welding (EGW) is similar in appearance to the one used for electroslag welding. However, EGW is an arc welding process and gives welds with properties close to those obtained by submerged arc welding.

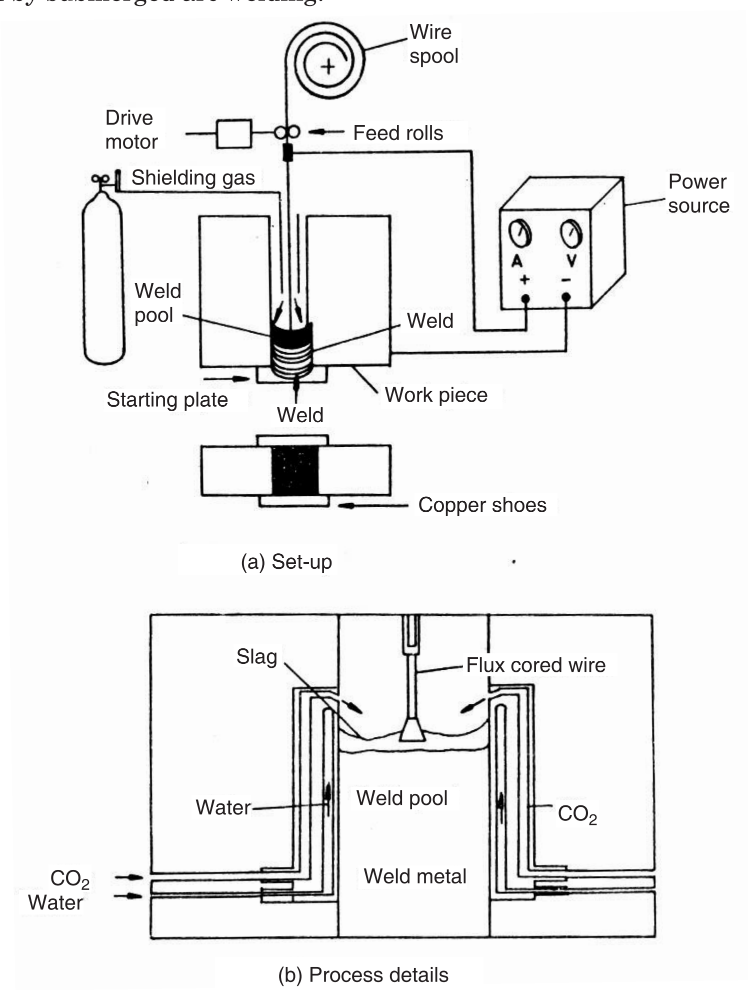

Fig. 1.14. Essential features of a set-up and process details for electrogas welding.

Electrogas welding uses the vertical orientation of the weld joint and employs copper shoes for retaining the molten metal in shape at the end of the plate width as in electroslag welding.

However, the wire used in EGW is of the flux-cored type which provides minimal covering to the weld pool. Additional protection is normally provided by the use of CO_2 or argon-rich shielding gas. The rating of the equipment is similar to that of gas metal arc welding equipment. The duty cycle of the power source, however, needs to be 100% as it is a continuous operation. The essential features of a set-up for electrogas welding are shown in *Fig. 1.14.*

Electrogas welding process is mainly used for joining metals with a thickness of 12 to 75 mm; more on the lower range. Typically EGW is used in shipbuilding, and site fabrication of storage tanks.

1.3.1.10. Electron Beam Welding

In electron beam welding (EBW), a beam of electrons is used to melt the metal for welding. The electron beam, emitted from a heated filament, is focussed on to the desired spot on the workpiece surface with the help of a focussing coil. The workpiece which is placed in a vacuum chamber can be moved to create the necessary welding speed.

The penetrating power of the electron beam depends upon the speed of the electrons which is controlled by the magnitude of accelerating voltage. Depending upon the accelerating voltage, the EBW guns are rated as low voltage and high voltage types with the range of voltages between 15–30 kV and 70–150 kV respectively. *Fig. 1.15* shows a schematic representation of a triode type EBW unit.

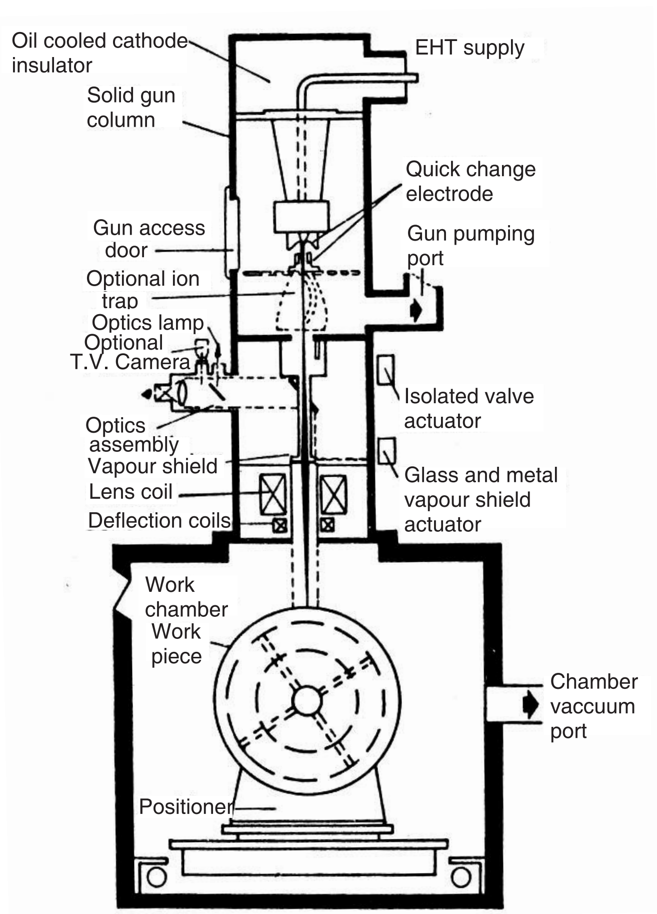

Fig. 1.15. Essential features of an electron beam welding unit.

The EBW welds are very narrow and can be of the full penetration type with width to penetration ratio of 1 : 20 compared with 5 : 1 of shielded metal arc welding, and 2 : 1 of gas metal arc welding. The energy density of electron beam (EB) being nearly 5×10^8 W/mm^2 it is, therefore, possible to melt and weld any known metal. Due to high energy density of the EB the HAZ is extremely narrow and high welding speeds can be reached.

Electron beam welding is widely used in the electronics, nuclear, missile, and aircraft industries. Typical applications of the process include cluster gears, intricate valve arrangements made of corrosion resistant alloys for automobile industry as well as pressure capsules, and missile hull frames. A portable EBW unit has also been developed for inflight repair welding of satellites.

1.3.1.11. Laser Beam Welding

In laser beam welding, a monochromatic (of one wavelength) coherent light beam is used as a heat source. A coherent light is one in which the waves are identical and parallel which can travel a long distance without loss in intensity or deviation. Laser light can be easily focussed without any decrease in intensity to a very small spot giving a very high energy density which may reach 10^9 W/mm^2. Thus, a laser beam like an electron beam, can weld any known material. Due to very high energy density, the HAZ is extremely narrow and high welding speeds can be attained.

There are three basic types of lasers *viz.*, the solid-state lasers, semi-conductor lasers, and gas lasers. Although at present the solid-state Nd:YAG (Neodymium doped Yttrium aluminium garnet) lasers are the most used lasers in industry but their heat conversion efficiency is very low usually below 1%. *Fig. 1.16* shows the essential features of one such laser unit. The CO_2 lasers with their heat conversion efficiency of 15–25% are now being increasingly installed.

Laser beam welding is more versatile than EBW in that it can weld metals in air, in a gas shield, and in vacuum. It can also weld through transparent materials as laser beam can easily pass through such media.

A laser must have a power rating of atleast about 2 kW to be used successfully for welding, however Nd:YAG lasers of 100 W to 1 kW power are used for welding in industry because they can achieve pulses with peak power of the order of 10 kW. Although CO_2 lasers of power

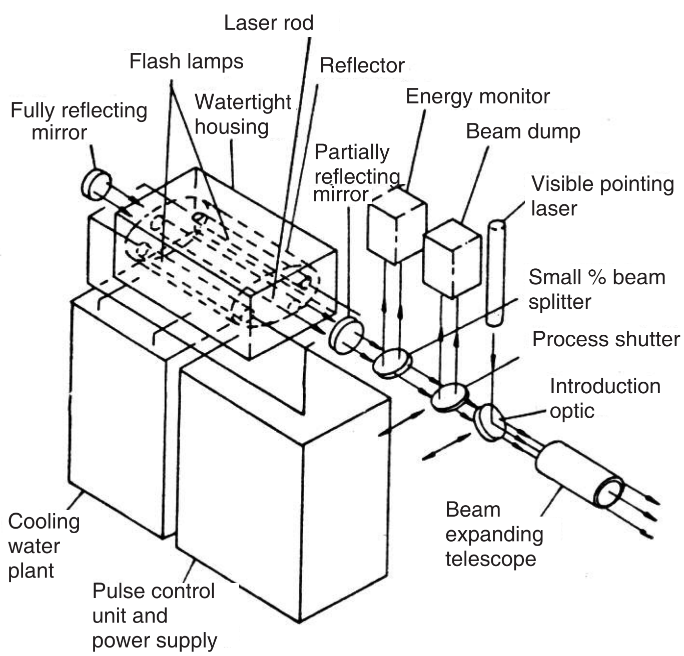

Fig. 1.16. Schematic representation of an Nd:YAG laser unit. (After Dawes)

rating up to 25 kW have reportedly been installed but presently such a unit is a rare piece of equipment and is extremely expensive.

Commercially laser welding is finding use in radio engineering and electronics where fine wires are often to be connected to films on micro-circuit boards, solid-state circuits, and micromodules. It is also expected to be used in high quality precision work as in aerospace industry and high speed mass production applications as in automobile industry.

1.3.1.12. Oxy-Acetylene Welding

In this process, acetylene gas is mixed with oxygen in the gas welding torch and is then burnt at the torch tip to give a flame with a temperature of about 3300°C which can melt most of the ferrous and non-ferrous metals in common use. *Fig. 1.17* shows a standard set-up for oxy-acetylene welding.

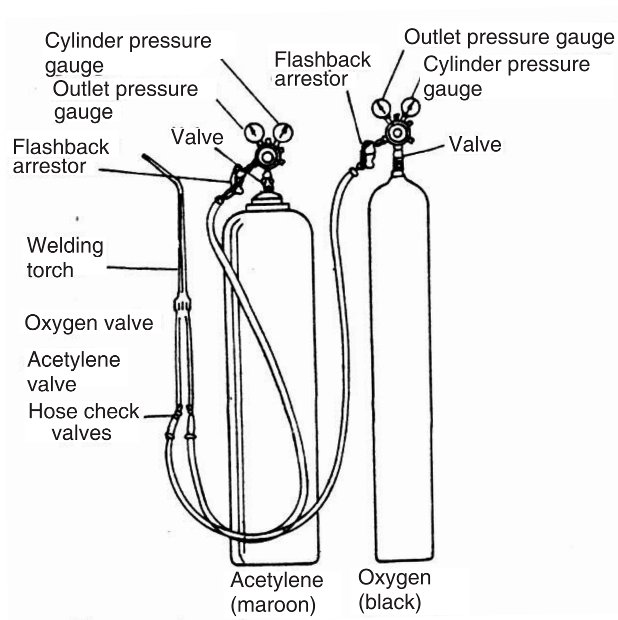

Fig. 1.17. A standard set-up for Oxy-acetylene welding.

Three types of flames are used in oxy-acetylene welding. The nature of the flame depends upon the ratio of the two gases. The neutral flame is most often used for the welding of most of the materials like low carbon steels, cast steel, cast iron, etc. The oxidising flame has higher proportion of oxygen than acetylene and is used for welding of Mn-steel, brass, and bronze whereas the carburising flame has higher proportion of acetylene in it and is used for welding aluminium, nickel, etc.

The heat transfer to the work in this process is very poor (about 30%) and may lead to a wide HAZ around the weld. The welding speed is also accordingly low.

Typical applications of oxy-acetylene welding include welding of root run in pipe and other multi-run welds, light fabrications like ventilation and air-conditioning ducts, and motor vehicle repairs. A large percent of general repair work is also done by this process.

1.3.2. Arc Spot Welding Processes

The processes in this class are used to join workpieces within a narrow zone of desired shape.

1.3.2.1. GTAW Arc Spot Welding

In this process, the equipment used is basically the same as for conventional GTAW except that the control system includes timing device and the torch nozzle is modified to develop a spot weld at the intended place. GTAW arc spot welding may be done with *AC* or *DCEN* (direct current with electrode negative). DCEN is used for all materials except aluminium for which *AC* with continuous superimposition of high frequency (HF) current is employed. The torch nozzle is made of copper or stainless steel and is often water-cooled as the arc is enclosed completely within the nozzle. The torch nozzle, usually about 12 mm inside diameter, is provided with venting ports to affect gas flow and escape.

The shielding gas used is either helium or argon with a flow rate of 2.5 to 4.5 lit/min.

To accomplish a spot weld, the arc is initiated by the HF discharge for which the outline circuitry is shown in *Fig. 1.18*. The arc continues for the preset time and the spot weld is achieved.

Normally no filler metal is used but when required it is fed with the help of special wire feeder. Filler wire addition improves nugget configuration and helps in overcoming crater cracking.

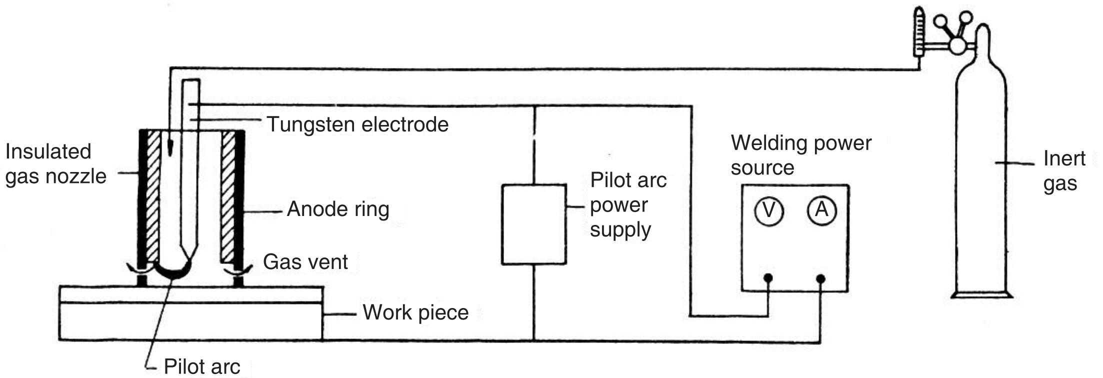

Fig. 1.18. Schematic illustration of a set-up for GTAW arc spot welding.

This process is mainly used in its semi-automatic mode but it can be mechanised and even controlled by numerically controlled (NC) system to achieve high rate of production.

GTAW arc spot welding is widely used in the manufacture of automatic parts, precision metal parts and parts for electronic components and appliances. It is particularly useful for applications where access to a lap joint can be gained only from one side.

1.3.2.2. GMAW Arc Spot Welding

Normal GMAW equipment can be used for making spot welds between the lapped sheets by providing a special torch with a nozzle attached to it. A vented metal nozzle of a shape to suit the application is fitted to GMAW gun and is pressed against the workpiece at the desired spot. The operation is carried out for a period of 1 to 5 seconds and a slug is melted between the parts to be joined, as is shown in *Fig. 1.19.* Timing is usually controlled automatically with the help of a timer.

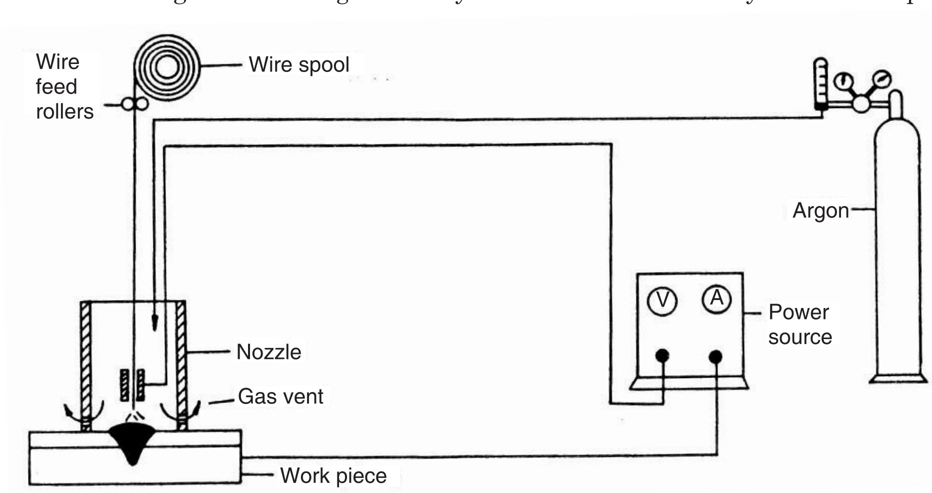

Fig. 1.19. Schematic illustration of a set-up for GMAW spot welding.

No joint preparation is required except proper cleaning of the overlapped areas. Argon and CO_2 are the shielding gases commonly used for GMAW arc spot welding.

GMAW arc spot welding process can be used most efficiently for downhand welding position. It can be successfully employed for horizontal position but fails for overhead welding position.

This process does not require a hole to be made in either member, thus it differs from plug welding in that respect. As the upper member is required to be melted through and through its thickness is normally restricted to 3 mm. The thickness of the second member is not important.

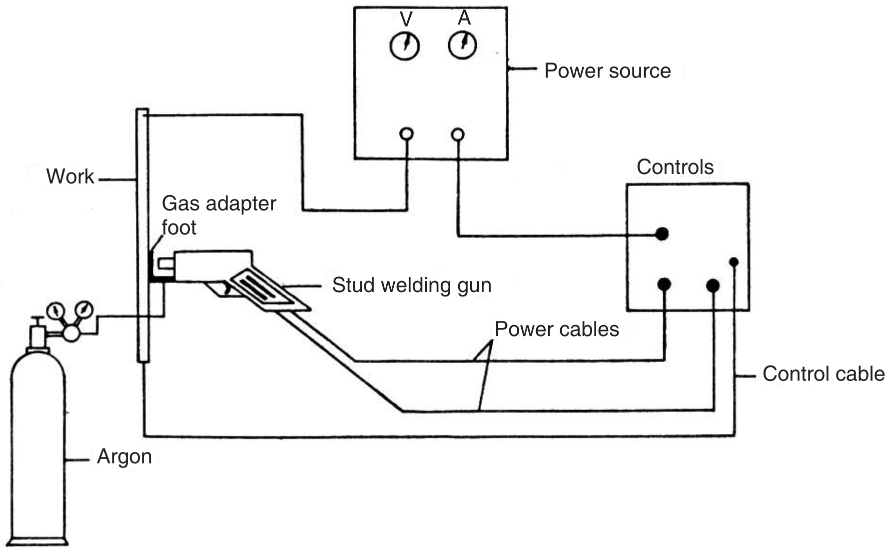

Fig. 1.20. A set-up for Arc Stud Welding of aluminium.

GMAW arc spot welding can be used successfully on aluminium, mild-, low alloy-, and stainless steels.

1.3.2.3. Stud Welding

This is a process of welding stud (a headless threaded bolt) or stud-like pieces (*e.g.* bolts, screws, rivets, rods, etc.) to flat pieces like plates.

The main equipment for stud welding consists of a stud welding gun, a time control unit, a *DC* power source of 300–600 amperes capacity, studs and ceramic protective caps called *ferrules.*

For stud welding, the stud is held in the welding gun and a ferrule is slipped on it. The stud is then made to touch the cleaned spot where it is to be welded and the switch, in the form of gun trigger, is pressed and the process is completed in a couple of seconds. *Fig. 1.20* shows the basic features of a stud welding unit.

Typical applications of stud welding include steel decks of ships, for attaching brackets, hangers, cover plates, piping, etc. to metal workpieces. The process also finds wide use in automotive rail road machinery manufacturing and construction industries.

1.4. RESISTANCE WELDING PROCESSES

In all resistance welding processes, the heat is generated at the interface of contacting workpieces due to the resistance offered to the flow of electric current and is expressed by Joule's Law,

$$H = \eta \frac{I^2 R t}{J} \qquad \text{...(1.1)}$$

where,

H = heat generated, calories,
I = welding current, amperes (rms),
R = contact resistance, ohms,
t = time for which the current flows, seconds,
J = the electrical equivalent of heat
η = thermal efficiency of the process.

The welds produced by resistance welding are normally without the addition of any filler material and are, therefore, sometimes referred to as *autogenous welds.*

Resistance welding processes can be divided into three categories *viz.*, spot, seam, and zonal type welds with some of them falling in more than one category. Brief description of industrially important processes, among them, follows.

1.4.1. Spot Welding Processes

In this class of processes the materials are joined at a spot the size of which depends upon the design specifications and is controlled by the electrode size and the magnitude of the welding current. Two main processes fall in this class *viz.*, resistance spot welding and projection welding.

1.4.1.1. Resistance Spot Welding

In resistance spot welding process overlapping sheets are welded by the flow of current between two cylindrical electrodes. The main equipment for spot welding is the spot welding machine which consists of a step down transformer, a time control unit, and a pair of copper alloy electrodes. As voltage plays no direct role in resistance welding it is, therefore, kept low between 5 to 25 volts but the current is usually heavy (100–50,000 A); however, it flows only for a short duration of time (0.06 to 3 seconds). Application of pressure to achieve forge between the two sheets is an essential aspect of the process. *Fig. 1.21* shows a general purpose spot welding machine.

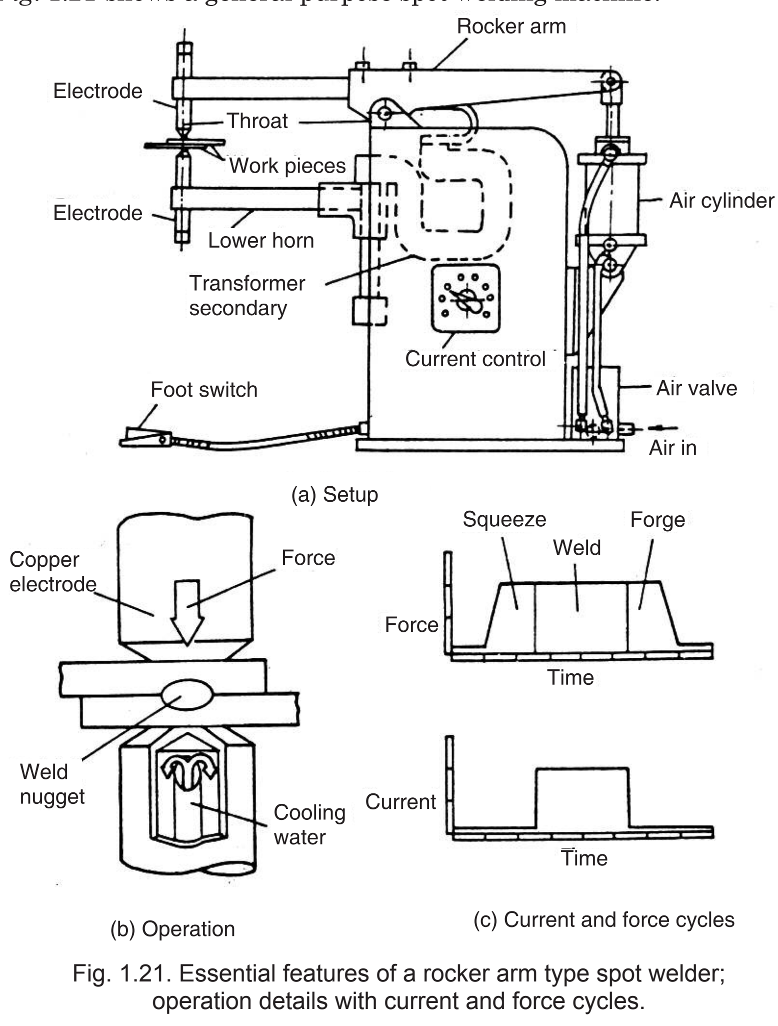

Fig. 1.21. Essential features of a rocker arm type spot welder; operation details with current and force cycles.

Spot welding is mainly used for lap welding of thin sheets particularly in the welding of automobile and refrigerator bodies, and high quality work in aircraft engines.

1.4.1.2. Projection Welding

Projection welding is a process of joining two sheets or a sheet and a thick component, or a small component like nut to a big body like automobile chasis, by making raised portions or projections on one of the components. The projections are made by embossing or intersection (*e.g.* cross of wires, etc.). There are several types of projections *viz.*, round button or dome type, ring type, elongated projection, shoulder projection, and radius projection. The projections act to localise the heat of welding circuit, because when placed together the sheets touch only at the points of the projections. Projection collapses due to heat and pressure and a fused nugget is formed at the interface.

Equipment used for projection welding is similar to that used for spot welding except that the rod electrodes are replaced by flat copper platens as shown in *Fig. 1.22*; which also shows the force and current cycles for the process.

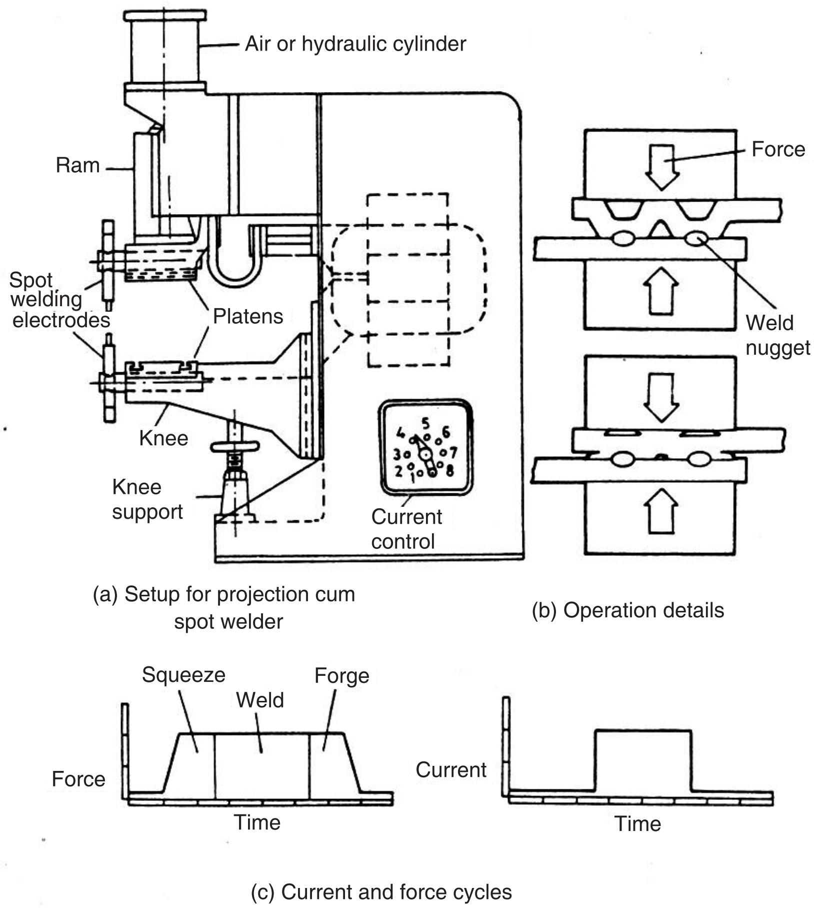

Fig. 1.22. Essential features of a projection welder; operation details with current and force cycle.

Typical applications of the process include projection welding of reinforcing rings around holes in sheet metal tanks, welding of threaded studs to backing bar or plate and cross-wire welding. Cross-wire products include such items as refrigerator racks, grills of all kinds, lamp shade frames, wire baskets, fencing, gratings and concrete reinforcing mesh.

1.4.2. Seam Welding Processes

In these processes, the weld is established along a seam so as to make a leakproof joint. The seam weld may be produced by making partially overlapping spot welds. Apart from projection welding the main processes in this class include resistance seam welding, electric resistance butt seam welding (ERW), high frequency resistance welding (HFRW), and high frequency induction welding (HFIW).

1.4.2.1. Resistance Seam Welding

In resistance seam welding, wheel electrodes are used to produce spot welds overlapping to the extent of 25 to 50%. Due to shunting of current through the already made weld, the current required is higher than in normal spot welding. Pressure is applied to fuse the metal properly into a nugget as in spot welding. *Fig. 1.23* shows the principle of resistance seam welding alongwith force and current cycles employed in the process.

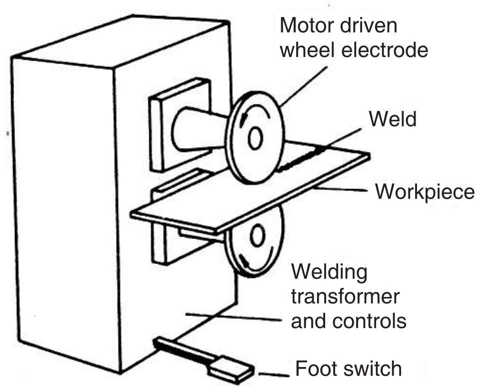

(a) Set-up

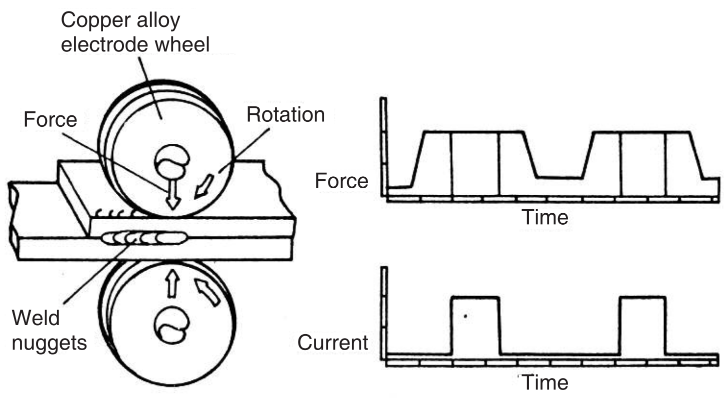

(b) Operation details (c) Current and force cycles

Fig. 1.23. Resistance seam welding.

Seam welding is used for producing leak-proof joints in tanks and boxes generally required for the automobile industry. This process is, however, restricted to welding thin materials ranging between 2.5 and 5.0 mm. Also, it is used mainly for welding materials with low hardenability rating, for example, hot-rolled grades of low alloy steels. This process is commonly used for making flange welds for use in water-tight tanks.

1.4.2.2. Electric Resistance Butt Seam Welding (ERW Process)

Large quantities of steel tube and pipe are manufactured by resistance butt seam welding from strip which is continuously edge sheared and rolled into tube of desired diameter before welding. Alternating current of up to 4000 A at about 5 volt is introduced across the joint by pressure rolls as shown in *Fig. 1.24.* For introducing heavy current directly to the moving electrodes a rotating transformer with slip rings on the primary side is employed. Unlike the normal resistance seam welding, current and work motion are continuous in this process.

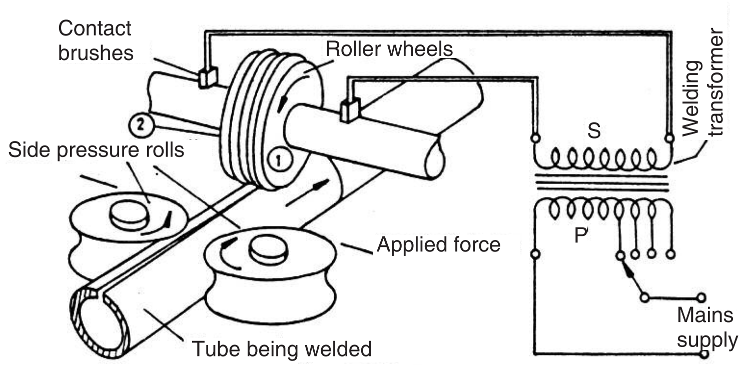

Fig. 1.24. ERW process of tube manufacturing.

The maximum rate of production is limited by the welding current frequency because as the welding speed is increased individual current half-cycles eventually lead to spot welding instead of seam welding. To overcome this difficulty current frequency is usually increased to 350 Hz to achieve welding speed of up to 36 m/min. The tube produced by this process has a fin of upset metal along the weld joint both inside and outside which is usually removed by installing appropriate cutters on the production line. The tube is cut to the desired lengths by employing a cutter which moves along the tube and is synchronised to cut the desired length in the available run in a given cycle.

1.4.2.3. High Frequency Resistance Welding (HFRW Process)

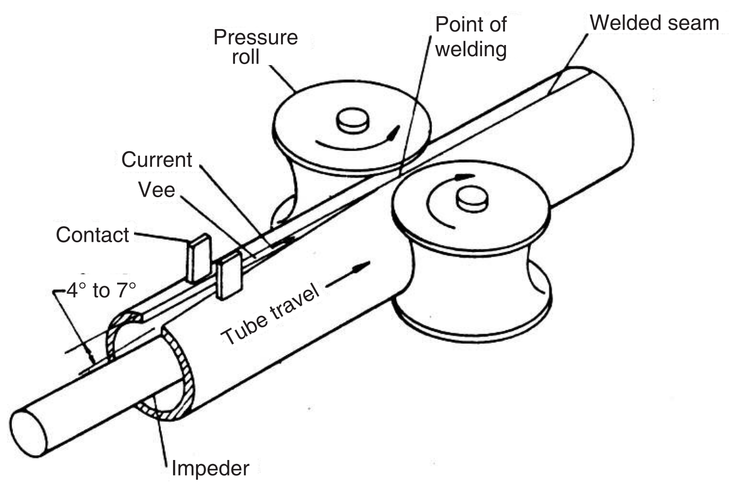

Fig. 1.25. HFRW process of tube manufacturing.

In this process, the tube is formed by rollers in the same way as in ERW process but the current in the range of 500 to 5000 A at a frequency (*f*) of up to 500 kHz and a voltage of about 100 volts is introduced through probes made of copper alloys and silver brazed to heavy water-cooled copper mounts. Contact tip sizes range between 15 and 650 mm^2 depending upon the amperage to be carried. Whereas in ERW process the heat is generated mainly by the interfacial contact resistance in HFRW process it is produced by the *skin effect* due to which the current flows in a shallow depth of the conductor and is proportional to $\sqrt{\frac{1}{f}}$.

Pressure rollers, to provide the forging pressure are installed a short distance down the line from the current probes as shown in *Fig. 1.25.* Due to the skin effect the current flow path lies along the strip through the apex of vee formed by the faying surfaces meeting at an angle of 4°– 7° as they close to form the tube. The depth of the heated region is generally less than 0.8 mm and thus affords the optimal condition for weld joint.

HFRW process is used to produce pipe and tubing of diameters ranging between 12 and 1270 mm, and with a wall thickness of 0.25 to 25 mm. Any metal can be welded by this process with a speed range of 5 to 300 m/min depending upon the wall thickness. This process can also be used to manufacture spiral and finned tubes and pipes. Various types of serrated or folded fins can also be welded to tubes.

1.4.2.4. High Frequency Induction Welding (HFIW Process)

High frequency induction welding of tubes is similar to high frequency resistance welding except that the heat generated in the work material is by the current induced into it. Because there is no electrical contact with the work this process can be used only where there is a complete current path or closed loop wholly within the work. The induced current flows not only through the weld area but also through other portions of the work.

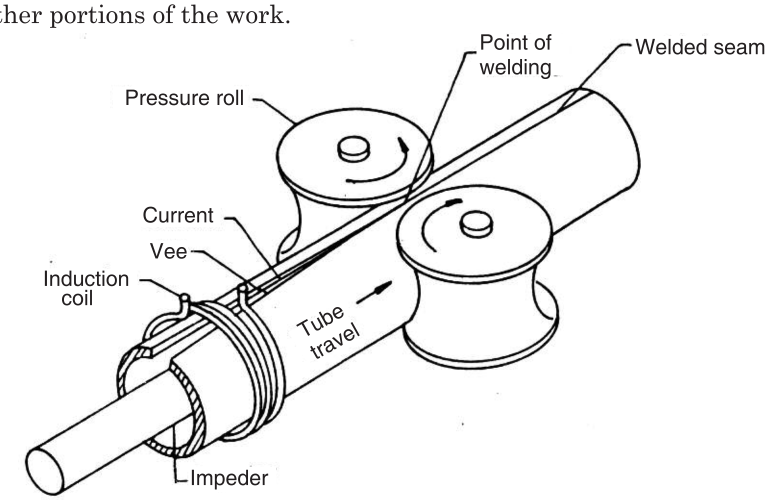

Fig. 1.26. HFIW process of tube manufacturing.

Tube edges are brought together in the same manner as in ERW and HFRW processes. A water-cooled induction coil or inductor made of copper encircles the tube at the open end of the vee as shown in *Fig. 1.26*. High frequency current flown through the coil induces a circulating current around the outside surface of the tube and along the edges of the vee, heating them to welding temperature. Pressure is applied to accomplish the weld as in HFRW process.

HFIW process is suitable for tubing made of any metal within a diameter range of 12 to 150 mm with a wall thickness of 0.15 to 10 mm at a welding speed ranging between 5 and 300 m/min.

HFIW process is not limited to tube manufacture but can also be employed to make circumferential welds for welding cap to tube. The process can as well be advantageously used for manufacturing tubing from coated material, small or thin-walled tubing; and it eliminates surface marking by electrical contacts. This process is, however, not suitable for welding high conductivity metals or those which form refractory oxides as there is no effective mechanism for oxide disposal.

1.4.3. Zonal Welding Processes

In these resistance welding processes, heat is generated simultaneously over the entire zone which is required to be welded. The processes included in this class are Resistance Butt Welding, Flash Butt Welding, and Percussion Welding.

1.4.3.1. Resistance Butt Welding

In Resistance Butt Welding or Upset Welding, the pieces to be welded are held in clamps supported on two platens, one of which is fixed and the other moveable; and form part of the single-turn secondary loop of a heavy duty transformer, as shown in *Fig. 1.27.* The ends to be welded touch each other before the current is switched on. A heavy current is then passed from one workpiece to another and the contacting faces are heated up due to the contact resistance. The two pieces are pressed together firmly after the desired welding temperature of 870 to 925°C, for steels, is reached. The pressing action which results in the increase in lateral dimension of the workpieces is called *upsetting*. Upsetting takes place both during and after the current flow. The upsetting action results in welding of end faces with squeezing of a part of the softened metal to form a fin, which can be removed later, if required, by machining.

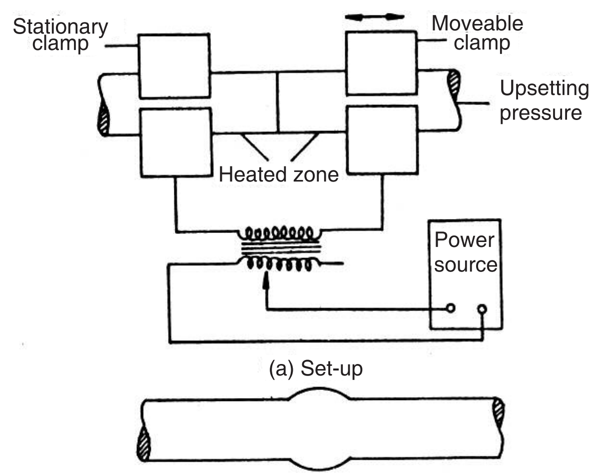

Fig. 1.27. Basic features of upset welding.

Resistance butt welding is used for end joining of rods, tubes, bars, and similar other sections for welding a cross-sectional area of up to 150 mm^2. Wire and rod from 1.25 mm to 30 mm diameters can be upset welded. Typical application of resistance butt welding is in wire mills for joining wire coils to each other to facilitate continuous processing.

1.4.3.2. Flash Butt Welding

Flash welding is similar to resistance butt welding except that it is accompanied by arcing and flashing. Flash welding consists of one fixed and one moveable clamp to hold and clamp the workpieces firmly as well as to force them together, a heavy duty single phase transformer with a single turn secondary, alongwith equipment to control welding current, movement of the clamp, force, and time. With a voltage of about 10 volts across the clamps, heavy current flows along the asperities across the contacting faces of workpieces. As the points of contact are melted and the metal is squeezed out in a shower of fine molten droplets, the contact is broken and arcing takes place across the gap. With further movement of the clamp, the process of melting, flashing and arcing repeats itself. Due to flashing contaminants from the contacting faces are removed and the surfaces are heated to a uniform temperature. Finally the movement of the platen (or moveable clamp) is rapidly increased and a high force is applied to achieve a weld with the expelled metal forming a rough fin or flash around the joint. The flash can be removed by subsequent machining. Basic arrangement for flash butt welding process is shown in *Fig. 1.28.*

Flash Butt Welding requires a heavy power supply, for example, currents in excess of 100,000 A can flow across the interface with a power input up to 200 kVA. Transformer used for flash butt welding are single phase which can, thus, place an unbalancing load on normal 3-phase supply from the mains. This necessitates the use of special transformer which can distribute the load uniformly.

In flash butt welding, the pieces to be welded must be held with enough force to avoid slipping and that requires a clamping force of up to twice that of the upsetting force. The upset force is around 70 MPa* for mild steel and nearly four times that for high strength materials.

* 1MPa = 1 N/mm^2.

Flash butt welding is extensively used for welding mild steels, medium carbon steels, and alloy steels as well as non-ferrous metals like aluminium alloys, nimonic alloys (80% Ni + 20% Cr) and titanium. Dissimilar metals may be flash welded if their flashing and upsetting characteristics are similar, for example aluminium can be flash butt welded to copper or nickel alloy to steel.

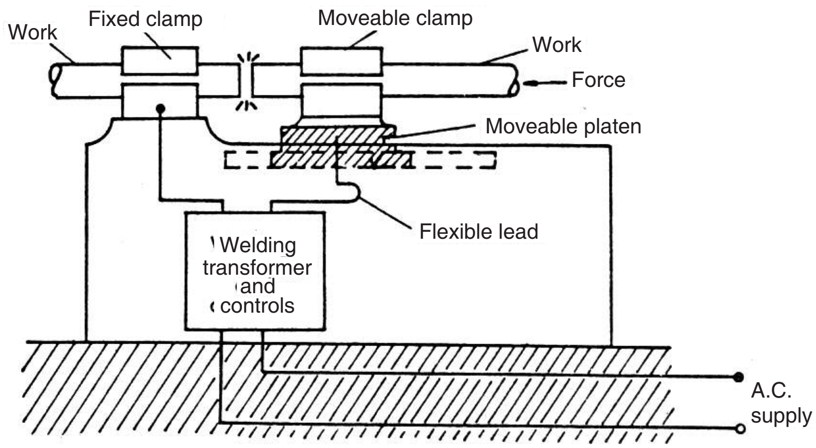

Fig. 1.28. Basic elements of a set-up for flash butt welding.

Typical uses of flash butt welding include welding of wheel rims, cylindrical transformer cases, circular flanges, and seals for power transformer cases. The aircraft industry utilises flash butt welding to manufacture landing gears, control assemblies, and hollow propeller blades while the petroleum industry uses oil drilling with fittings attached by flash welding. Other uses of the process include welding of rails, steel strips, window frames, and heavy duty chain links *e.g.*, anchor chains for ships. To avoid shunting of current the ring-type workpieces are made by welding two halves of each link simultaneously.

1.4.3.3. Percussion Welding

Percussion welding is an arc welding process of joining, end-to-end, two parts of equal cross-section. The arc is produced by a short pulse of electrical energy and pressure is applied in a percussive* manner to produce coalescence simultaneously over the entire abutting surface. In general percussion welding is the term used in the electronics industry for joining wires, contacts, loads, and similar items to a flat surface.

There are two variants of this process *viz.*, magnetic force percussion welding and capacitor discharge percussion welding. Essential steps involved in the process involves, (*i*) establishing an arc between the surfaces, to be joined, with high voltage to ionize the gas between the parts or with high current to melt and vapourise a projection on the part, and (*ii*) move the parts together percussively with an applied force to extinguish the arc to accomplish a weld.

Welding heat is generated by a high current arc between the two parts to be joined. The extremely short duration arc limits melting to a very thin layer on the two surfaces being welded. Consequently, there is very little upset or flash on the periphery of the welded joint. Filler metal is not used nor flux or special atmosphere required.

Percussion welding is usually employed for welding dissimilar metals difficult to weld by other processes and where the avoidance of upset at the joint is imperative.

Percussion welding is particularly good for joining small diameter (0.050–0.400 mm) wires even with widely different properties in electronic industry. Large contact assemblies for relays and contactors are often produced by percussion welding. This process is also used to weld electronic components to terminals as shown in *Fig. 1.29*.

*Forcible striking of one solid body against another.

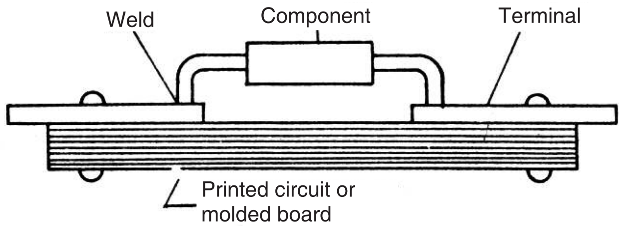

Fig. 1.29. Electronic component welded to terminals by percussion welding.

1.5. SOLID-STATE WELDING PROCESSES

In solid-state welding processes, the material to be welded is heated to a temperature below or just up to the solidus. The coalescence between the parts is achieved under pressure and thus forging or impact action plays an important role in all these processes.

Solid-state welding processes may be divided into two groups *viz.*, high heat input processes and low heat input processes.

1.5.1. High Heat Input Processes

High heat input solid-state welding processes include Forge Welding, Friction Welding and Diffusion Bonding.

1.5.1.1. Forge Welding

Forge welding or *smith welding* is the oldest known welding process and its use has been reported from about 1400 B.C. By this process the pieces to be welded are heated to above 1000°C and then placed together and given impact blows by hammering. In the more recent form of welding of large components the pressure is applied by rolling, drawing and squeezing to achieve the forging action. The oxides are excluded by virtue of design of the workpieces and or by the use of appropriate temperature as well as fluxes. Fluxes commonly used for forge welding low carbon steels are sand, fluorspar, and borax. They help in melting the oxides, if formed.

Proper heating of the workpieces is the major welding variable that controls the joint quality. Insufficient heating may not affect a joint while overheating results in a brittle joint of low strength. Also, the overheated pieces tend to be oxidised which shows itself by spongy appearance. The joints most commonly employed are scarf, cleft and lap types, as shown in *Fig. 1.30.*

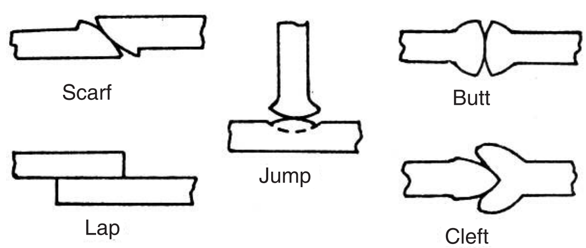

Fig. 1.30. Types of joints used in forge or smith welding.

Forge welding is now mainly used in under-developed countries for welding small agriculture implements and chains, etc.

1.5.1.2. Friction Welding

In friction welding one piece is held stationary and the other is rotated in the chuck of a friction welding machine. As they are brought to rub against each other under pressure, they get heated due to friction. When the desired forging temperature is reached throughout the rubbing cross-section of the workpieces, the rotation is stopped suddenly and the axial pressure is increased to cause a forging action and hence welding.

The machine used for friction welding resembles a lathe, as shown in *Fig. 1.31*, but is strudier than that. The essential features of the machine are that it should be able to withstand high axial pressure of the order of up to 500 N/mm^2 and be able to provide a high spindle speed of up to 12,000 rpm though the usual working range may rarely exceed 5000 rpm.

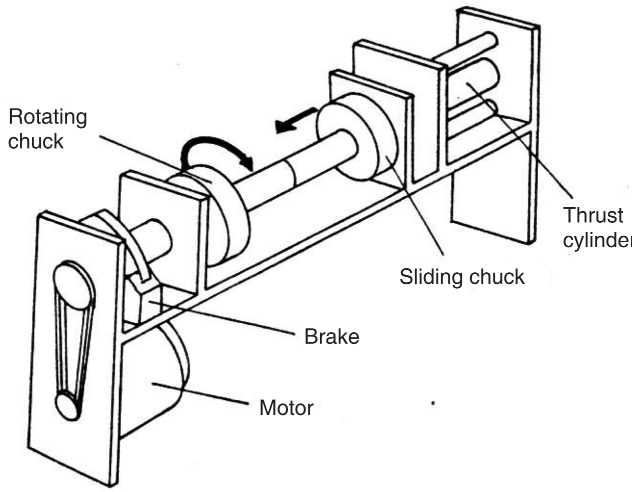

Fig. 1.31. A continuous drive friction welding machine.

Friction welding is a high speed process suited to production welding. However, initial trials are required to standardise the process parameters for a given job. Friction welding of two pieces rarely takes more than 100 seconds though it may be just about 20 seconds for small components.

Friction welding can be employed to weld most of the metals and their dissimilar combinations such as copper and steel, aluminium and steel, aluminium and titanium, etc. Typical applications of the process include welding of drill bits to shanks, *i.c.* engine valve heads to stems, automobile rear-axle hub-end to axle casing.

1.5.1.3. Diffusion Bonding

In diffusion bonding or *diffusion welding,* a weld is achieved by the application of pressure, of the order of 5 to 75 N/mm^2, while the pieces are held at a high temperature, normally about 70% of the melting point in degrees absolute *i.e.* about 1000°C for steel. The process is based on solid-phase diffusion which, obviously, is accelerated with rise in temperature.

Depending upon the extent of diffusion required the process may be completed in 2 to 3 minutes or may take many minutes or even hours. The quality of the surfaces to be welded plays an important role; surfaces machined to a standard of 0.4 to 0.2 μm CLA (centreline average) is usually adequate. The surfaces must be degreased before welding by using acetone or petroleum ether swab.

Diffusion bonding can be achieved by three methods *viz.*,

(*i*) gas pressure bonding,

(*ii*) vacuum fusion bonding,

(*iii*) eutectic fusion bonding.

In *Gas Pressure Bonding*, the parts are held together in an inert atmosphere and heated to a temperature of 800°C by a system resembling an autoclave*. During heating the high pressure provides uniform pressure over all the surfaces. This method is used for bonding non-ferrous metals only because it necessitates high temperatures for steels.

In *Vacuum Fusion Bonding* the parts are held in an intimate contact in a vacuum chamber. The pressure on the parts is applied by mechanical means or a hydraulic pump, and heating is done

* An autoclave is a vessel in which chemical reactions take place at high temperature and pressure.

in the same way as in gas pressure welding. *Fig. 1.32* shows the essential features of a set-up for vacuum fusion bonding. A vacuum pumping system which can quickly reduce pressure to about 10^{-3} torr (mm of mercury) needs to be used. High pressure created by the use of mechanical or hydraulic means makes it possible to diffusion bond steels by this method. Successful joining of steel can be achieved at a temperature of about 1150°C under an applied pressure of nearly 70 N/mm^2.

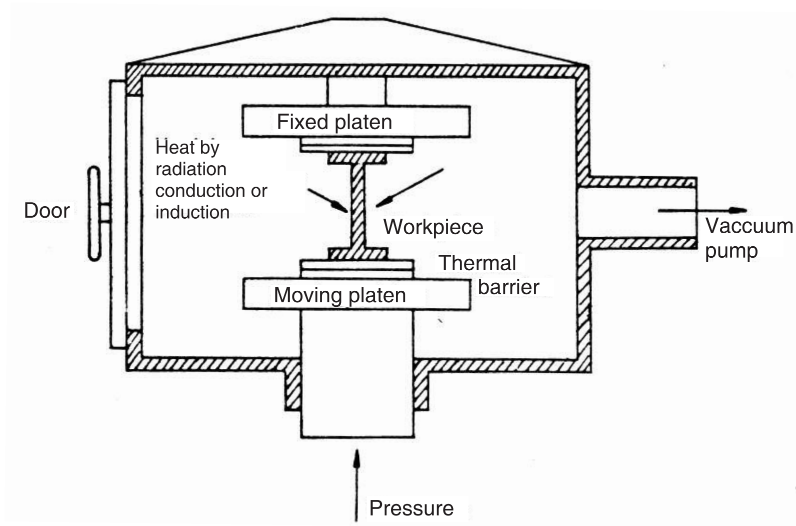

Fig. 1.32. Essential features of a setup for vacuum diffusion bonding.

In *Eutectic Fusion Bonding* a thin piece of a particular material is placed between the surfaces to be welded. This results in the formation of a eutectic compound by diffusion at an elevated temperature and the piece may completely disappear and form eutectic alloy at the interface. The material used for being placed in-between the two parts is usually in a dissimilar metal foil form with a thickness of 0.005 mm to 0.025 mm.

Diffusion bonding finds use in radio engineering, electronics, instrument making, missile, aircraft, nuclear, and aerospace industries. Typical applications of this process include tipping of heavy cutting tools with carbide tips or hard alloys, joining of vacuum tube components, fabrication of high temperature heaters from molybdenum disilicide for resistor furnace that can operate in an oxidising atmosphere up to 1650°C. In aerospace industry, it is used for fabricating complex shaped components of titanium from simple structural shapes. It is also used for surfacing components to resist wear, heat or corrosion.

1.5.2. Low Heat Input Processes

Low heat input solid-state welding processes include Ultrasonic Welding, Explosion Welding, Cold Pressure Welding, and Thermo-Compression Bonding.

1.5.2.1. Ultrasonic Welding

In ultrasonic welding a metallic tip vibrating at ultrasonic frequency (*i.e.* the vibrations which produce sound beyond the range of human hearing) is made to join a thin piece to a thicker piece supported on an anvil. The frequency used is mainly around 20 kHz though higher frequencies up to 60 kHz have reportedly been used. Higher the frequency of vibration higher is the rate at which energy is transmitted.

Ultrasonic welding equipment consists of two main parts *viz.*, a power source, and a transducer. The power source converts the 50 Hz mains supply to a high frequency electric power and that is converted by the transducer to magnetic flux and then the kinetic motion which is amplified through a velocity transformer. The schematic illustration of the set-up is shown in *Fig. 1.33*.

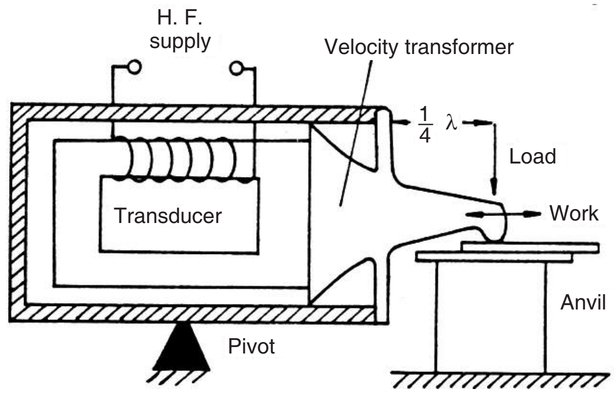

Fig. 1.33. Schematic illustration of the set-up for ultrasonic welding.

The transducer and the horn-shaped velocity transformer form a unit called *sonotrode*. The tip of the velocity transformer which is used for welding is made of high speed steel (*i.e.* steel containing 14 to 20% tungsten and 4% chromium) or Nimonic alloy (80/20 Ni/Cr) and is shaped to a spherical contour of about 75 mm radius. These tips are brazed or welded to the horn.

A velocity transformer is made of low-loss, high strength metal like titanium and is shaped to achieve the desired frequency based on the relationship,

$$f = \lambda E \qquad \text{...(1.2)}$$

where, f = vibration frequency,

λ = wavelength,

E = modulus of elasticity of horn material.

Since the welding tip has to be an anti-node thus the length of the horn has to be a multiple of $\lambda/2$ and any support must be at nodal points at $\lambda/4$. A vibrator, thus, can operate at one definite frequency only.

The work to be welded is placed under the sonotrode tip in lap joint formation and is supported on an anvil. Force is applied on the sonotrode tip with the help of pneumatic, hydraulic or a spring-actuated device. This set-up can be used for spot and seam welds. To make an annular or ring type ultrasonic weld, the force is applied tangentially on a cylindrical tip to give torsional vibration to the welding tip.

Due to the ultrasonic vibrations the oxide layer over the metal is broken and a clean metal to metal contact is achieved. The temperature at the interface rises to between 35 to 50% of the absolute melting point temperature of the metal and, thus, a solid-state weld is achieved. The strength of the weld is 65 to 100% of the base metal strength. The process is fast and seam welding with a speed of up to 10 m/min. have been reported. Energy required (E) for ultrasonic welding unit depends upon the thickness (t) and hardness (h) of the material to be welded and may be calculated from the following relationship,

$$E = Kt^{3/2} h^{3/2} \qquad \text{...(1.3)}$$

With adequate power a spot weld can be made in less than a second but the maximum thickness of the thinner piece should not exceed 3 mm.

Ultrasonic welding can be used for welding thin to thick parts as well as for welding dissimilar metal combinations like aluminium to steel, aluminium to tungsten, aluminium to molybdenum, nickel to brass, etc. The major users of the process are semiconductor, micro-circuit, and electrical contact industries. It is also used by automotive and aerospace industries.

Typical applications of the process include fabrication of small motor armatures, aluminium and gold lead wire connections to transistors and diodes, helicopter access doors, dissimilar metal joints in solar collectors. The unique applications of ultrasonic welding, however, is welding of containers of explosives like nitroglycerine, pyrotechnic (fire works), and reactive chemicals.

1.5.2.2. Explosion Welding

In explosive or explosion welding process, the weld is achieved by making one part strike against the other at a *very high but subsonic velocity*. This is achieved by the use of explosives usually of the ammonium nitrate base. The process is completed in micro-seconds.

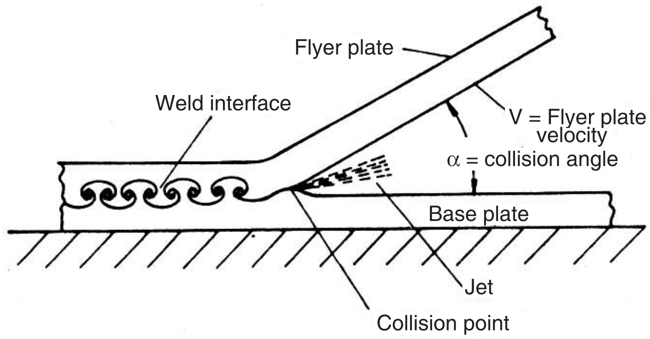

Fig. 1.34. Basic features of a set-up for explosion welding.

The set-up, in principle, used for explosion welding is shown in *Fig. 1.34*. It shows the two plates to be welded placed at an inclination to each other. The included angle varies between 1° and 10°. The thicker plate called the *target plate* is placed on an anvil and the thinner plate called the *flyer plate* has a *buffer plate* of PVC or rubber, between it and the explosive charge, for protection against surface damage. The charge is exploded by a detonator placed at one end of the flyer plate. When the charge explodes, the flyer plate moves towards the target plate at a velocity of 150 to 550 m/sec and the pressure produced at the interface of the impacting plates by such a high velocity is of the order of 700 to 7,000 N/mm^2. Under such a high velocity and pressure the metal flows ahead of the joining front acting like a fluid jet resulting in a bond of the interlocking type as shown in *Fig. 1.35*. The interlocking is an essential aspect of an explosion weld and is the cause of its strength. The weld strength equal to the strength of the weaker of the two components (metals) can be achieved.

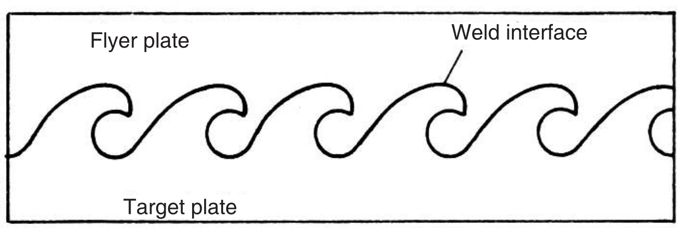

Fig. 1.35. Nature of another type of interlocking bond for explosion welding.

Explosion welding is normally an outdoor activity and needs a large area to ward off the persons coming close to the explosion site particularly when an explosive charge of high strength may have to be exploded.

Explosion welding can be used for joining dissimilar metal combinations like copper and steel, aluminium and mild steel, aluminium and inconel (76% Ni + 15% Cr + 9% Fe), aluminium and stainless, etc. Typical applications of explosion welding include cladding of thick plates by thin sheets, even foils. Tube to tube-plate joints in boilers and heat exchangers, valve to pipe joint, as well as blocking of leaking tubes in boilers can be successfully achieved by this process.

1.5.2.3. Cold Pressure Welding

Cold pressure welding or *cold welding* is a solid-state welding process in which a weld joint is produced solely by the application of pressure at room temperature. No heat is involved in this process. The main requirement of the process is that atleast one of the components being welded should be of ductile metal without much tendency for workhardening. Thus metals with FCC (face centred cubic) lattice structure are best suited for this purpose. Aluminium and copper are the major metals joined by this process.

The amount of deformation is a major factor in cold pressure welding and it depends upon the properties and thickness of the metal as well as the type of joint and surface preparation.

The parts to be joined by cold welding are cleaned thoroughly by degreasing, wire brushing, and scraping to remove any contaminants on the surfaces.

Cold pressure welding is used to make usually lap and butt types of joints. In lap welding the sheet thickness may vary between 0.2 and 15 mm and the joint is affected with the help of a single or a double die and the joint shape varies accordingly. The die radius varies with the workpiece thickness and the rough rule is $r = (1 - 3)\,t$, where t is the sheet thickness.

Butt joints by cold welding are made by clamping the two parts to be welded in a split die. Before clamping, however, a short section is usually sheared from the ends of the parts to expose fresh, clean surfaces with square ends. Butt welds usually have higher strength than the parent metal because the joint is workhardened.

Pressure for cold welding may be applied, to the properly aligned components, with hydraulic or mechanical presses, rollers, or specially designed manual or pneumatically operated tools. The rate at which the pressure is applied has no effect on weld joint properties hence welding can be done at high speed.

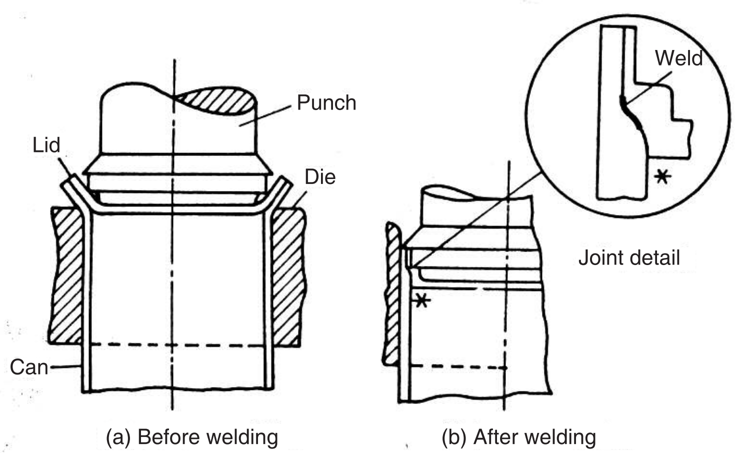

Fig. 1.36. Details of can joint produced by cold pressure welding.

Commercial applications of cold welding include can joints (*Fig. 1.36*) for packaging food, closing of aluminium cable sheaths, and cases of semi-conductor devices, lap and butt joints of wires and busbars for electrolysis cells, communication lines and trolley wires.

1.5.2.4. Thermo-Compression Bonding

It is a pressure welding process which is employed at temperatures above 200°C. The process deals with mainly small components in the electrical and electronic industries for welding fine wires of about 0.025 mm diameter to metal films on glass or ceramic.

There are many versions of the process, three out of which are shown in *Fig. 1.37* and are referred to as chisel or wedge bond, ball bond, and parallel gap bond. In the *chisel* or *wedge bond* a wire is deformed under pressure and welded to the film with the help of wedge shaped indentor.

In the *ball bond* a wire is heated by a micro-hydrogen flame to form a ball at the wire tip as shown in *Fig. 1.37*(*b*), which is subsequently welded to the heated film on substrate by the pressure exerted through the pierced indentor.

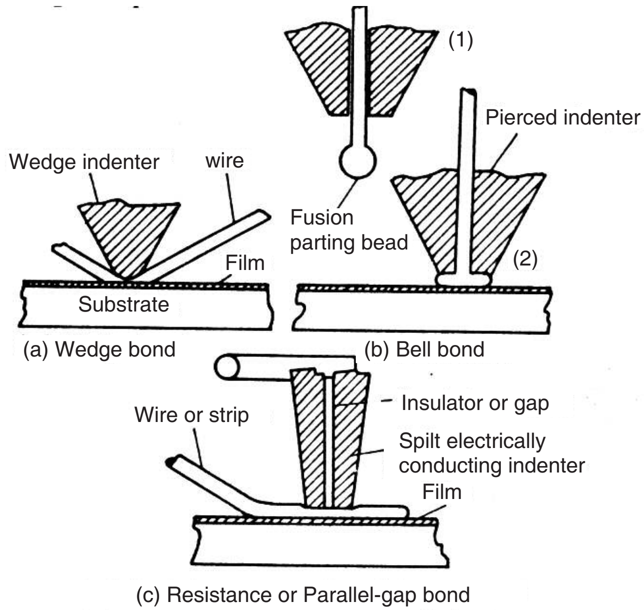

Fig. 1.37. Different methods of thermo-compression bonding. (After Houldcroft).

In the *parallel gap bond* the wire or strip is pressed to the film with the help of twin electrode made of high resistance material like tungsten. The flow of current through the wire or strip heats it up locally thus keeping the heat confined to small zone around it.

For all these variants of the process local inert atmosphere is created around the joint being bonded. Ultrasonic variations replace heating in some of the applications of all these modes of the process.

Commercial applications of the process include welding of noble metals, aluminium, and copper to substrates of glass or ceramics.

1.6. ALLIED PROCESSES

The processes allied to welding are of three types *viz.*, (*i*) *joining processes* involving no melting of the parent metal with consequential lower joint strength; (*ii*) *metal depositing processes* which often employ the welding process and or equipment to lay or spray material on to a substrate for repair to accomplish certain desired properties in the base material; and (*iii*) *thermal cutting processes* which help in cutting the material to the desired size for welding; alternatively the process may be employed for edge preparation by gouging. Brief descriptions and typical applications of the industrially important allied processes are given in the following sections.

1.6.1. Material Joining Processes

The processes allied to welding used for joining of materials include Soldering, Brazing, and Adhesive Bonding.

1.6.1.1. Soldering

Soldering is a process of joining metal pieces usually in the form of overlapped joints by making a filler metal flow into the gap between them by capillary action. The filler used is called a *solder* and has a melting point lower than 450°C.

The solder most commonly used is a compound of tin and lead in the ratio of 40/60, 50/50 or 60/40 having a melting point between 185 and 275°C, depending upon composition.

Soldering is done by thoroughly cleaning the pieces with the help of wire brush, emery cloth, file or even steel wool. The pieces are then fitted closely with a gap of about 0.08 mm between the mating surfaces. A flux is applied to the surfaces to be joined so as to avoid the formation of oxide due to subsequent heating as also to dissolve any flux still present on them. A commonly employed general purpose flux is zinc chloride while for soldering electrical connections resin, being non-corrosive, is best suited.

After the application of flux, the pieces are heated by any of the available methods *viz.*, oxy-acetylene torch, soldering iron, hot plate, electrical resistance, induction heating, oven heating, or dip heating; *Fig. 1.38* shows a general purpose electrical soldering iron in common use. The solder is then applied to the gap. It melts and flows into the interface of the mating surfaces by capillary action. On cooling it solidifies and provides a joint of adequate strength. If the gap between the surfaces is small as mentioned above, then the strength of the joint is more than that of the strength of solder. However, if a thick layer of solder is deposited then the maximum strength attained by the joint equals that of the solder. On cooling the joint is cleaned by hot water to avoid corrosive action of the flux residue.

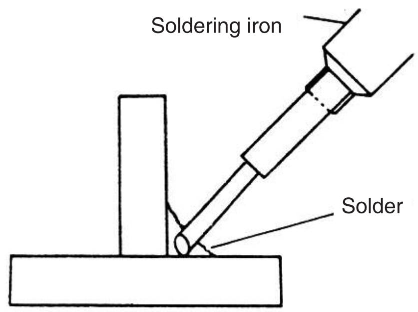

Fig. 1.38. Use of electrically heated soldering iron for making a fillet weld.

Commercially, soldering is used extensively for joining thin sheets of ferrous and non-ferrous metals where the joint is not stressed in tension. It is also widely used in the electrical and electronics industries.

Typical uses of soldering include joining of electrical conductors, and plumbing of copper tubing to copper fittings.

1.6.1.2. Brazing

Brazing is a process of joining metals by using a non-ferrous filler metal having a melting point above 450°C but below the solidus of the base metal. No melting of the base metal is involved and the filler spreads by capillary action between the pieces being joined.

The workpieces to be brazed are usually prepared for lap or butt joints. Both square butt and scarfed butt are used. The cleaning of the pieces is done by mechanical methods like filing, grinding, etc. or by the use of chemicals like carbon tetrachloride (CCl_4).

Joints to be brazed are made with small clearances of 0.025 mm to 0.25 mm. Brazing flux is then applied to dissolve solid metal oxide still present and to prevent further oxidation. Brazing fluxes usually contain chlorides, fluorides, and borates of alkali metals. *Borax*, however, is one of the most popular brazing fluxes.

Heating of workpieces is achieved by oxy-acetylene flame, induction heating or furnace heating. *Fig. 1.39* shows the induction heating system employed for brazing. The brazing filler material, if not already placed in position over the joint, can be applied in the form of a rod or a wire and melted to make it flow into the joint by capillary action. The fillers most commonly used are brass (60/40 Cu–Zn) and silver-copper-zinc- cadmium alloy like 35 Ag, 26 Cu, 21 Zn, 18 Cd.

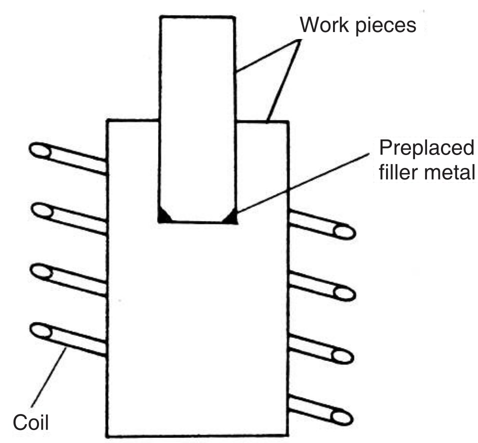

Fig. 1.39. Schematic illustration of induction brazing.

Residual flux left on the brazed joint can be removed by washing with hot water followed by air drying.

Commercially brazing is used widely throughout the industry. The major industries using brazing, however, are electrical, electronics, and maintenance industries. Typically brazing is used for joining carbide tips to the steel shanks for cutting tools.

A variant of Brazing is called *Braze Welding* or *Bronze Welding*.

Braze Welding is a process in which the metal pieces are joined in the same way as in brazing but the filler material is made to flow into the joint gap without the use of capillary action. Base metal is melted, if at all, to a limited extent.

All joints used for oxy-acetylene welding can be braze welded. Heat is also applied usually with the help of oxy-acetylene torch. However, carbon arc, gas tungsten arc, and plasma arc can be utilised equally effectively and without the use of flux. The filler is dipped in the flux and is melted with the help of flame or arc to make it flow into the joint gap. The force of the flame can be used to make the molten filler flow into the desired position. The fluxes used for bronze welding are propriety type and the filler is often a copper alloy brazing rod of 60/40 copper-zinc composition.

Joints for braze welding are of the square butt type for sheet thickness up to 2 mm but need single or double vee preparation above that thickness. However, efforts are made to eliminate sharp corners in edge preparation to avoid overheating.

Braze welding was initially developed for repair welding of cracked or broken cast iron parts, but is now-a-days used conveniently for joining dissimilar metals like copper to steel, copper to cast iron, nickel and copper alloys to cast iron and steel.

Typical applications of braze welding include rapid joining of thin gauge mild steel, welding of galvanised steel ducts using carbon arc, thin sheets to thick parts of cast iron and for joining telescoping pipes.

1.6.1.3. Adhesive Bonding

In adhesive bonding, a metal is joined to another metal or a non-metal by the use of an adhesive which usually consists of synthetic organic polymers of the thermosetting type, for example epoxy, and phenol formaldehyde.

The pieces to be joined are thoroughly cleaned by chemical or mechanical means. Whereas chemical cleaning may involve degreasing in a vapour bath followed by dipping in suitable acids, mechanical cleaning may include shot blasting, grinding, filing, wire brushing or sanding.

Adhesives are applied to the cleaned surfaces by brushing, spraying, roller coating or dipping. The thickness of the layer of adhesive, applied depends upon the metal being bonded, type of adhesive, solvent used and the strength aimed at, *e.g.*, to achieve an ultimate glue thickness of 0.025 mm to 0.75 mm anywhere from 0.125 mm to 0.375 mm of 20% solid wet adhesive must be applied.

Typical joints used for adhesive bonding include lap, inset, butt-strap, and tee type, as shown in *Fig. 1.40.*

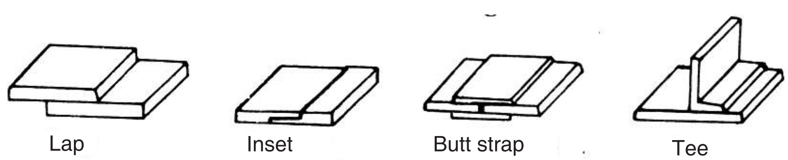

Fig. 1.40. Typical joints used for Adhesive bonding.

The adherends (workpieces) after being joined in the desired joint configuration are placed under a pressure of 10 to 100 N/cm^2 and are cured usually at a temperature of about 150°C for about 30 minutes. Adhesion is generally due to molecular attraction between the adhesive and the adherend. *Fig. 1.41* shows the joint mechanism of an adhesive bond.

Commercial uses of adhesive bonding include a large number of applications in manufacture of railway cars, microwave reflectors, refrigerators, storage tanks, etc. But, by far the major users of this method are the aircraft and automobile industries.

Typical applications of the process include fastening of stiffners to aircraft skin, attaching of brake linings to brake shoes, and joints in the aircraft wing and tail assemblies.

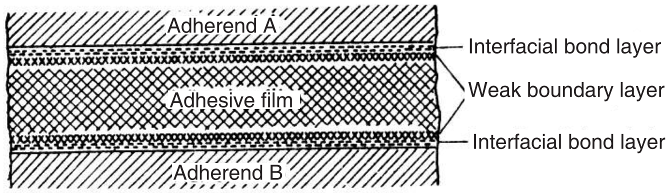

Fig. 1.41. Joint mechanism of an adhesive bond.

1.6.1.4. Surfacing

Surfacing or overlaying is the process of depositing filler metal over the surface of a base metal with a view to achieving desired properties which include corrosion resistance, wear resistance, dimension control and metallurgical needs. Usually four variants of the process are recognised *viz. cladding*, *hardfacing*, *build-up,* and *buttering*, the aims of which are respectively to provide increased corrosion resistance, increased wear resistance, dimensional requirement, and to achieve metallurgical compatibility.

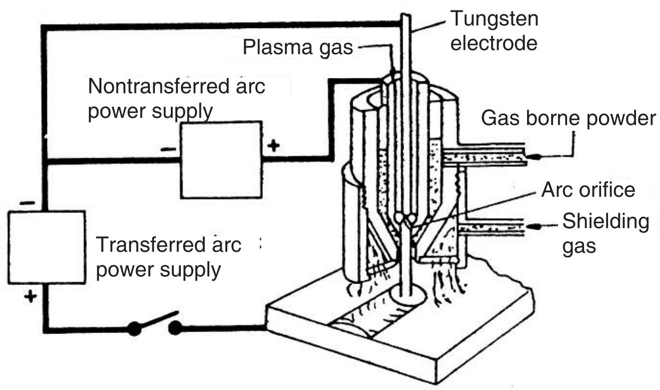

Fig. 1.42. Schematic illustration of a set-up for Plasma arc surfacing.

Surfacing can be done by a number of welding processes like shielded metal arc welding, submerged arc welding, electroslag welding, plasma welding, explosion welding, and even oxyacetylene welding. *Fig. 1.42* shows a set-up for plasma arc surfacing process. Cladding can be done even by mechanical rolling operation.

Surfacing by welding is carried out by the usual welding techniques but quite often the beads are laid overlapping to the extent of 30 to 50% to achieve complete union between them. Shallow penetration with low dilution but adequate joint strength are the desired aims of the process. This may necessitate proper cleaning of the surface before surfacing. Cleaning method employed will depend upon the material and the surface integrity of the base metal. Grinding, shot blasting, and chemical cleaning may be employed to achieve the desired quality of the surface. The thickness of the material laid usually varies between 3 and 5 mm.

Commercially, submerged arc and plasma arc are the most often used for surfacing. The industries using surfacing are many including pressure vessel industry, railways, automobile industry, and the earth moving machinery industry. Apart from overlaying the inside of the newly made pressure vessels and boilers, the process is used mainly for reclamation of equipment such as coal and cement crushing equipment, drill rigs, coal cutters, forges and press components like dies and punches.

Typical applications of the process include surfacing of engine valve facings and seats of internal combustion engines, building-up broken or wornout gear and sprocket teeth, repairing of digesters used in pulp and paper mills, rock crusher cones and bulldozer tips.

1.6.1.5. Thermal Spraying

Thermal spraying is the process of depositing a metallic or a non-metallic material over a base material to protect it from corrosion, or to reduce abrasion, erosion, cavitation, or wear. It is also used to restore the defective or worn surfaces to their original shape and dimensions.

Thermal spraying process has three main variants *viz.,* electric arc spraying, flame spraying, and plasma spraying. Whereas the electric arc spraying uses material in wire form, plasma arc spraying uses it in powder form while flame spraying can use material both in wire and powder forms. *Fig. 1.43* shows the schematic of flame spraying set-up using material in wire form.

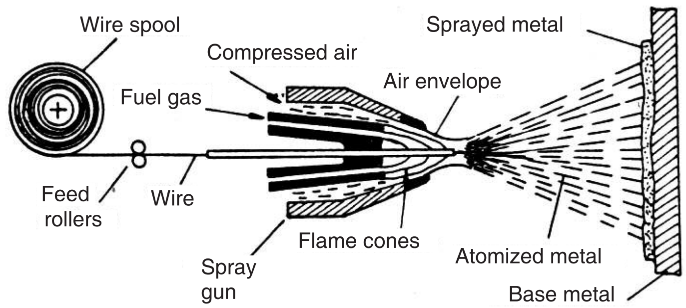

Fig. 1.43. Schematic of a set-up for flame spraying.

The principle of operation in all three methods of spraying is that the material to be sprayed is melted by electric arc or plasma arc, or gas flame and is atomised with the help of high pressure air or inert gas and is projected on to the base material. The sprayed material sticks to the base material due to its fluid state and high impact. Depending upon the temperature and pressure the bond between the coating and the base material is of mechanical nature or a complete coalescence.

For achieving a good bond between the coating and the base material it is very important to prepare the workpiece properly. Depending upon the nature of base material it may be machined, shot blasted, chemically cleaned, or even bond coated. Overall a clean but rough surface gives the best result if it is sprayed immediately after preparation. Apart from metals, the base material can be cloth, leather, wood, concrete, or any other porous surface.

Commercially, the process of thermal spraying is used in machinery repairs and maintenance, and for providing protective coatings. Material deposited by spraying is usually of much less thickness than that deposited by surfacing. The bond in spraying is also normally of the mechanical nature whereas in surfacing it is of the coalscence type.

Typical applications of the process include zinc coating on turbine blades, armature shafts and cam shafts. Decorative work by spraying includes spraying of furniture, toys and sign boards.

1.7. THERMAL CUTTING PROCESSES

Thermal cutting processes is a family of processes in which heat of an electric arc, radiation energy, or an exothermic reaction is utilised to melt or oxidise a metal at an accelerated rate to achieve a cut. There are a number of processes which utilise the heat of the arc to cut metals and they include shielded metal arc, air carbon arc, plasma arc, gas tungsten arc, and gas metal arc. Electron beam and laser beam use the high density radiation energy to achieve cutting of metals. Oxy-fuel gas flame in conjunction with oxygen jet is utilised to initiate and sustain an exothermic oxidising reaction which generates enough heat and affects parting of metals particularly low carbon ferrous alloys. Out of these processes oxy-acetylene flame cutting and plasma arc cutting are the two major thermal cutting processes, while air carbon arc process is used both for cutting and gouging in the industry.

Oxy-Acetylene Flame Cutting Process is the most used process for economic and high speed cutting of low carbon steels. In this process, a gas cutting torch, shown in *Fig. 1.44*, having some resemblance to gas welding torch is employed. The gas cutting torch not only provides a means to obtain an oxy-acetylene flame but also has a separate lever controlled passage to provide a high pressure pure oxygen gas jet which impinges upon the heated metal to cause oxidation and generation of heat by the following reaction.

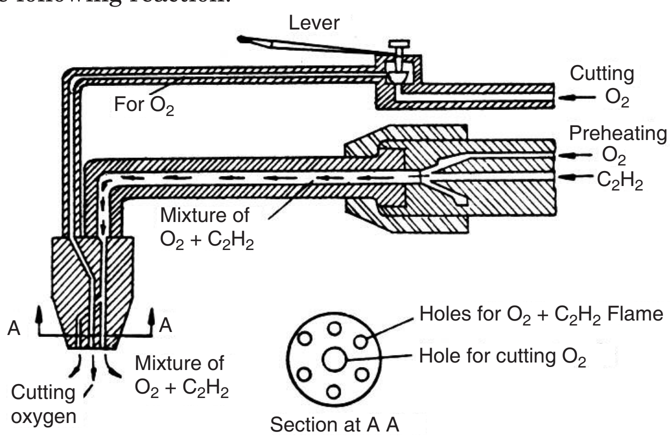

Fig. 1.44. Constructional features of a flame cutting torch.

$$3Fe + 2O_2 \longrightarrow Fe_3O_4 + \text{heat (1120 kJ/mol)} \qquad ...(1.4)$$

However, the initiation of this reaction is possible only if the metal to be cut has achieved the ignition temperature of 870°C or above for steel. Once the reaction is initiated the flame is required only to sustain it so a neutral flame of low energy is used. The metal which is oxidised (Fe_3O_4) has a lower melting point than the melting point of steel, thus the cut is achieved faster than that by melting of steel. The oxygen jet also helps in blowing the oxidised metal or slag out of the cut or kerf.

Commercially, oxy-acetylene cutting process is extensively used for cutting mild and low alloy steels for straight or contoured cuts as well as for joint edge preparation for welding. It also finds though a limited use in cutting cast iron and stainless steels *e.g.* in foundries to remove gates and risers, etc. from the castings.

In *Plasma Arc Cutting* a metal is parted by melting using a high velocity jet of ionised hot gas. The equipment employed is similar to that used for plasma arc welding, however, the gas pressure used is higher than that employed for welding.

The plasma arc cutting torch is of the transferred plasma arc type with the workpiece connected to the anode of the *DC* power source, as shown in *Fig. 1.45*. The power source used is of the drooping volt-ampere characteristic type with an open circuit voltage (OCV) range of 120 to 400 volts. Higher OCV is used for cutting thicker sections. The output current range required is usually 70 to 1000 amperes.

The gas used for producing plasma jet depends upon the metal to be cut, for example, carbon steel can be cut by compressed air while most non-ferrous metals can be cut by using nitrogen, hydrogen, argon and their mixtures.

Almost all metals can be cut by plasma arc cutting but it is particularly suited to cutting aluminium and stainless steels. It can also be used for stack cutting, shape cutting, and plate bevelling.

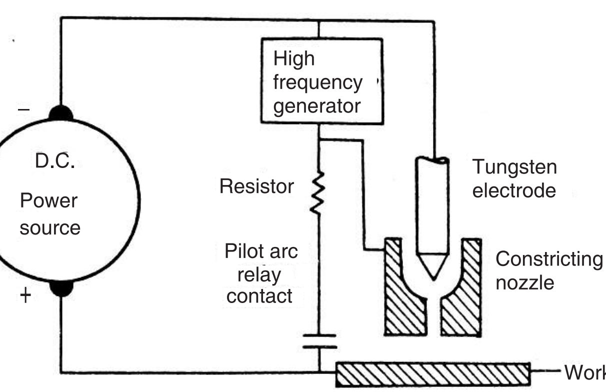

Fig. 1.45. Circuit diagram for plasma arc cutting.

Air Carbon Arc Gouging and Cutting is a process of removing unwanted metal to produce grooves in plates and to bevel edges in preparation for welding. In this process heat is produced by an electric arc between a graphite rod and the workpiece to melt and blow it out of the cut by compressed air which may also partially oxidise the material and hence help in lowering its melting point. The compressed jet usually follows the arc for blowing out the molten metal as shown in Fig. 1.46. Apart from gouging the process can also be used for cutting the metals.

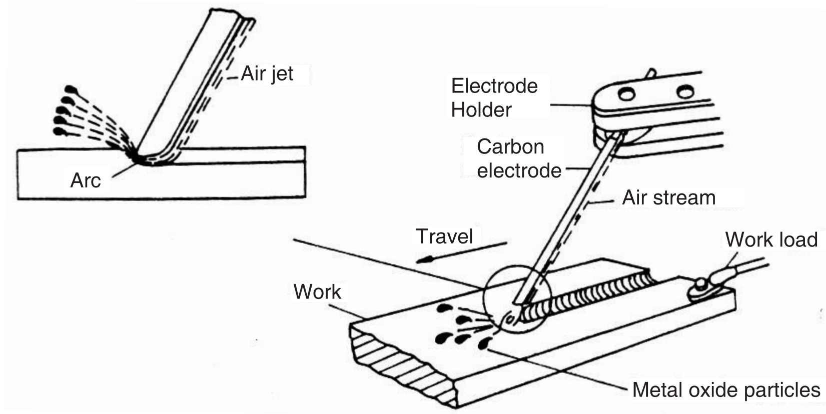

Fig. 1.46. Schematic illustration of the process of air carbon arc gouging.

As oxidation of metal is not an essential requirement of the process therefore all metals can be gouged or cut regardless of how rapidly they oxidise. Material can be removed approximately five times faster by arc gouging than by chipping. A 10 mm groove, for example, can be gouged at a speed of 60 cm/min. Depth of cut can be controlled closely, and welding slag does not deflect or hinder the cutting action as it would with cutting tools. The cost of operating gouging equipment is generally less than for chipping hammers or gas-cutting torches, and the arc-gouging equipment also requires less space. An arc-gouged surface is clean and smooth and can usually be welded without further preparation.

Most of the standard arc welding power sources, both *AC* and *dc*, with an open circuit voltage of 60 volts can be used for air carbon arc gouging and cutting. The 150 to 300 mm long electrodes used vary from 4 mm to 25 mm in diameter. Both bare and copper coated electrodes are used, however the latter type finds more extensive use because they erode far less during operation than the bare electrodes and because of better groove uniformity achieved by them.

The air pressure used is 55 to 70 N/cm^2 with an airflow rate of 85 to 145 lit/min. Where compressed air lines are not available, arc gouging torches suitable for light work can be operated on gas from compressed gas cylinders at pressures as low as 30 N/cm^2.

Arc gouging torches are generally air-cooled but those intended for applications at higher currents are water-cooled.

The correct use of arc gouging with carbon-based electrodes usually causes no carbon pick-up and does not affect corrosion resistance of the parent material. A thin hardened zone may appear, by gouging, in some metals but subsequent welding remelts this zone and reduces the hardness.

Heat penetration is shallower with arc gouging than with oxygen cutting, so arc gouging produces less distortion.

Air carbon arc process is widely used for gouging, joint edge preparation and for removing defective weld metal. It is also used for scraping of metal objects by cutting.

1.8. MODES OF WELDING

All the afore described welding and allied processes are used in fabrication industries in different modes depending upon the volume of production involved, nature of joint, material and its thickness, and the accessibility of the spot to be welded.

In most of the welding methods the following sequence is required to be followed to achieve the end product assuming, however, that the preliminary operations like cleaning, edge preparation, and the fixing of tab-in and tab-out plates have already been accomplished.

1. Assemble parts by tack welding or by employing jigs and fixtures.
2. Present the assembled workpiece to the machine or vice versa.
3. Initiate welding by striking the arc for fusion welding or by bringing electrodes in contact with the work and switching on the current for resistance welding.
4. Create relative movement between the welding head and the work to attain the desired welding speed.
5. Control the welding variables like arc voltage, welding current, wire feed rate, etc. to control the arc length in the case of arc welding processes and to control the depth of molten metal and slag pool in Electroslag welding.
6. Stop welding by stopping the relative movement between the welding head and the work. If weld pool crater is to be filled then the crater filler will become operative before the current is switched off automatically.
7. Shift the welding head to the position wherefrom the next welding cycle is to be initiated.
8. Remove the completed work. This operation may be done before or after repositioning the welding head or both operations may be carried out simultaneously.

To accomplish the above task anyone of the following four techniques may be employed.

(*i*) Manual welding, (*ii*) Semi-automatic welding,
(*iii*) Automatic welding, (*iv*) Automated welding.

1.8.1. Manual Welding

It implies that all the eight operations of welding sequence are carried out manually. Note, however, that stage 4 that is 'the relative movement between the welding head and the work' may include some mechanical assistance such as a welding manipulator which moves the workpiece at approximately the right speed for welding. One such manipulator called *gravity welder* is shown in *Fig. 1.47* in which the welder winds up the weight, then controls rotational speed of the circular table by holding the edge and letting it run through his fingers at the desired speed enabling him to produce neater, continuous welds on circular seams in the downhand welding position.

Manual welding is most popular with SMAW, GTAW, plasma arc welding, and oxy-fuelgas welding processes.

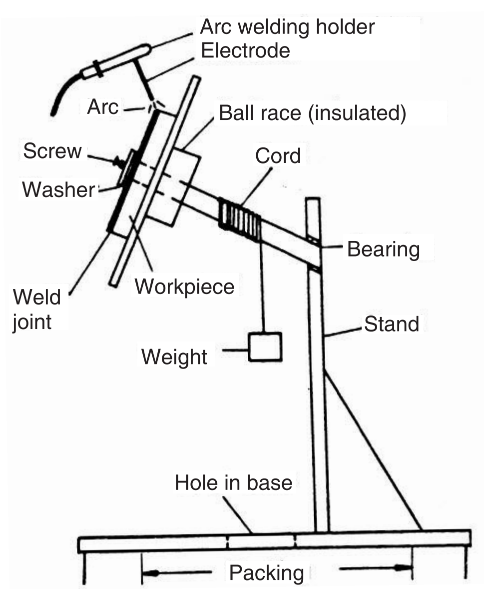

Fig. 1.47. Gravity motor for work manipulation in welding.

1.8.2. Semi-Automatic Welding

In this mode of operation stage 5 that is 'the control of welding variables such as wire feed speed in GMAW or the duration of current in resistance welding with a gun welder is automatic' but the means of welding are held in hand. Stage 4, that is 'the relative movement between the welding head and the work' is normally manual but mechanical means like conveyor belt or work manipulator may be employed. Thus, GMAW process can be used in conjunction with gravity motor to improve the quality and productivity in welding.

Various operations in stages 3 and 6 that is 'initiation and stoppage operation' can be carried out in sequence automatically with the help of a single on-off switch.

The semi-automatic welding mode is most popular with GMAW and FCAW. Though it is possible to use this technique with GTAW, SAW, and ESW processes but it is rarely done.

1.8.3. Automatic Welding

It is a welding mode in which at least stage 5, that is 'the control of welding variables' and stage 4 *i.e.* 'the relative movement between the welding head and the work' are automatic. Usually a single switch working through a sequencing device operates the controls for power and consumables like wire and gas. This may also bring crater-filling device, if incorporated, into action automatically. *Fig. 1.48* shows a block diagram for a typical automatic welding system.

In an automatic welding mode stages 1, 2, 7 and 8 are carried out by hand or initiated manually. By above logic, *gravity welding** is classified as a portable automatic welding method.

The automatic welding mode is most popular with SAW and ESW processes. It is also used, to a limited extent, with GTAW, GMAW, FCAW, and plasma arc welding processes.

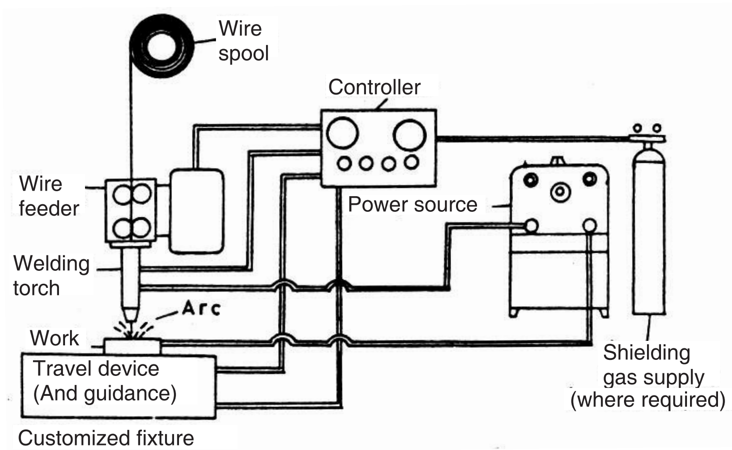

Fig. 1.48. Block diagram for an automatic welding system.

1.8.4. Automated Welding (Flexible Welding System)

In automated welding mode all eight stages from assembly and transfer of the parts to the welding head are performed without adjustment of controls by a welding operator. The welding which may be completed in one or more stages, and the final ejection of the completed parts, are carried out mechanically without manual intervention. An important aspect of automated welding is that the operator need not continuously monitor the operation. Compared to automatic welding this tends to increase productivity, improve quality, and reduce operator fatigue.

Fig. 1.49 shows a schematic diagram for an automated welding system employing mini-computer, multi-programmer, and a seam tracing unit. The automated welding mode is populary used with SAW, GMAW, and FCAW processes. To a limited extent GTAW, PAW, and ESW processes are also used in automated modes.

Automated welding systems often employ *Adaptive Controls* to accomplish two aims *viz.*, seam tracking and quality control.

Apart from the conventional automated systems this mode of welding is used for *remote welding* and robotic welding.

* Refer to author's book entitled, 'Welding Processes and Technology' for description of Gravity Welder.

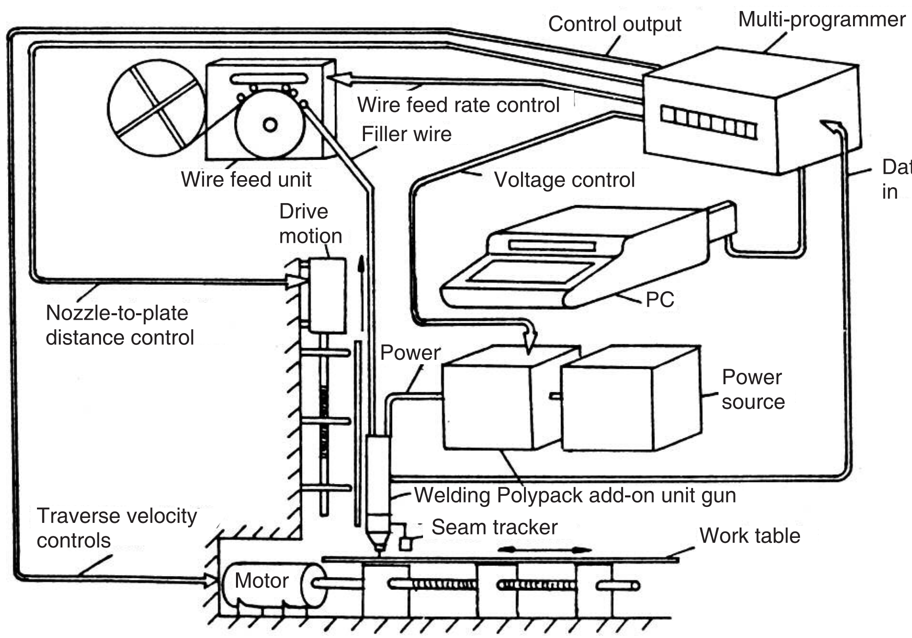

Fig. 1.49. Schematic representation of an automatic welding system.

1.8.4.1. Remote Welding

Remote welding is similar to automated welding in that the welding operator is not at the welding location and may be at a great distance from it. While conventional automated system is designed normally for making the same identical weld time after time, Remote welding usually involves maintenance operations where each weld may be different from the previous one. Remote welding is becoming more widely used with the increased establishment of nuclear power plants. In general, it is performed where humans cannot be present because of a hostile atmosphere, such as where high level of radioactivity exists.

One of the typical applications of remote welding is the sealing of radioactive materials into metal containers. Sealing of fuel elements and target rods in nuclear industry is also accomplished by remote welding.

1.8.4.2. Robotic Welding

Robotic welding is a more fascinating aspect of automated welding as *articulated robots** can closely emulate the productive actions of a man in the welding environment, and within limits provide an acceptable alternative for performing many of the monotonous and thus fatiguing tasks that are to be encountered in industry in abundance. In such situations a robot can be cost effective solution to many welding tasks. Apart from cost reduction by increased productivity; other advantages of robots are that of consistent accuracy, minimum wastage of materials and stabilized labour charges.

Although welding robots can be used for any weld joint for which software programme can be produced but it is best suited to batch production.

1.9. POSITIONS IN WELDING

Depending upon the position during welding all butt and fillet welds in plates are classified into four basic groups *viz.*, downhand or flat, horizontal, vertical, and overhead welds.

According to internationally accepted norms a *downhand or flat weld* is a weld in any direction

* Articulated robot is a robot with flexible joints including wrist movement.

on a horizontal surface; a *horizontal weld* is one running horizontally on a vertical surface, a *vertical weld* is that which runs vertically on a vertical surface and an *overhead weld* is one that is deposited above the operator's head.

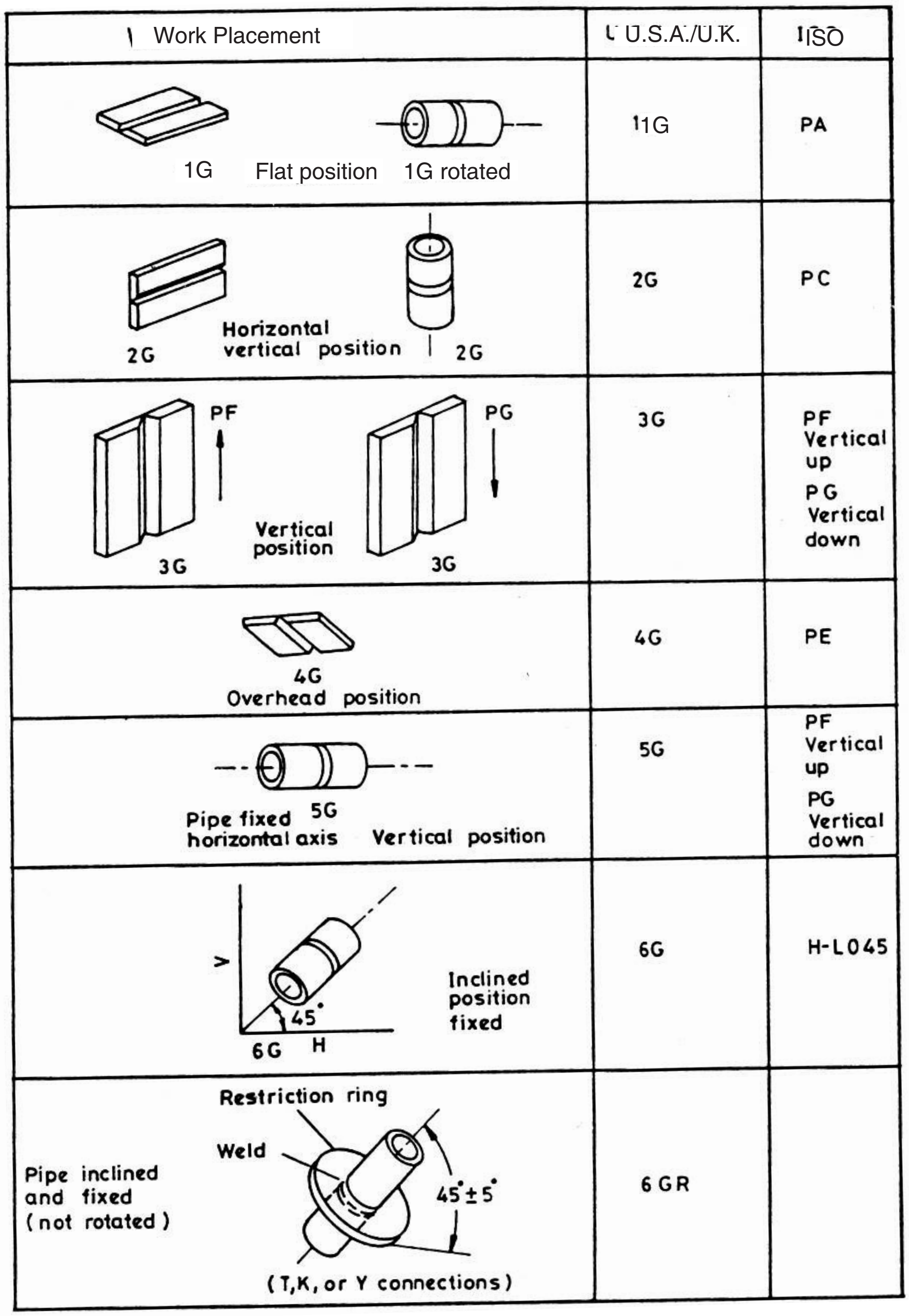

Work Placement	U.S.A./U.K.	ISO
1G Flat position 1G rotated	1G	PA
2G Horizontal vertical position 2G	2G	PC
PF PG Vertical position 3G 3G	3G	PF Vertical up PG Vertical down
4G Overhead position	4G	PE
Pipe fixed horizontal axis 5G Vertical position	5G	PF Vertical up PG Vertical down
V 45° 6G H Inclined position fixed	6G	H-L045
Pipe inclined and fixed (not rotated) Restriction ring Weld 45°±5° (T,K, or Y connections)	6GR	

Fig. 1.50. Standard welding positions for butt welds in plates and pipes.

Butt and fillet welds in pipes are classified in a slightly different way depending upon not only the type of weld *i.e.* butt or fillet weld but also whether the pipe is held stationary or rotated. Further classification is also based on the inclination of the pipe and whether there is any restricting ring on it to interfere with the welding operation. All these positions of welds as per US (UK) and ISO (International Standards Organisation) standards are given in *Figs. 1.50* to *1.54*. While *Fig. 1.50* gives the standard welding positions for butt welds in plates and pipes, *Fig. 1.51* gives detailed configurations for test welds in positions 5G and 6 GR for pipes.

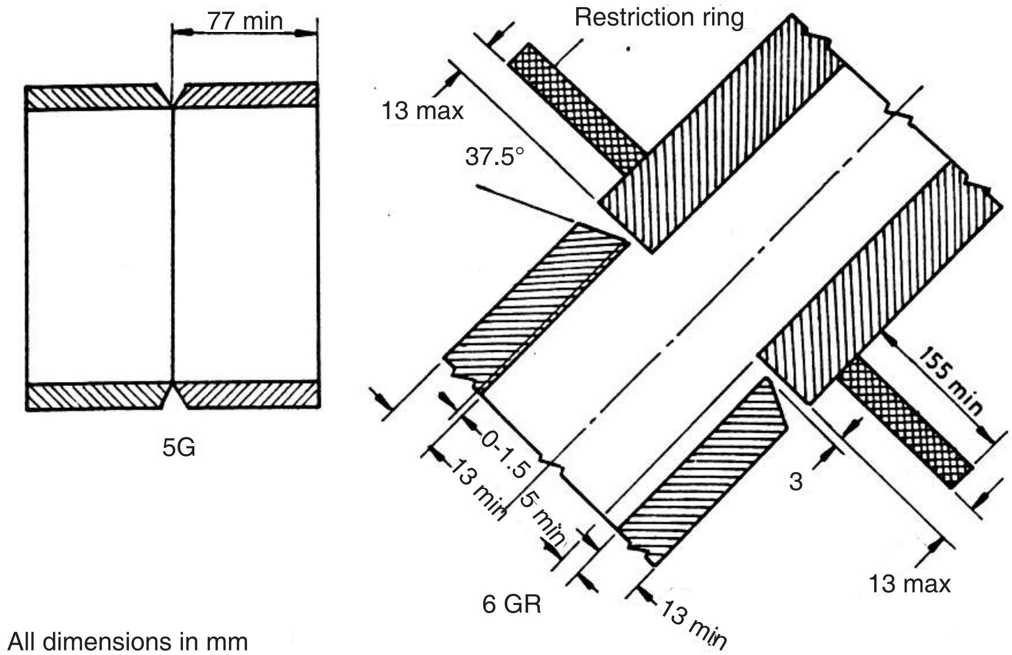

Fig. 1.51. Detailed configurations for standard welding positions 5G and 6GR in pipes.

The standard welding positions for fillet welds in plates and pipes are illustrated in *Fig. 1.52*, and *Fig. 1.53* shows the basis on which the main welding positions are defined as per ISO. *Fig. 1.54* shows the standard welding positions for stud welding alongwith their limits of operation.

Work Placement	US/UK	ISO
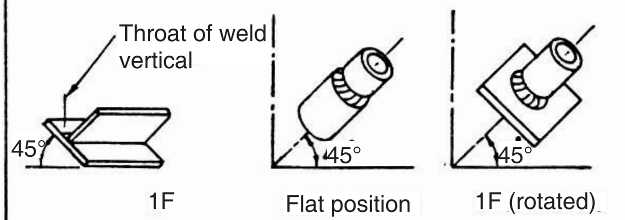 Throat of weld vertical 45° 1F Flat position 1F (rotated)	1F 1FR	L45/PA L45/PA
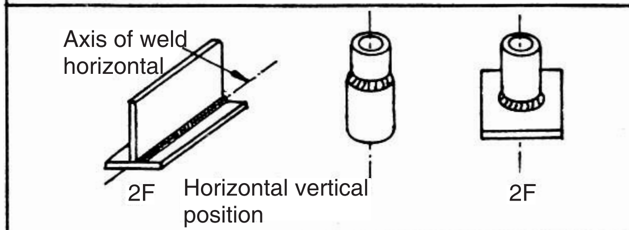 Axis of weld horizontal 2F Horizontal vertical position 2F	2F	PB
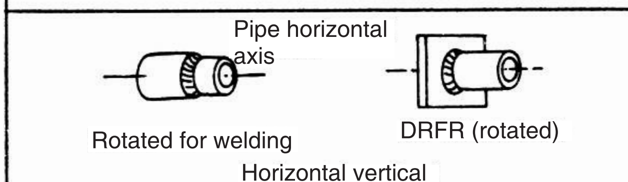 Pipe horizontal axis Rotated for welding DRFR (rotated) Horizontal vertical	2FR	PB
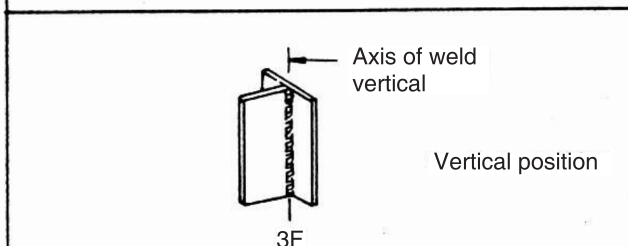 Axis of weld vertical Vertical position 3F	3F	PF Vertical up PG vertical down
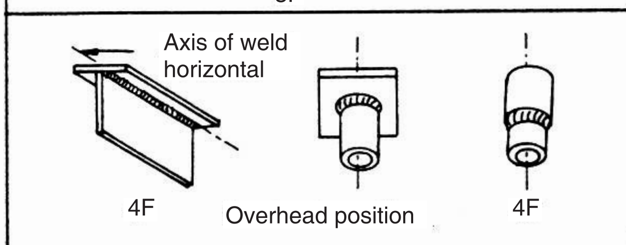 Axis of weld horizontal 4F Overhead position 4F	4F	PD
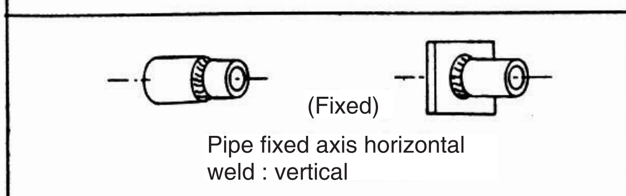 (Fixed) Pipe fixed axis horizontal weld : vertical	5F	PF Vertical up PG vertical down

Fig. 1.52. Standard welding positions for fillet welds in plates and pipes.

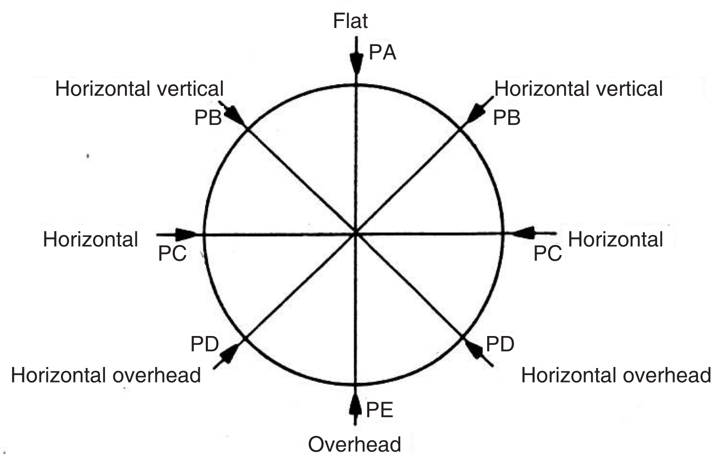

Fig. 1.53. Basis for nomenclature of welding positions as per ISO.

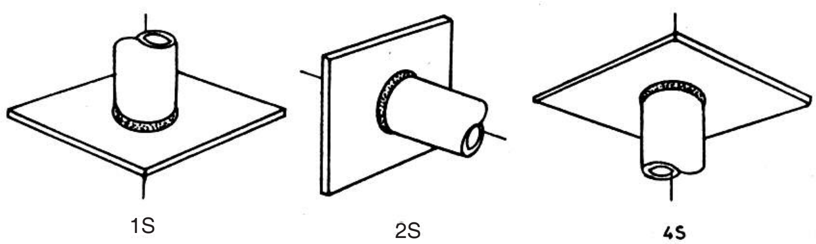

(a) Stud welding positions

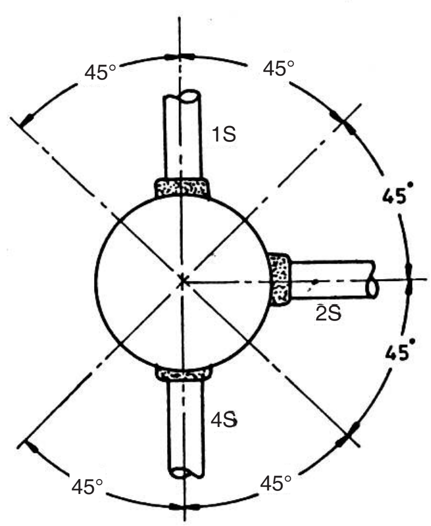

(b) Limits of positions for plate or pipe

Fig. 1.54. Standard stud welding positions and their limits of operation.

2

Heat Flow in Welding

All fusion welding processes involve heat flow during welding to accomplish the desired joint. Depending upon the heating and cooling cycles involved different types of microstructures are obtained in weld bead and the heat affected zone (HAZ). This leads to varying mechanical properties of different zones of a weldment, necessitating PWHT (post weld heat treatment) to obtain uniform structure and the required service behaviour. Apart from the metallurgical effects of heat flow in welding there are other phenomena involved including distortion, residual stresses, physical changes, and chemical modifications. Thus, to achieve a weldment of desired specifications to perform satisfactorily in service it is essential to know the effects of heat during welding. This can well be achieved by knowing the temperature distribution during welding so as to determine the *cooling rates* in different directions with respect to the weld axis.

2.1. TEMPERATURE DISTRIBUTION IN WELDING

Temperature distribution in welding depends upon the nature of the welding process used, type of the heat source employed, energy input per unit time, configuration of the joint (linear or circular), type of joint (butt, fillet, etc.), physical properties of the metal being welded, and the nature of the surrounding medium *i.e.* ordinary atmospheric conditions or underwater. Although it is beyond the scope of this book to analyse all these aspects of heat flow in detail but brief descriptions of the following cases are included.

(A) Arc Welding

(*i*) Linear butt welds, (*ii*) Circular butt welds,

(*iii*) Fillet welds.

(B) Resistance Welding

(*i*) Upset butt welding, (*ii*) Spot welding.

(C) Electroslag Welding,

(D) Underwater Welding.

2.1.1. Temperature Distribution in Arc Welding

Nearly 90% of welding in world is carried out by one or the other arc welding process, therefore it is imperative to discuss the problem of temperature distribution in arc welding in the maximum possible detail to arrive at the best possible understanding of the problem. Because linear butt welds are perhaps the most used type of welds in welded fabrication therefore this type of joint will be detailed the most.

2.1.1.1. Temperature Distribution in Linear Butt Welds

Heat flow in welding is mainly due to the heat input by welding source in a limited zone, and its subsequent flow into the body of the workpiece by conduction. A limited amount of heat loss is by way of convection and radiation as well but that can be accounted for by allotting heat transfer efficiency factor at the accounting of heat input. So, the problem of temperature distribution can be seen as a case of heat flow by conduction when the heat input is by a moving heat source. This case can be further simplified by assuming workpiece of large dimensions to approach the infinity concept *i.e.* the temperature at the farthest end of the workpiece in all directions remains unchanged. This leads to a condition of *quasi-stationary state* which can be defined as a condition in which an observer at the arc will see a fixed temperature field all around the arc at all times. In other words under a condition of quasi-stationary state of heat flow isotherms representing different temperatures remain at a fixed distance with respect to the heat source. Mathematically stated it means $\frac{\partial T}{\partial t} = 0$, where T is the temperature at any time and t is the time unit. *Fig. 2.1* represents the condition of quasi-stationary state with observation points at A and B for welding along centreline of the plate.

To determine the temperature at any point, in a workpiece, during welding, the problem can be solved by considering from the basic Fourier's Equation of heat flow by conduction.

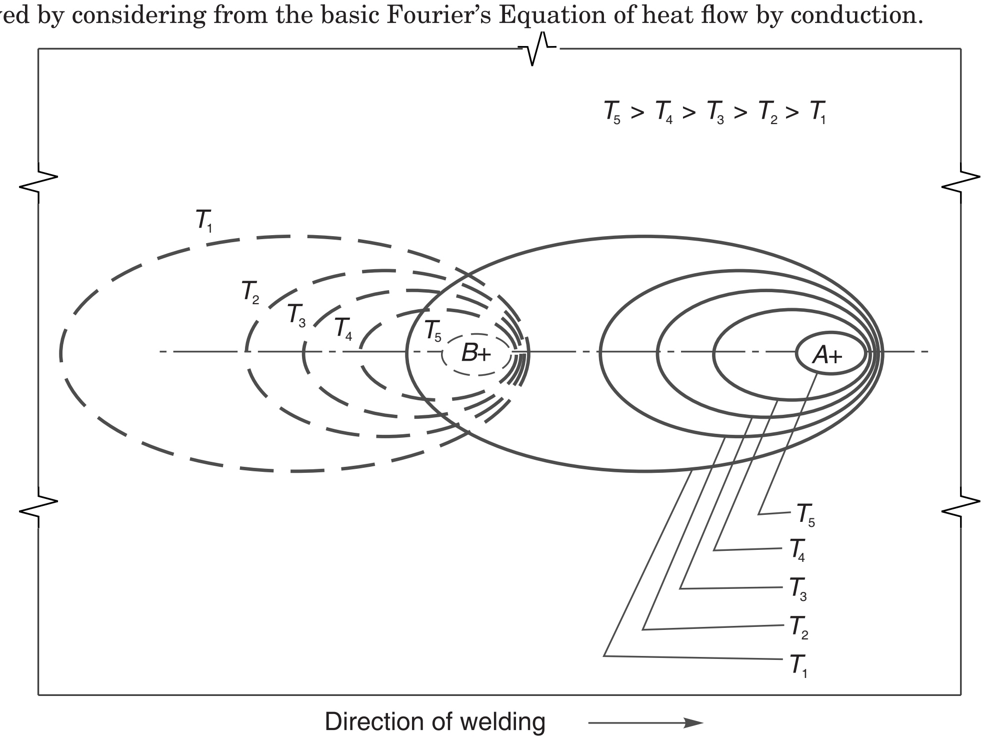

Fig. 2.1. Temperature fields in quasi-stationary state of welding.

If one dimensional form of heat conduction is considered as shown in *Fig. 2.2*, Fourier's Law states that the rate of heat transfer per unit time, q, is a product of,

(*a*) area, A, normal to heat flow path,

(*b*) $\frac{\partial T}{\partial x}$, the temperature gradient at the section *i.e.* the rate of change of temperature with reference to the distance in the direction of heat flow,

(*c*) k, thermal conductivity of the material of the body.

Mathematically stated,

$$q = \frac{dQ}{dt} = -k \cdot A \cdot \frac{\partial T}{\partial x} \qquad \text{...(2.1)}$$

where, dQ = quantity of heat conducted in time, dt.

Note : (i) Since the heat flow always occurs in the direction of decreasing temperature, the temperature gradient $\left(\frac{\partial T}{\partial x}\right)$ will, therefore, always be –ve, hence the negative sign on the right hand side of the equation (2.1).

(ii) The following assumptions have been made in the above equation,

(a) the heat flow in y and z directions is zero,

(b) the temperature in any plane perpendicular to the x-axis is uniform throughout the plane.

The equation (2.1) represents the fundamental heat conduction law for uni-directional flow of heat. As normally the heat will flow in all the three directions in a given body, therefore a comprehensive equation must deal with 3-dimensional heat flow.

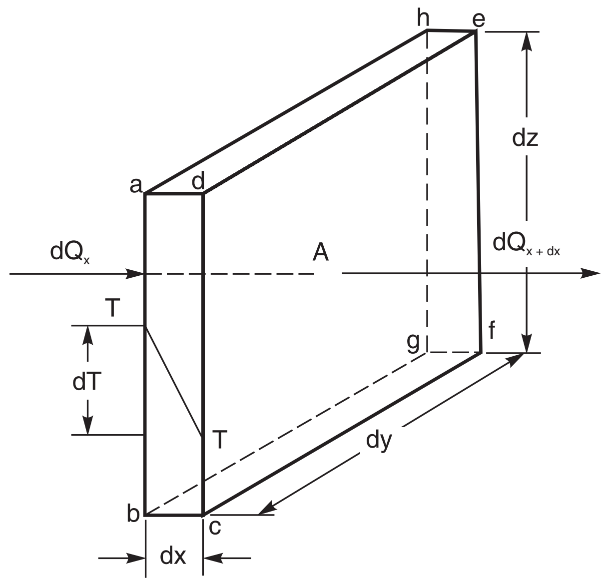

Fig. 2.2. A case of one dimensional heat flow by conduction.

Three Dimensional Heat Flow Equation

Consider an infinitely small solid cubic body as shown in *Fig. 2.3.*

Let the edges parallel to the three axes be respectively dx, dy and dz. The volume of the cubic element is, therefore, given by the relation,

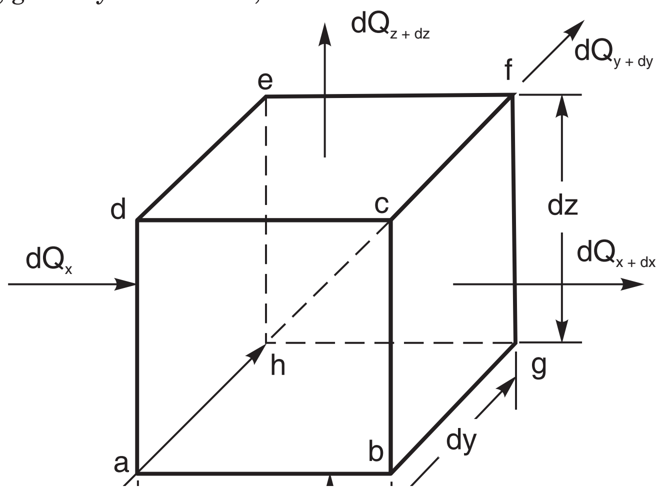

Fig. 2.3. An infinitely small solid cubic body with heat flow by conduction in 3-directions.

$$dv = dx \,.\, dy \,.\, dz \qquad \text{...(2.2)}$$

Let dQ_x represent the total quantity of heat entering the face area $dy \cdot dz$ in time dt as shown in *Fig. 2.3*. So, on the basis of equation (2.1), we have,

$$\frac{dQ_x}{dt} = -k\,(dy \cdot dz)\,\frac{\partial T}{\partial x} \qquad \text{...(2.3)}$$

Note : The gradient in equation (2.3) is expressed as a partial derivative of the temperature T as it is a function of x, y, z and t.

Now, a corresponding quantity of heat will be leaving the cubic element $(dx \cdot dy \cdot dz)$. Let it be dQ_{x+dx}, the value of which may be obtained by Taylor Expansion of dQ_{x+dx}, whereby,

$$dQ_{x+dx} = dQ_x + \frac{\partial}{\partial x}\,(dQ_x) \cdot dx + \ldots\ldots \qquad \text{...(2.4)}$$

Ignoring the higher terms of Taylor expansion in equation (2.4), the net heat gained by the element $(dx \cdot dy \cdot dz)$ due to conduction in x-direction will, thus, be,

$$dQ_x - dQ_{x+dx} = -\frac{\partial}{\partial x}\,(dQ_x) \cdot dx \qquad \text{...(2.5)}$$

By substituting the value of dQ_x from (Eqn. 2.3) in the right hand side of equation (2.5), we get,

$$dQ - dQ_{x+dx} = -\frac{\partial}{\partial x}\left\{-k\,(dy \cdot dz)\frac{\partial T}{\partial x}\right\} dx \cdot dt$$

$$= \frac{\partial}{\partial x}\left(k\,.\,dy\,.\,dz\,.\,\frac{\partial T}{dx}\right) dx \cdot dt$$

$$= \frac{\partial}{\partial x}\left(k\,.\,\frac{\partial T}{dx}\right)(dx \cdot dy \cdot dz) \cdot dt \qquad \text{...(2.6)}$$

From eqns. (2.6) and (2.2), we get,

$$dQ_x - dQ_{x+dx} = \frac{\partial}{\partial x}\left(k\,.\,\frac{\partial T}{dx}\right) dv \cdot dt \qquad \text{...(2.7)}$$

Similarly, the net heat gained by the cubic element by conduction in y and z directions may be obtained as follows,

$$dQ_y - dQ_{y+dy} = \frac{\partial}{\partial y}\left(k\,.\,\frac{\partial T}{dy}\right) dv \cdot dt \qquad \text{...(2.8)}$$

and

$$dQ_z - dQ_{z+dz} = \frac{\partial}{\partial z}\left(k\,.\,\frac{\partial T}{dz}\right) dv \cdot dt \qquad \text{...(2.9)}$$

The total heat gained (dQ) by the cubic element $(dx \cdot dy \cdot dz)$ is the sum of the heat gained by conduction in x, y, and z direction. Thus, from equations (2.7), (2.8) and (2.9), we get,

$$dQ = (dQ_x - dQ_{x+dx}) + (dQ_y - dQ_{y+dy}) + (dQ_z - dQ_{z+dz})$$

$$= dv\left\{\frac{\partial}{\partial x}\left(k\,.\,\frac{\partial T}{\partial x}\right) + \frac{\partial}{\partial y}\left(k\,.\,\frac{\partial T}{\partial y}\right) + \frac{\partial}{\partial z}\left(k\,.\,\frac{\partial T}{\partial z}\right)\right\} . dt \qquad \text{...(2.10)}$$

Now, the heat gained by the cubic element $(dx \cdot dy \cdot dz)$ can also be expressed in terms of increase in internal energy dE, expressed as,

$$dE = m \cdot s \cdot t = (\rho \cdot dv) \cdot c_p \cdot \frac{dT}{dt} \cdot dt \qquad \text{...(2.11)}$$

where, m = mass of the cubic element,
s = specific heat of the material of the element,
t = change in temperature of the material of the element,
ρ = density of material of cubic element,
c_p = specific heat of material at constant pressure.

Now, $dQ = dE$

Therefore, equating equations (2.10) and (2.11), we get,

$$dv\left\{\frac{\partial}{\partial x}\left(k\,\frac{\partial T}{\partial x}\right)+\frac{\partial}{\partial y}\left(k\,\frac{\partial T}{\partial y}\right)+\frac{\partial}{\partial z}\left(k\,\frac{\partial T}{\partial z}\right)\right\}dt = c_p\rho dv\frac{dT}{dt}\,.\,dt \qquad ...(2.12)$$

Assuming k uniform in all directions of the cubic element, equation (2.12) can be written as,

$$k\left[\frac{\partial^2 T}{\partial x^2}+\frac{\partial^2 T}{\partial y^2}+\frac{\partial^2 T}{\partial z^2}\right].\,dt = c_p\,\rho\,\frac{dT}{dt}\,.\,dt$$

i.e.,

$$\frac{\partial^2 T}{\partial x^2}+\frac{\partial^2 T}{\partial y^2}+\frac{\partial^2 T}{\partial z^2} = \frac{c_p\,\rho}{k}\cdot\frac{dT}{dt} \qquad ...(2.13)$$

Now,

$$\frac{k}{c_p\,\rho} = \alpha \qquad ...(2.14)$$

where α is known as the thermal diffusivity of the material of cubic element and its unit is m^2/sec.

From equations (2.13) and (2.14), we get,

$$\frac{\partial^2 T}{\partial x^2}+\frac{\partial^2 T}{\partial y^2}+\frac{\partial^2 T}{\partial z^2} = \frac{1}{\alpha}\,\frac{dT}{dt} \qquad ...(2.15)$$

This is known as Fourier's Equation of three dimensional heat conduction in solids.

To apply equation (2.15) to welding, let us consider the situation in arc welding as expressed in *Fig. 2.4.*

Let O be the origin (*i.e.* the starting point for welding) for the Cartesian coordinates (x, y, z). Suppose, we are interested in finding temperature at any point $A\,(x, y, z)$. Because of moving heat source the distance of point A is changing every moment with respect to the arc or the tip of the electrode. If the origin of coordinate system is shifted from O to the tip of the electrode (which is assumed to lie in the plane of top surface of the plate) then the temperature at any point A located at a fixed distance from the tip of the electrode remains fixed because of the establishment of a quasi-stationary state and can thus be determined mathematically.

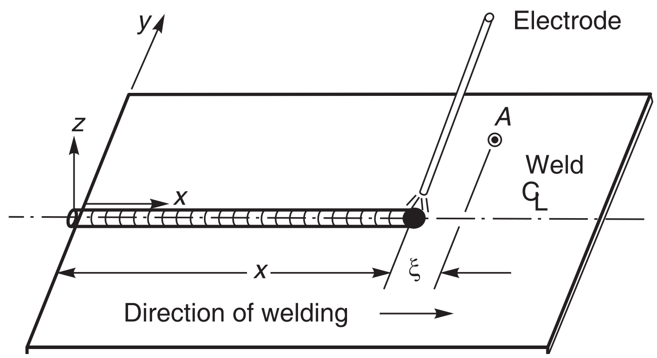

Fig. 2.4. Arc welding on a large plate.

Let point A in the new coordinate system with respect to the tip of the electrode have the co-ordinates (ξ^*, y, z)

$$\therefore \qquad \xi = x - vt \qquad ...(2.16)$$

where, v = the welding speed,

t = time taken by welding, starting from the origin, O.

Now, to determine the temperature distribution in the plate with respect to the tip of the electrode, we are required to change equation (2.15) from Cartesian coordinate system (x, y, z) to a new coordinate system (ξ, y, z).

Differentiating (2.16), we get,

$$\frac{\partial \xi}{\partial x} = 1 \qquad ...(2.17)$$

* ξ is pronounced as *Xi*.

and $$\frac{\partial \xi}{\partial t} = -\, v \qquad ...(2.18)$$

Because temperature T is a function of distance ξ and time t, it can be expressed as,

$$T = f(\xi, t) \qquad ...(2.19)$$

Differentiating T w.r.t. t, we get,

$$\frac{\partial T}{dt} = \frac{\partial T}{dt} \cdot \frac{d\xi}{dt} + \frac{\partial T}{dt} \cdot \frac{dt}{dt}$$

$$= \frac{\partial T}{d\xi}(-v) + \cdot \frac{\partial T}{dt} \cdot 1 \qquad \text{(from 2.18)}$$

$$= -\, v\ \frac{\partial T}{\partial \xi} + \frac{\partial T}{\partial t} \qquad ...(2.20)$$

Also, $$\frac{\partial T}{\partial x} = \frac{\partial T}{\partial \xi} \cdot \frac{\partial \xi}{dx} = \frac{\partial T}{\partial \xi} \cdot 1 \qquad (\because\ \partial\xi = \partial x)$$

$$\frac{\partial T}{\partial x} = \frac{\partial T}{\partial \xi} \qquad ...(2.21)$$

Differentiating (2.21), we get,

$$\frac{\partial^2 T}{\partial x^2} = \frac{\partial}{\partial x}\left(\frac{\partial T}{\partial \xi}\right) = \frac{\partial}{d\xi}\left(\frac{\partial T}{\partial \xi}\right)\frac{d\xi}{dx} = \frac{\partial^2 T}{\partial \xi^2} \cdot 1$$

$\therefore$ $$\frac{\partial^2 T}{\partial x^2} = \frac{\partial^2 T}{\partial \xi^2} \qquad ...(2.22)$$

In the new coordinate system of (ξ, y, z), because there is no change in y and z of Cartesian coordinate system, therefore their derivatives also remain unchanged in equation (2.15).

Substituting the values of $\frac{\partial T}{dt}, \frac{\partial T}{\partial x}$ and $\frac{\partial^2 T}{\partial x^2}$ and from equations (2.20), (2.21) and (2.22) respectively in equation (2.15), we get,

$$\frac{\partial^2 T}{\partial \xi^2} + \frac{\partial^2 T}{\partial y^2} + \frac{\partial^2 T}{\partial z^2} = \left(-v\frac{\partial T}{\partial \xi} + \frac{\partial T}{\partial t}\right)\frac{1}{\alpha} \qquad ...(2.23)$$

For convenience in further derivations,

Let $$\frac{1}{\alpha} = 2\lambda \qquad ...(2.24)$$

From Eqns. (2.23) and (2.24), we get,

$$\frac{\partial^2 T}{\partial \xi^2} + \frac{\partial^2 T}{\partial y^2} + \frac{\partial^2 T}{\partial z^2} = -\,2\ \lambda v\ \frac{\partial T}{\partial \xi} + 2\lambda\frac{\partial T}{\partial t} \qquad ...(2.25)$$

When a quasi-stationary state is established then with respect to the tip of the electrode, the temperature at any given distance undergoes no change with time *i.e.*, $\frac{\partial T}{\partial t} = 0$.

Therefore, equation (2.25) changes to,

$$\frac{\partial^2 T}{d\xi^2} + \frac{\partial^2 T}{dy^2} + \frac{\partial^2 T}{dz^2} = -\,2\ \lambda v\ \frac{\partial T}{\partial \xi} \qquad ...(2.26)$$

Equation (2.26) is thus the differential equation of the quasi-stationary state of welding.

Equation (2.26) is more easily handled if T is replaced by the following expression,

$$T = T_0 + e^{-\lambda v\xi}\,\phi\,(\xi, y, z) \qquad ...(2.27)$$

where, T_0 = initial temperature of the plate,

and $\phi\,(\xi, y, z)$ = a function to be determined.

Thus, the aim is to replace T by ϕ in equation (2.26). Differentiating (2.27) w.r.t. ξ, we get,

$$\frac{\partial T}{\partial \xi} = -\lambda v e^{-\lambda v\xi}\,\phi + e^{-\lambda v\xi}\,\frac{\partial \phi}{\partial \xi} \qquad ...(2.28)$$

Differentiating (2.28), we get,

$$\frac{\partial^2 T}{\partial \xi^2} = \lambda^2 v^2 e^{-\lambda v\xi}\,\phi - \lambda v e^{-\lambda v\xi}\,\frac{\partial \phi}{\partial y} - \lambda v e^{-\lambda v\xi}\,\frac{\partial \phi}{\partial y} + e^{-\lambda v\xi}\,\frac{\partial^2 \phi}{\partial \xi^2}$$

i.e.

$$\frac{\partial^2 T}{\partial \xi^2} = \lambda^2 v^2 e^{-\lambda v\xi}\,\phi - 2\lambda v e^{-\lambda v\xi}\,\frac{\partial \phi}{\partial y} + e^{-\lambda v\xi}\,\frac{\partial^2 \phi}{\partial \xi^2} \qquad ...(2.29)$$

Differentiating eqn. (2.27) w.r.t. y, we get,

$$\frac{\partial T}{\partial y} = e^{-\lambda v\xi}\,\frac{\partial \phi}{\partial y}$$

and

$$\frac{\partial^2 T}{\partial y^2} = e^{-\lambda v\xi}\,\frac{\partial^2 \phi}{\partial y^2} \qquad ...(2.30)$$

Similarly, by double differentiation of eqn. (2.27) w.r.t. z, we get,

$$\frac{\partial^2 T}{\partial z^2} = e^{-\lambda v\xi}\,\frac{\partial^2 \phi}{\partial z^2} \qquad ...(2.31)$$

Putting the values of $\frac{\partial^2 T}{d\xi^2} + \frac{\partial^2 T}{dy^2} + \frac{\partial^2 T}{dz^2}$ and $\frac{\partial T}{\partial \xi}$, from equations (2.29), (2.30), (2.31) and (2.28) respectively in equation (2.26), we get,

$$\left(\lambda^2 v^2 e^{-\lambda v\xi}\phi - 2\lambda v e^{-\lambda v\xi}\,\frac{\partial \phi}{\partial \xi} + e^{-\lambda v\xi}\,\frac{\partial^2 \phi}{\partial \xi^2}\right) + \left(e^{-\lambda v\xi}\,\frac{\partial^2 \phi}{\partial y^2}\right) + \left(e^{-\lambda v\xi}\,\frac{\partial^2 \phi}{\partial z^2}\right)$$

$$= -\,2\lambda v\,\left\{-\lambda v e^{-\lambda v\xi}\,\phi + e^{-\lambda v\xi}\,\frac{\partial \phi}{\partial \xi}\right\}$$

or

$$e^{-\lambda v\xi}\left\{\frac{\partial^2 \phi}{\partial \xi^2} + \frac{\partial^2 \phi}{\partial y^2} + \frac{\partial^2 \phi}{\partial z^2}\right\} + \lambda^2 v^2 e^{-\lambda v\xi}\phi - 2\lambda v e^{-\lambda v\xi}\,\frac{\partial \phi}{\partial \xi}$$

$$= 2\lambda^2 v^2 e^{-\lambda v\xi}\,\phi - 2\lambda v e^{-\lambda v\xi}\,\frac{\partial \phi}{\partial \xi}$$

or

$$\frac{\partial^2 \phi}{\partial \xi^2} + \frac{\partial^2 \phi}{\partial y^2} + \frac{\partial^2 \phi}{\partial z^2} - (\lambda^2 v^2)\phi = 0 \qquad ...(2.32)$$

Equation (2.32) is a more convenient form of heat flow equation for a quasi-stationary state of welding. It can be used for determining temperature distribution in specific cases for example, in a semi-infinite plate which is representative of welding a large thick plate.

2.1.1.2. Temperature Distribution in a Semi-Infinite Plate (3- dimensional case)

Considering a case of laying a single weld bead, using a point heat source, on the surface of a very large and thick plate (workpiece), as shown in *Fig. 2.5.*

Let us assume that the Z-axis is placed in the direction of thickness of the plate downwards. For determining the temperature distribution the solution of equation (2.32) must satisfy the following conditions.

(1) Since welding is done by a point heat source, the heat flux through the surface of the hemisphere drawn around the source must tend to the value of the total heat, Q_p, delivered to the plate, as the radius of the sphere tends to zero. If R is the radius of the sphere, then the total heat flowing through the hemispherical surface of heat source as given by Fourier's Equation will be,

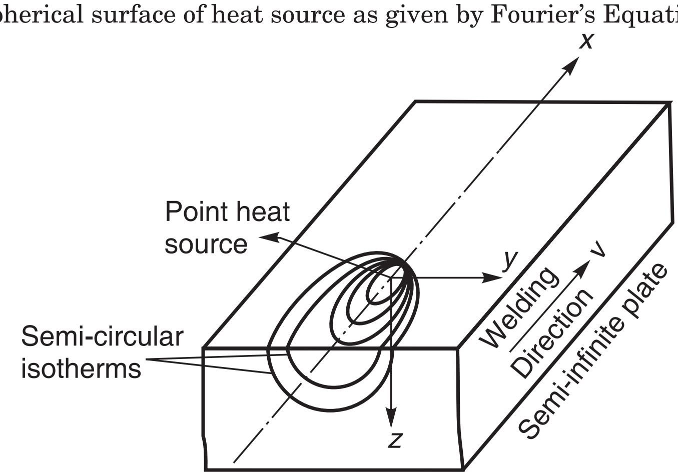

Fig. 2.5. Isotherms in semi-infinite plate with a point heat source on the surface.

$$q = -2\pi R \cdot k \cdot \frac{\partial T}{\partial R} \quad ...(2.33)$$

$$q \to Q_p \text{ as } R \to 0 \quad ...(2.34)$$

where $R = \sqrt{\xi^2 + y^2 + z^2}$ ...(2.35)

(2) Heat losses through the surface of the plate (workpiece) being negligible, there is no heat transmission from the plate to the surroundings

i.e., $$\frac{\partial T}{\partial z} = 0 \text{ for } z = 0 \text{ and } R \neq 0 \quad ...(2.36)$$

(3) The temperature of the plate remains unchanged at a great distance from the heat source

$\therefore$ $$T = T_0 \quad \text{for} \quad R \to \infty \quad ...(2.37)$$

Now, condition (2) *i.e.* equation (2.36) assigns a semi-circular form to the isotherms located at sections parallel to plane *YZ* (Fig. 2.5), thus they are dependent only on radial distance 'l' from the heat source.

Keeping in view the semi-circular form of isotherms, equation (2.32) can be written more conveniently in cylindrical coordinates, ξ, l, ψ* as shown in *Fig. 2.6.*

where, $$l^2 = y^2 + z \quad ...(2.38)$$

From Fig. 2.6, we have,

$$y = l \cos \psi$$

and $$z = l \sin \psi$$

i.e., $$\psi = \tan^{-1}\left(\frac{z}{y}\right) \quad ...(2.39)$$

*ψ is pronounced as psi.

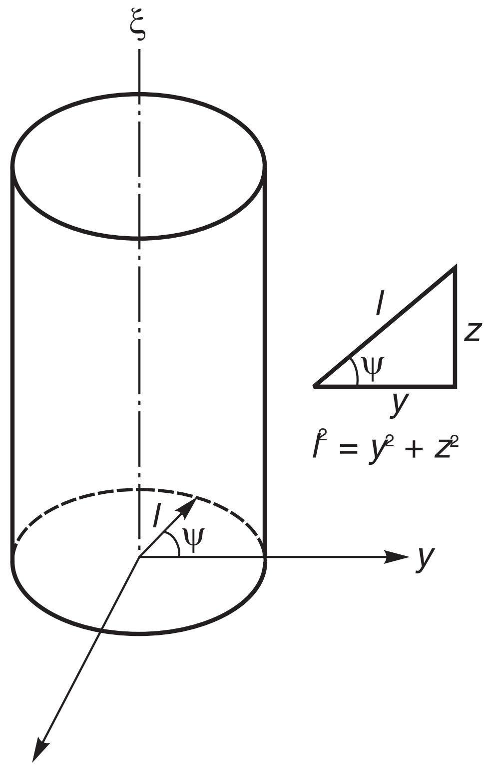

Fig. 2.6. Nomenclature of cylindrical coordinate system employed.

Now, because y is a function of l and ψ

$$\therefore \quad \frac{\partial T}{\partial y} = \frac{\partial T}{\partial l} \cdot \frac{\partial l}{\partial y} + \frac{\partial T}{\partial \psi} \cdot \frac{\partial \psi}{\partial y} \qquad \text{...(2.40)}$$

Now, temperature ϕ is a function of y and z while y and z are functions of l and ψ therefore equation (2.32) can be converted into polar coordinates by determining the double differential of ϕ w.r.t. y and z in terms of l and ψ.

Using equations (2.38), (2.39) and (2.40), we get,

$$\frac{\partial^2 \phi}{\partial y^2} = \cos^2 \psi \frac{\partial^2 \phi}{\partial \psi^2} + \frac{\sin^2 \psi}{l} \cdot \frac{\partial \phi}{\partial l} + \frac{\sin^2 \psi}{l^2} \frac{\partial^2 \phi}{\partial \psi^2} - \frac{\sin 2\psi}{l} \cdot \frac{\partial^2 \phi}{\partial \psi \partial l} + \frac{\sin 2\psi}{l^2} \frac{\partial \phi}{\partial \psi} \qquad \text{...(2.41)}$$

and

$$\frac{\partial^2 \phi}{\partial z^2} = \sin^2 \psi \frac{\partial^2 \phi}{\partial \psi^2} + \frac{\cos^2 \psi}{l} \cdot \frac{\partial \phi}{\partial l} + \frac{\cos^2 \psi}{l^2} \frac{\partial^2 \phi}{\partial \psi^2} + \frac{\sin 2\psi}{l} \cdot \frac{\partial^2 \phi}{\partial \psi \partial l} - \frac{\sin 2\psi}{l^2} \frac{\partial \phi}{\partial \psi} \qquad \text{...(2.42)}$$

Adding eqns. (2.41) and (2.42), we get,

$$\frac{\partial^2 \phi}{\partial y^2} + \frac{\partial^2 \phi}{\partial z^2} = \frac{\partial^2 \phi}{\partial l^2} + \frac{1}{l} \frac{\partial \phi}{\partial l} + \frac{1}{l^2} \frac{\partial^2 \phi}{\partial \psi^2} \qquad \text{...(2.43)}$$

Substituting eqns. (2.43) in (2.32), we get,

$$\frac{\partial^2\phi}{\partial\xi^2}+\frac{\partial^2\phi}{\partial l^2}+\frac{1}{l}\frac{\partial\phi}{\partial l}+\frac{1}{l^2}\frac{\partial^2\phi}{\partial\psi^2}-(\lambda v)^2\phi=0 \quad \text{...(2.44)}$$

But as there is no effect of angle ψ on temperature ϕ,

$$\therefore \qquad \frac{\partial\phi}{\partial\psi}=0$$

Hence equation (2.44) reduces to,

$$\frac{\partial^2\phi}{\partial\xi^2}+\frac{\partial^2\phi}{\partial l^2}+\frac{1}{l}\frac{\partial\phi}{\partial l}-(\lambda v)^2\phi=0 \quad \text{...(2.45)}$$

Equation (2.45) is satisfied by the following function,

$$\phi = c\cdot\frac{e^{-\lambda vR}}{R} \quad \text{...(2.46)}$$

where, $R=\sqrt{\xi^2+l^2}$ ...(2.47)

Putting c = ——, we get {Refer to eqns. (2.33) and (2.34)}

$$T-T_0=\frac{Q_p}{2\pi k}e^{-\lambda v\xi}\frac{e^{-\lambda vR}}{R} \quad \text{...(2.48)}$$

As already stated, for the present case of semi-infinite plate,

$$\frac{\partial T}{\partial z}=0, \text{ for } z=0 \text{ and } R\neq 0 \quad \text{...(eqn. 2.36)}$$

and $T=T_0$ for $R\to\infty$ ...(eqn. 2.37)

Equation (2.48) when converted to Cartesian coordinate system leads to,

$$T=\frac{Q_p}{2\pi kr}e^{-v(r-x)/2\alpha} \quad \text{...(2.49)}$$

where $r=\sqrt{x^2+y^2+z^2}$ ...(2.50)

and $\alpha=\dfrac{k}{\rho c_p}$ ...(eqn. 2.14)

Equations (2.48) and (2.49) are important relationships for determining temperature distribution in a semi-infinite plate.

2.1.1.3. Temperature Distribution in a Large (infinite) Plate of Finite Thickness

Equation (2.48) can help in determining temperature distribution in semi-infinite plate but the normal cases encountered are those of large plates (in ship-building and pressure vessel fabrication, etc.) of finite thickness. Thus, equation (2.48) must be modified to account for the limited range of Z dimension.

Let, the plate thickness = g

Thus, no heat losses must take place at level $z=g$, *i.e.*

$$\frac{\partial\phi}{\partial z}=0 \qquad \text{for} \qquad z=g \quad \text{...(2.51)}$$

Equation (2.48) can be further generalised by putting it into another form

Now, $$\frac{e^{-\lambda vR}}{R}=\int_0^\infty e^{-\lambda vz\sqrt{l^2+1}}J_0(\lambda vrl)\frac{ldl}{\sqrt{l^2+1}} \quad \text{...(2.52)}$$

where $r=\sqrt{\xi^2+y^2}$ ...(2.53)

and J_0 is the so-called *Bessel Function of First kind and zero order*. Thus, equation (2.48) can be written as,

$$T - T_0 = \frac{Q_p}{2\pi k} \cdot e^{-\lambda v \xi} \int_0^{\infty} e^{-\lambda v z\sqrt{l^2+1}} \cdot J_0(\lambda vrl) \cdot \frac{l \cdot dl}{\sqrt{l^2+1}} \quad \text{...(2.54)}$$

To get a solution for finite thickness, g, of plate, let us replace in equation (2.54),

$$e^{-\lambda vz\sqrt{l^2+1}} \text{ by } \frac{\cosh[\lambda v(g-z)\sqrt{l^2+1}]}{\sinh[\lambda ug\sqrt{l^2+1}]} \quad \text{...(2.55)}$$

where cosh and sinh mean hyperbolic cosine and sine respectively.

Then,
$$\frac{\partial T}{\partial z} = -\frac{Q_p}{2\pi k} e^{-\lambda v \xi} (\lambda v)^2 \cdot \int_0^{\infty} M(z) \cdot J_0(\lambda vrl)\, l \cdot dl \quad \text{...(2.56)}$$

where,
$$M(z) = \frac{\cosh[\lambda v\,(g-Z)\sqrt{l^2+1}]}{\sinh[\lambda v \cdot g\sqrt{l^2+1}]} \quad \text{...(2.57)}$$

But, for $z = g$,

$$M(z) = 0, \qquad \text{hence } \frac{\partial T}{\partial z} = 0 \quad \text{...(2.58)}$$

hence,
$$\frac{\partial T}{\partial z} = -\frac{Q_p}{2\pi k} e^{-\lambda v \xi} \cdot (\lambda v)^2 \int_0^{\infty} J_0(\lambda vrl) \cdot l \cdot dl \quad \text{...(2.59)}$$

However,
$$(\lambda v)^2 \int_0^{\infty} J_0(\lambda vrl) \cdot l \cdot dl = \int_0^{\infty} \frac{d}{dx}[J_1(x) \cdot x] = 0 \quad \text{...(2.60)}$$

Therefore, boundary condition of equation (2.51) is satisfied. However, it remains to be proved that conditions of equations (2.33) and (2.35), *viz.*,

$$-2\pi Rk^{\,\partial T} \to Q_p \quad \text{as} \quad R = \sqrt{\xi^2 + y^2 + z^2} \quad \text{...(eqn. 2.33)}$$

and
$$T = T_0 \text{ for } R \to \infty \quad \text{...(eqn. 2.35)}$$

To do so let us write,

$$\frac{\cosh(a-x)}{\sinh x} = \frac{e^{-x} + e^{x} \cdot e^{-2a}}{1 - e^{-2a}} = [e^{-x} + e^{-(2a-x)}]\,[1 + e^{-2a} + e^{-4a} + \ldots]$$

$$= e^{-x} + \sum_{n=1}^{n=\infty} (e^{-(2na-x)} + e^{-(2na+x)}) \quad \text{...(2.61)}$$

Substituting eqn. (2.61) in (2.54), we get,

$$\mathbf{T - T_0} = \frac{Q_p}{2\pi k} e^{-\lambda v \xi} \left[\frac{e^{-\lambda vR}}{R} + \sum_{n=1}^{n=\infty} \left(\frac{e^{-\lambda vR_n}}{R_n} + \frac{e^{-\lambda vR'_n}}{R'_n} \right) \right] \quad \text{...(2.62)}$$

where $R_n \sqrt{(2ng-z)^2 + \xi^2 + y^2}$

and $R'_n = \sqrt{(2ng+z)^2 + \xi^2 + y^2}$

Equation (2.62) satisfies equations (2.33) and (2.35).

To sum up it can be said that the following two equations can be used for determining temperature distribution during butt welding of large (semi-infinite) plates of infinite thickness and finite thickness respectively.

$$T - T_0 = \frac{Q_p}{2\pi k} \cdot e^{-\lambda v \xi} \cdot \frac{e^{-\lambda v R}}{R} \quad \text{...(eqn. 2.48)}$$

$$T - T_0 = \frac{Q_p}{2\pi k} \cdot e^{-\lambda v \xi} \left[\frac{e^{-\lambda v R}}{R} + \sum_{n=1}^{n=\infty} \left(\frac{e^{-\lambda v R_n}}{R_n} + \frac{e^{-\lambda v R'_n}}{R'_n} \right) \right] \quad \text{...(eqn. 2.62)}$$

The efficacies of these equations can be checked up by solving actual problems.

Problem 2.1. *Calculate the temperature of a point (– 50, 15, 0) mm with respect to the arc as origin for laying a single weld bead on a wide steel plate by GTAW process using 200 A and 18 V at a welding speed of 125 mm/min. Assume thermal conductivity of steel (K) = 55 KCal/m.hr.°c and diffusivity (α) = 0.0625 m^2/hr. Consider the following two cases,*

(*i*) *the plate of an infinite thickness (semi-infinite plate),*

(*ii*) *the plate of 5 mm thickness.*

Solution. (*a*) *For Semi-infinite plate of infinite thickness*

$$T - T_0 = \frac{Q_p}{2\pi k} \cdot e^{-\lambda v \xi} \cdot \frac{e^{-\lambda v R}}{R} \quad \text{...}(i) \text{ [from (2.48)]}$$

Now, $\xi = -50$ mm, $y = 15$ mm, $z = 0$ mm

$$\therefore \quad R = \sqrt{\xi^2 + y^2 + z^2} = \sqrt{(-50)^2 + (15)^2 + (0)^2}$$

$$= 52.2015 \text{ mm} = 0.0522015 \text{ m} \quad \text{...}(ii)$$

$$k = 55 \text{ kCal/m.hr.°C}$$

$$= \frac{55 \times 4.2 \times 1000}{60 \times 60} = 64.167 \text{ J/m.sec.°C} \quad \text{...}(iii)$$

$Q_p = \eta VI$ where $V = 18$ volt, $I = 200$ A

and heat transfer efficiency, η, for GTAW = 0.65

$$\therefore \quad Q_p = 0.65 \times 18 \times 200 = 2340 \text{ J/sec} \quad \text{...}(iv)$$

$$v = 125 \text{ mm/min} = \frac{125}{1000 \times 60} = 0.002083 \text{ m/sec} \quad \text{...}(v)$$

$$\frac{Q_p}{2\pi k} = \frac{2340}{2 \times \pi \times 64.167} \quad \text{[from } (iv) \text{ and } (iii)\text{]}$$

$$= 5.80 \quad \text{...}(vi)$$

$$\lambda = \frac{1}{2\alpha} = \frac{1}{2 \times \frac{0.0625}{60 \times 60}} = \frac{60 \times 60}{2 \times 0.0625} = 28800 \quad \text{...}(vii)$$

$$-\lambda v \xi = 28800 \times 0.002083 \times \frac{50}{1000} = 2.99952 \quad \text{[from } (vii) \text{ and } (v)\text{]}$$

$$\therefore \quad e^{-\lambda v \xi} = (e)^{2.99952} = 20.076 \quad \text{...}(viii)$$

$$\frac{e^{-\lambda v R}}{R} = \frac{e^{-2.88 \times 10^4 \times 2.083 \times 10^3 \times 0.522015}}{0.0522015} = \frac{(e)^{-3.1315}}{0.0522015} = 0.836 \quad \text{...}(ix)$$

Putting the values of (*vi*), (*viii*), and (*ix*) in (*i*), we get,

$$T - T_0 = \frac{Q_p}{2\pi k} \cdot e^{-\lambda v \xi} \cdot \frac{e^{-\lambda v R}}{R}$$

$$= 5.80 \times 20.076 \times 0.836 = 97.37 \text{°C}$$

Let $T_0 = 20°C$

$\therefore$ $T = 97.37 + 20 = 117.37°C$ **Ans. 117.37°C**

(*b*) *For Semi-infinite plate of 5 mm thickness*

Temperature distribution in a semi-infinite plate of finite thickness is given by (eqn. 2.62), reproduced as follows.

$$T - T_0 = \frac{Q_p}{2\pi k} \cdot e^{-\lambda v \xi}\left[\frac{e^{-\lambda v R}}{R} + \sum_{n=1}^{n=\infty}\left(\frac{e^{-\lambda v R_n}}{R_n} + \frac{e^{-\lambda v R'_n}}{R'_n}\right)\right] \quad ...(i)$$

All other terms in (*i*) are calculated, in part (*a*) above, except the last two terms. For determining those, let

$n = 1$

$$\therefore R_n = \sqrt{(2ng - z)^2 + \xi^2 + y^2} = \sqrt{(2 \times 1 \times 5 - 0)^2 + (-50)^2 + (15)^2}$$

$$= \sqrt{100 + 2500 + 225} = \sqrt{2825} = 53.15 \text{ mm} \quad ...(ii)$$

Similarly, $$R'_n = \sqrt{(2ng + z)^2 + \xi^2 + y^2} = R_n = 53.15 \text{ mm} \quad ...(iii)$$

$$\therefore \quad \frac{e^{-\lambda v R_n}}{R_n} = \frac{e^{-\lambda v R'_n}}{R'_n}$$

$$\lambda v = 2.8 \times 10^4 \times 2.083 \times 10^{-3} = 58.324 \quad ...(iv)$$

$$\lambda v R_n = \frac{58.324 \times 53.15}{1000} = \frac{3100}{1000} = 3.1 \quad ...(v)$$

$$\frac{e^{-\lambda v R_n}}{R_n} = \frac{e^{-(3.1)}}{\frac{53.15}{1000}} = 0.847586122 \quad ...(vi)$$

$$\therefore \quad \frac{e^{-\lambda v R_n}}{R_n} + \frac{e^{-\lambda v R'_n}}{R'_n} = 2\frac{e^{-\lambda v R_n}}{R_n} = 2 \times 0.847586122 = 1.695 \quad ...(vii)$$

Similarly,

for $n = 2$, $$\frac{e^{-\lambda v R_n}}{R_n} + \frac{e^{-\lambda v R'_n}}{R'_n} = 1.37325 \quad ...(viii)$$

$n = 3$ $$\frac{e^{-\lambda v R_n}}{R_n} + \frac{e^{-\lambda v R'_n}}{R'_n} = 0.993 \quad ...(ix)$$

$n = 4$, $$\frac{e^{-\lambda v R_n}}{R_n} + \frac{e^{-\lambda v R'_n}}{R'_n} = 0.6565 \quad ...(x)$$

$n = 5$, $$\frac{e^{-\lambda v R_n}}{R_n} + \frac{e^{-\lambda v R'_n}}{R'_n} = 0.408 \quad ...(xi)$$

$n = 6$, $$\frac{e^{-\lambda v R_n}}{R_n} + \frac{e^{-\lambda v R'_n}}{R'_n} = 0.2432 \quad ...(xii)$$

$n = 7$, $$\frac{e^{-\lambda v R_n}}{R_n} + \frac{e^{-\lambda v R'_n}}{R'_n} = 0.1406 \quad ...(xiii)$$

$n = 8$, $$\frac{e^{-\lambda v R_n}}{R_n} + \frac{e^{-\lambda v R'_n}}{R'_n} = 0.0798 \quad ...(xiv)$$

$n = 9,$ $$\frac{e^{-\lambda v R_n}}{R_n} + \frac{e^{-\lambda v R'_n}}{R'_n} = 0.0449 \quad \ldots(xv)$$

$n = 10,$ $$\frac{e^{-\lambda v R_n}}{R_n} + \frac{e^{-\lambda v R'_n}}{R'_n} = 0.0246 \quad \ldots(xvi)$$

Putting the values of $\frac{e^{-\lambda v R_n}}{R_n} + \frac{e^{-\lambda v R'_n}}{R'_n}$ for $n = 1$ to 10, and other terms in equation (*i*), we get,

$$T - T_0 = \frac{Q_p}{2\pi k} \cdot e^{-\lambda v \xi} \left[\frac{e^{-\lambda v R}}{R} + \sum_{n=1}^{n=10} \left(\frac{e^{-\lambda v R_n}}{R_n} + \frac{e^{-\lambda v R'_n}}{R'_n} \right) \right]$$

$$= 5.80 \times 20.076\ [0.836 + (1.695 + 1.3735 + 0.993 + 0.6565 + 0.408 + 0.2432 + 0.1406 + 0.0798 + 0.0449 + 0.0246)]$$

$$= 5.80 \times 20.076\ [0.836 + (5.6591)] = 5.80 \times 20.076 \times 6.4951 = 756.3°C$$

Let $T_0 = 20°C$

$\therefore$ $T = 756.3 + 20 = 776.3°C$ **Ans.** $\boldsymbol{T_{(-50,\,15,\,0)} = 776.3°C}$.

2.2. EFFICIENCY OF HEAT SOURCES

It is evident from the solution of Problem 2.1 that to solve the temperature distribution problems we require to know the efficiency (η) of the heat source used for welding ; where η is defined as,

$$\eta = \frac{\text{Energy transferred to the workpiece}}{\text{Energy generated by the heat source}} \quad \ldots(2.63)$$

Energy generated by the heat source

Thus, if the efficiency (η) of the heat source is known, the energy (Q) transferred from it to the workpiece, can be determined. In arc, electroslag, and electron beam welding,

$$Q = \eta V I \quad \ldots(2.64)$$

where V and I are the arc voltage and welding current respectively.

In gas tungsten arc welding (GTAW) with DCEN (direct current, electrode negative) the majority of the heat is produced by electrons bombarding the workpiece (anode) that is as a result of the release of the work function* and the conversion of their kinetic energy into heat at the workpiece. In GTAW with a.c., however, electrons bombard the workpiece only during straight polarity half cycle *i.e.* for a period when electrode is negative thus resulting in significantly lower arc efficiency. Also, the heat loss to the surrounding can be rather high; particularly so for long arc lengths. A part of the heat generated is taken away by the cooling water employed to keep the electrode cool.

In consumable electrode welding processes like SMAW, SAW, GMAW and FCAW, using dcep or a.c. the heat going to both the electrode and the workpiece finally lands up on the workpiece through transfer of molten metal. Thus, the heat transfer efficiencies of these processes are high. In SAW process, the heat transfer η is further increased because the arc remains under a blanket of flux, the heat loss to the surroundings is, thus, minimised.

The efficiency of heat transfer in ESW is lower than that in SAW, mainly owing to heat loss to the water-cooled copper shoes and, to lesser extent, by radiation and convection from the surface of the molten slag.

**Work Function* of a material is defined as the energy required, in electron volts (eV) or joules, to get one electron released from the surface of the material to the surrounding space.

In EBW (electron beam welding) process the welds are produced by the phenomenon of *keyholing*. These keyholes act like black bodies to the heat source and trap most of its energy; leading to very high efficiency of heat transfer in EBW process.

In laser welding the heat transfer efficiency can be strongly affected by the wavelength and energy density of the laser beam, the workpiece material and its surface condition, and the joint design. For example, with well polished Al or Cu, the surface reflectivity can be around 99%, *i.e.* the efficiency can be only about 1% for a 10.6 μm* continuous wave CO_2 laser. For steels, especially when coated with thin layers of materials that enhance absorption of the beam energy (for example, graphite and zinc phosphate), quite reasonable efficiencies can be obtained. When keyholes are established during laser welding, the efficiency of the process can rather be impressive.

In Oxy-acetylence welding the energy transferred is given by,

$$Q \text{ (watts)} = \eta \times \frac{48 \text{ kJ}}{\text{litre } C_2H_2} \times V_{C_2H_2} \times \frac{h}{3600s} = 13.3\, \eta\, V_{C_2H_2} \quad ...(2.65)$$

where $V_{C_2H_2}$ = volumetric flow rate of C_2H_2, lit/hr,

48 kJ = the heat of combustion of C_2H_2.

Both these values refer to standard state of 1 atm and 25°C temperature.

The heat source efficiency in Oxy-acetylene gas welding varies over a rather wide range as the efficiency decreases significantly with increasing fuel consumption rate VC_2H_2, because of incomplete combustion. Efficiency of oxy-acetylene gas welding is also found to depend on the torch nozzle diameter, welding speed, material thickness, and thermal conductivity of the workpiece. In Table 2.1 are listed the efficiencies of most of arc, beam and flame welding processes.

Table 2.1. Heat Source Efficiencies of Arc, Beam and Flame Welding Processes (After Sindo Kou)

S.No.	*Welding Processes*	*Efficiency, η (%)*
1.	Gas tungsten arc welding (GTAW)	
	(*a*) DCEN	50—80
	(*b*) A.C.	20—50
2.	Shielded metal arc welding (SMAW)	65—85
3.	Gas metal arc welding (GMAW)	65—85
4.	Submerged arc welding (SAW)	80—99
5.	Electroslag welding (ESW)	55—82
6.	Electron Beam Welding (EBW)	80—95
7.	Laser Beam Welding (LBW)	0.5—70
8.	Oxy-acetylene gas welding (OAW)	25—80

Thermal properties required for solving the temperature distribution problems are listed in Table 2.2 for some of the commonly welded materials.

**1 μm (one micron) = 0.001 mm.

Table 2.2. Thermal Properties of Some Commonly Welded Materials

S. No.	*Material*	*Thermal diffusivity* (α) (m^2/sec)	*Volume thermal capacity* (ρc_p) $J/m^3 . °C$	*Thermal conductivity (k)* ($J/m. sec. °C$)	*Melting point (°C)*
1.	Aluminium	$(8.5–10) \times 10^{-5}$	2.7×10^6	229	660
2.	Carbon steel	9.1×10^{-6}	4.5×10^6	41.0	1527
3.	9% Ni-steel	1.1×10^{-5}	3.2×10^6	35.2	1400
4.	Austenitic steel	5.3×10^{-6}	4.7×10^6	24.9	1500
5.	Inconel 600*	4.7×10^{-6}	3.9×10^6	18.3	1400
6.	Ti-alloy	9.0×10^{-6}	3.0×10^6	27.0	1650
7.	Copper	9.6×10^{-5}	4.0×10^6	384.0	1063
8.	Monel 400**	8.0×10^{-6}	4.4×10^6	35.2	1300

* Inconel 600 contains 76% Ni, 15.5% Cr, 8% Fe and 0.5% Mn.
** Monel 400 contains 66.5% Ni, 31.5% Cu, 1% Mn and 1% Fe.

2.3. FURTHER MODIFICATIONS OF TEMPERATURE DISTRIBUTION EQUATIONS

Different researchers have tried to modify Rosenthal's equations to determine more accurately the temperature distribution under different sets of welding conditions. The ones put forward by Adams, and Wells have received wide recognition and are included in the following sub-sections.

2.3.1. Adams Modification

In the earlier treatment of problem based on Rosenthal's solution the heat source has been assumed to be a point heat source which is obviously not true, particularly for small sized workpieces. Thus, recognising the existence of finite sized weld pools, Adams used the fusion line as the boundary condition and modified Rosenthal's equations *viz.*, equations (2.48) and (2.62). The following equations were derived by Adams for the peak temperature, T_p, at a distance y from the fusion boundary at the workpiece surface.

For 2-dimensional Heat Flow

$$\frac{1}{T_P - T_0} = \frac{4.13\, vyg\rho c}{Q_p} + \frac{1}{T_m - T_0} \qquad ...(2.66)$$

For 3-dimensional Heat Flow

$$\frac{1}{T_P - T_0} = \frac{5.44\, \pi k\alpha}{Q_p\, .\, v}\left[2 + \left(\frac{vy}{2\alpha}\right)^2\right] + \frac{1}{T_m - T_0} \qquad ...(2.67)$$

where T_m = melting point of workpiece material,
T_0 = ambient temperature. Other symbols have the usual meanings.

2.3.2. Wells Modification

The relationship between the heat flow and weld bead dimensions is given by the Wells simplification of Rosenthal's Equation by the following relationship.

$$Q_p = 8kT_m\left(\frac{1}{5} + \frac{v.d}{4\alpha}\right) \qquad ...(2.68)$$

where, Q_p = heat input, cals/sec. cm of work thickness,
d = bead width, T_m = melting point of work material,
v = welding speed, d = weld pool width,
α = thermal diffusivity.

From this equation it has been derived that time t for the material to cool between two temperatures T_1 and T_2 $(T_1 > T_2)$ on the centreline of the weld for the two dimensional case of complete penetration in a single pass and the 3-dimensional case of a bead on plate are as follows:

$$t_{(2-d\ case)} = \frac{d}{v} \cdot \frac{5\left(\frac{vd}{4\alpha}\right)+2}{4}\left[\left(\frac{T_m}{T_2}\right)^2 - \left(\frac{T_m}{T_1}\right)^2\right] \quad ...(2.69)$$

$$t_{(3-d\ \text{case})} = \frac{d}{v} \cdot \frac{5\left(\frac{vd}{4\alpha}\right)+2}{8}\left[\left(\frac{T_m}{T_2}\right) - \left(\frac{T_m}{T_1}\right)\right] \quad ....(2.70)$$

The main difficulty in the use of heat flow equations is the variation of physical constants (like k, ρ, C, etc.) with temperature. Energy absorption within the weld pool by latent heat and its subsequent release at the tail end of the weld pool on solidification is one reason why actual isotherms around a moving weld pool are more elongated than indicated by calculations. Wells equations (2.68) to (2.70) give good correlation with experimental data for low carbon steel and can be adjusted to apply more accurately to metals having high latent heats by using a specific heat value corrected by the following relationship.

$$C_{(\text{corrected})} = C\left(1 + \frac{L}{CT_m}\right) \text{Cal/h} - °\text{C} \quad ...(2.71)$$

where L = Latent heat of fusion,
C = the relevant constants.

Problem 2.2. *Determine the average cooling rate for cooling from 800°C to 500°C along the weld axis of a 1 cm thick steel plate for a bead-on-plate weld made by GTAW process at a welding speed of 12 cm/min. using welding current of 175 A at 20 volts. Take the melting point of steel at 1527°C, k = 41 W/m.°C, $\alpha = 9.1 \times 10^{-6}$ m²/sec and efficiency of GTAW process equal to 0.7.*

Solution.

Procedure (*i*) Using equation (2.68), find d, (*ii*) Using equation (2.70), find t,

(*iii*) $\frac{\partial T}{\partial t} = \frac{T_1 - T_2}{t}$

Using Wells equation (2.68), we get,

$$Q = 8kT_m\left(\frac{1}{5} + \frac{vd}{4\alpha}\right)$$

Now, $Q = \eta VI = 0.7 \times 20 \times 175 = 2450$ watts

(for 1 cm thickness of plate)

$$\therefore \quad Q_{(\text{metre thickness})} = 2450 \times 100 \text{ watts} \quad ...(i)$$

Now in (2.65), we need to find $\frac{vd}{4\alpha}$

$$v = \frac{120}{60} \text{ mm/sec} = \frac{120}{60 \times 1000} \text{ m/sec} = \frac{1}{500} \text{ m/sec}$$

$$\therefore \quad \frac{vd}{4\alpha} = \frac{\frac{1}{500} \cdot d}{4 \times 9.1 \times 10^{-6}} = 54.945d \quad ...(ii)$$

Putting values of different parameters in (2.65), we get,

$$2450 \times 100 = 8 \times 41 \times 1527\left(\frac{1}{5} + 54.945\, d\right)$$

$$\therefore \qquad d = \frac{\left(\dfrac{2450 \times 100}{8 \times 41 \times 1527} - \dfrac{1}{5}\right)}{1153.85} = \frac{(0.489 - 0.2)}{54.945} = 0.00526 \text{ m} = 5.26 \text{ mm}$$

(*ii*) Using equation (2.70), we have,

$$t = \frac{d}{v} \cdot \frac{5\left(\dfrac{vd}{4a}\right) + 2}{8} \left[\frac{T_m}{T_2} - \frac{T_m}{T_1}\right]$$

Putting the values of different parameters in equation (2.70), we have,

$$t = \frac{0.00526}{\dfrac{1}{500}} \left[\frac{5\left(\dfrac{\dfrac{1}{500} \times 0.00526}{4 \times 9.1 \times 10^{-6}}\right) + 2}{8}\right] \left[\frac{1527}{500} - \frac{1527}{800}\right]$$

$$= 500 \times 0.00526 \left[\frac{5\,(0.289) + 2}{8}\right] [3.054 - 1.90875]$$

$$= 2.63 \times 0.431 \times 1.145 = 1.297 \text{ secs.}$$

$\therefore$ Cooling rate from 800°C to 500°C is,

$$\frac{\partial T}{\partial t} = \frac{800 - 500}{1.297} = \frac{300}{1.297} = 231.3\text{°C/sec}$$ **[Ans. 231.3°C]**

Problem 2.3. *Determine the cooling rate at 550°C along weld axis for welding a wide thick steel plate using GTAW process at a welding speed of 12.5 cm/min with a welding current of 200 A at 18 volts. Compare the results if the plate has a preheat temperature of 250°C. Take heat conversion efficiency = 0.65, k = 35 W/m°C and the room temperature as 20°C.*

Solution. For semi-infinite plates, the temperature distribution is given by equation (2.49), *i.e.*,

$$T - T_0 = \frac{Q_p}{2\pi \,.\, k \,.\, r} e^{-v(r-x)/2\alpha} \qquad \text{...}(i)$$

Along the weld axis, $y = z = 0$

$$\therefore \qquad r = \sqrt{x^2 + y^2 + z^2} = x \qquad \text{...}(ii)$$

From (*i*) and (*ii*), we get,

$$T - T_0 = \frac{Q_p}{2\pi k \,.\, x} \qquad \text{...}(iii)$$

Now, $Q_p = \eta VI = 0.65 \times 18 \times 200 = 2340$ watts

$k = 35$ W/m.°C

$$v = 125 \text{ mm/min} = \frac{125}{1000 \times 60} = \frac{1}{480} \text{ m/sec.}$$

By differentiating equation (*iii*) w.r.t. x, we get,

$$\left.\frac{\partial T}{\partial x}\right|_t = \frac{Q_p}{2\pi k} \cdot \frac{-1}{x^2} \qquad \text{...}(iv)$$

From (*iii*) and (*iv*), we get

$$\left.\frac{\partial T}{\partial x}\right|_t = -\frac{Q_p}{2\pi k} \cdot \frac{4(T - T_0)^2\, \pi^2 k^2}{Q_p^2} = -\frac{2\pi k\,(T - T_0)^2}{Q_p} \qquad \text{...}(v)$$

Also $$\left.\frac{\partial T}{\partial x}\right|_t = v \qquad \text{...}(vi)$$

Now, cooling rate $$\left.\frac{\partial T}{\partial x}\right|_t = \left.\frac{\partial T}{\partial x}\right|_t \cdot \left.\frac{\partial x}{\partial t}\right|_T = \frac{-2\pi k\,(T-T_0)^2}{Q_p}\,.\,\nu \qquad \text{[from } (v) \text{ and } (vi)] \text{ ...}(vii)$$

(*a*) *With no preheat*

$$\left.\frac{\partial T}{\partial t}\right|_x = -\,2\pi \times 35\ \frac{W}{m\,.\,°\text{C}} \times \frac{(500-20)^2\ (°\text{C})^2}{(2340)\,W} \times \frac{1}{480}\ \frac{\text{m}}{\text{sec.}}$$

$$= -2\,.\,\pi\,.\,35\,\frac{(530)^2}{(2340)} \times \frac{1}{480}\,°\text{C/sec}$$

$$= -\ 55\ °\text{C/sec}$$

negative sign indicates that temperature decreases in the direction of heat flow.

(*b*) *With 250°C preheat*

$$\left.\frac{\partial T}{\partial t}\right|_x = -2\,.\,\pi\,.\,35 \times \frac{(550-250)^2}{(2340)} \times \frac{1}{480}\,°\text{C/sec}$$

$$= -\ 17.62°\text{C/sec.}$$

Thus it can be seen that the cooling rate is significantly reduced by the use of preheating. Preheating is particularly important for single run welds because in multi-run welds the interpass temperature is equivalent to the preheat temperature in single pass welding.

2.3.2.1. Weld Characteristic

With the processes in which heat is used, the pattern of energy conversion to heat and its subsequent dissipation after welding is a major factor influencing the utilization of the process and the properties of the joint. The efficiency of energy conversion, as already discussed, varies considerably from one process to another. However, the efficiency with which the input energy is converted is not of prime importance; greater importance is attached to efficiency of heat transfer, energy level and energy intensity. These factors influence,

(*i*) the welding speed, and

(*ii*) the size of the heat affected zone.

The former has economic implications and the latter may affect the joint properties.

Not all the heat reaching the work is available for melting the workpiece. Some heat must be utilized for building up the temperature gradient. With high heat input conditions, allowing high welding speeds, heat dissipated in the workpiece is minimised but can never be reduced below half the total heat available. Inefficient processes or processes used at relatively low speeds result in losses three to four times greater than this. A measure of the efficiency of utilisation of heat is given for the 2-dimensional heat flow case by *Weld Characteristic* devised by Wells. For fusion welds this is a non-dimensional term $\frac{Vd}{4\alpha}$ encountered in equations (2.68) to (2.70). Thus,

$$\text{Weld characteristic (W.C.)} = \frac{Vd}{4\alpha} \qquad \text{...}(2.72)$$

where, V = weld speed, mm/sec,

d = melted width, mm,

α = thermal diffusivity, mm²/sec.

The corresponding weld characteristic for resistance spot welds is,

$$\text{W.C.} = \frac{d^2}{4\alpha t} \qquad \text{...(2.73)}$$

where, d = spot diameter, mm,
α = thermal diffusivity, mm^2/sec,
t = time, sec.

Welds in which there is a high heat input rate and the heat is therefore used efficiently $\frac{Vd}{4\alpha}$ will exceed 1. A low heat input rate, allowing wasteful spread of heat, will be indicated by a weld characteristic of less than 0.1. For the majority of situations the weld characteristic lies between 0.25 and 1. Heat input is frequently expressed in terms of Joules/mm of weld length for a moving heat source and Joules/second for a stationary heat source.

2.3.2.2. Weld Bead Dimensions

Based on Rosenthal's equation for 3-dimensional heat flow Christensen et. al. have derived theoretical relationships between the weld dimensions and the welding conditions using dimensionless parameters D and n which are related to each other as shown in *Fig. 2.7*, and can be expressed by the following relationships.

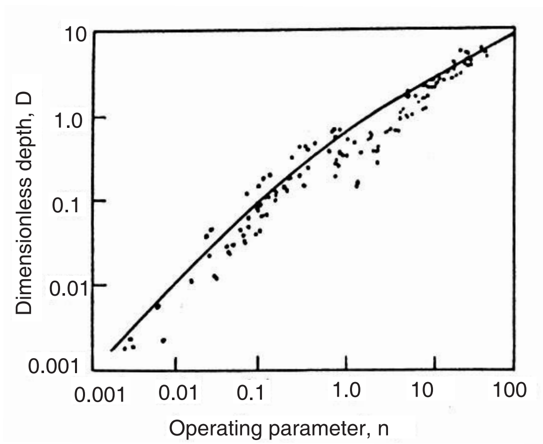

Fig. 2.7. Relationship between dimensionless operating parameter *n* and the dimensionless weld depth *D*.

Dimensionless depth, $$D = \frac{p \cdot v}{2\alpha} \qquad \text{...(2.74)}$$

and Dimensionless operating parameter,

$$n = \frac{Q_p \cdot v}{4\pi\alpha^2 \rho c\,(T_m - T_0)} \qquad \text{...(2.75)}$$

where p = weld penetration,
T_m = melting point of work material.

Since, by Rosenthal's equation weld bead is symmetrical with respect to the x-axis therefore the width of the weld bead, $d = 2p$ and thus the cross-sectional area of the weld bead can be determined. Also, equations (2.74) and (2.75) can be equally effectively used to determine HAZ width by substituting T_m with T_s *i.e.* the solidus temperature of the work material as is done in the following problem.

Problem 2.4. D*etermine the width of HAZ for welding thick plates of 9% Ni steel using GTAW process at a welding speed of 125 mm/min using welding current of 200 A at 20 volt. The melting point of steel is 1400°C and solidus temperature 1325°C.*

Solution.

(*a*) *For Weld Bead*. Using equation (2.75), determine the dimensional parameter, n,

$$n = \frac{Q \cdot v}{4\pi\alpha^2 \rho c\,(T_m - T_0)} \quad \text{...(eqn 2.75)}$$

Now, $$Q = \eta VI = 0.7 \times 20 \times 200 = 2800 \text{ watts} \quad \text{...}(i)$$

(assuming heat transfer efficiency = 0.7)

$$v = 125 \text{ mm/min} = \frac{125}{60 \times 1000} \text{ m/sec} = \frac{1}{480} \text{ m/sec} \quad \text{...}(ii)$$

Putting values of different parameters in equation (2.75), we get,

$$n = \frac{2800 \times \frac{1}{480}}{4 \times \pi \times (1.1 \times 10^{-5})^2 \times 3.2 \times 10^6 (1400 - 20)}$$

$$= \frac{2800}{480 \times 4 \times 4 \times 1.21 \times 10^{-10} \times 3.2 \times 10^6 \times 1380} = 0.868$$

Putting the values of $n = 0.868$ in Fig. 2.7, we get dimensionless depth $D = 0.8$.

Now from equation (2.74), we have,

$$D = \frac{p \cdot v}{2\alpha} \quad \text{...(2.74)}$$

$\therefore$ Weld bead penetration, $$p = \frac{D \cdot 2\alpha}{v} \quad \text{...}(iii)$$

Putting the values of D, α and v in the above equation (*iii*), we get,

$$p = \frac{0.8 \times 2(1.1 \times 10^{-5})}{\frac{1}{480}} = 480 \times 0.8 \times 2\,(1.1 \times 10^{-5})$$

$$= 0.008448 \text{ m} = 8.448 \text{ mm} \quad \text{...}(iv)$$

(*b*) *For HAZ* $T_s = 1325°\text{C}$

Dimensionless operating factor, $$n = \frac{Q \cdot v}{4\pi \cdot \alpha^2\, \rho c(T_s - T_0)} \quad \text{...}(v)$$

Putting the values of different parameters in (*v*), we get,

$$n = \frac{2800 \times \frac{1}{480}}{4\pi(1.1 \times 10^{-5})^2 \times 3.2 \times 10^6 \times (1325 - 20)}$$

$$= \frac{2800}{480 \times 4\pi \times 1.21 \times 10^{-10} \times 3.2 \times 10^6 \times 1305} = 0.918$$

Putting the value of n in *Fig. 2.7*, we get the value of dimensionless depth, $D = 0.9$.

Now, to determine the penetration of HAZ, use can be made of equation (2.74), *i.e.,*

$$D = \frac{p \cdot v}{2\alpha} \quad \text{...(2.74)}$$

or $$p = \frac{D \cdot 2\alpha}{v} \quad \text{...}(vi)$$

Putting the values of different parameters in (*vi*), we get, HAZ penetration, $p = \dfrac{0.9 \times 2(1.1 \times 10^{-5})}{\dfrac{1}{480}}$

$= 480 \times 0.9 \times 2\,(1.1 \times 10^{-5}) = 0.009504$ m

$= 9.504$ mm ...(*vii*)

$\therefore$ HAZ width $= (vii) - (vi) = 9.504 - 8.448 = 1.056$ mm

[Ans. HAZ width = 1.056 mm.]

2.4. HEAT FLOW IN FILLET WELDS

A simple approach to analyse heat flow in T-type fillet welds is to assume that the total heat supplied from the arc is distributed in the three plates in the ratio of their thicknesses. Temperature distribution in the three plates forming the fillet joint can then be determined individually with the help of formulas used for determining temperature distribution for laying bead-on-plate on moderately thick plates *i.e.* equation (2.62). This approach implies that if three plates have equal thicknesses, temperatures at points equidistant from the centre of the weld should be same in the three plates. This, however, does not hold good at early stages of heat flow from the weld centre though all three heat distributions approach similarity as the time passes. This leads to a conclusion that the bead-on-plate analysis can be applied successfully to fillet welds for determining temperature distribution except (*i*) at the early stages of welding, and (*ii*) to the points close to the arc. The deviation is large when the arc is passing just over the point under consideration. However, it decreases and ultimately the temperature distributions show no differences as the time passes, as shown in *Fig. 2.8*. Such a deviation at earlier stages of welding a fillet joint can be accommodated by introducing a factor which approaches unity with time. If equation (2.62) is multiplied by this factor, the temperature deviations at earlier stages can be duly accounted for finding the true temperature distribution in fillet welds. For this purpose an exponentially varying factor of the form $(1 - Ae^{-Bt})$ is considered most appropriate where A and B are constants, the magnitudes of which depend upon the thickness ratios of three plates, etc. If equation (2.62) is expressed in a simple form as,

$$(T - T_0)_b = Qf(\xi, y, z) \qquad ...(2.76)$$

(where b stands for bead-on-plate welds) then the modified relationship is obtained by multiplying equation (2.76) by a factor mentioned above. Thus, for fillet welds the temperature distribution can be expressed as

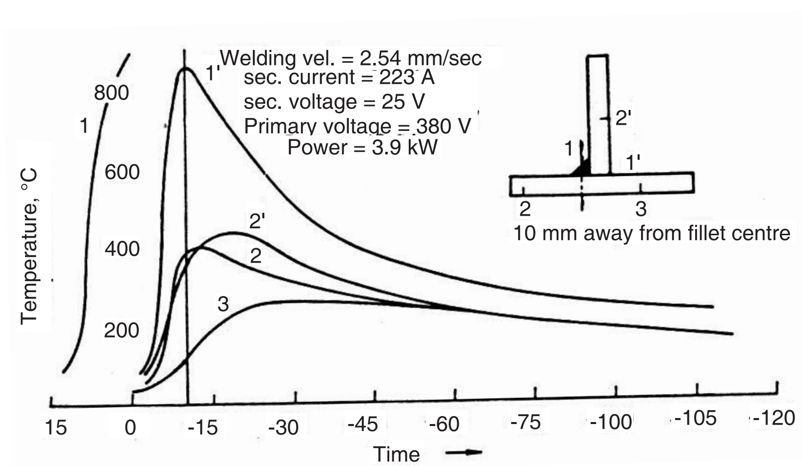

Fig. 2.8. Time-temperature distribution curves for three plates of a fillet welded joint.

$$(T - T_0)_f = Qf(\xi, y, z)\,(1 - Ae^{-Bt}) \quad ...(2.77)$$

$$(T - T_0)_f = (T - T_0)_b\,(1 - Ae^{-Bt}) \quad ...(2.78)$$

where f stands for fillet welds.

The values of the constants A and B as reported by Gupta and Gupta are, $A = 0.598$ and $B = 0.029$

$$A = 0.598 \text{ and } B = 0.029$$

It is further reported by the same authors that in T-type fillet welds the vertical plate shares the maximum instantaneous heat while the back portion of the flange, that is the one opposite to where the weld is laid shares the least amount of heat. This condition makes fillet welds susceptible to high degree of distortion and non-uniform metallurgical changes compared to butt welded joints.

2.5. HEAT FLOW IN CIRCULAR WELDS

The highest strain in welded structures form after making welds that do not finish on the free edges of the workpiece. This includes a large group of circular welded joints *i.e.* the welding of various types of patches, flanges, nipples, connecting pipes and many other cylindrical components. The strains in such welds may be considerably reduced by altering the design of the weld and the fabrication technology employed. To do so, it is imperative to evaluate the temperature field formed in the component during welding, and to select correctly the optimum parameters that control this field.

Considering the temperature dependence of the thermophysical properties of the material *i.e.* $K(T) = K_0(1 + \zeta T)$* and the heat transfer from the surfaces of the workpiece, the volume non-equilibrium distribution of heat in workpiece in the welding of circular joints is described in the cylindrical system of coordinates (r, ψ, z) by the following equation,

$$T = \frac{1}{\zeta}\left\{(\sqrt{1+2\zeta\theta}) - 1\right\} \quad ...(2.79)$$

where, K_0 = the reference coefficient of heat conductivity (W/cm°C),
ζ = temperature coefficient of heat conductivity (1/°C),
θ = Kirkhhof's variable, defined by the following equation.

$$\theta = \frac{q}{2\pi k_0 g}\sum_{n=1}^{\infty} B_n \,.\, A_n(z)$$

$$\int_0^t e^{\left\{-\frac{r^2 + r_0^2 - 2rr_0\cos\left[\psi - \frac{v_w(t-\tau)}{r_0}\right]}{4\alpha t} - \frac{\mu_n^2\,\alpha t}{g^2}\right\}}\frac{d\tau}{\tau} \quad ...(2.80)$$

where, q = specific power of the welding arc, cal/sec,
g = work thickness, cm.

$$B_n = \frac{\mu_n \cos\mu_n \frac{z_0}{g} + S_1 \sin\mu_n \frac{z_0}{g}}{\mu_n^2 + S_1^2 + \frac{\mu_n^2 - S_1^2}{\mu_n}\cos\mu_n \sin\mu_n + 2S_1\sin^2\mu_n} \quad ...(2.81)$$

and $A_n(z) = \mu_n \cos\mu_n \frac{z}{g} + S_1 \sin\mu_n \frac{z}{g}$ ...(2.82)

where, r_0 = radius of the circular weld, cm,
V_w = welding speed, cm/sec,
α = thermal diffusivity, cm^2/sec,
μ_n = roots of the characteristic equation (2.83),

* ζ is a Greek letter, and is pronounced *zeta*.

$$\tan \mu_n = \frac{(S_1 + S_2)\,\mu_n}{\mu_n^2 - S_1 S_2} \qquad \text{...(2.83)}$$

z_0 = depth of immersion of the arc under the work surface, cm,

$$S_1 = \frac{a_1 g}{k_0} L \qquad \text{...(Eqn. 2.82)}$$

and

$$S_2 = \frac{a_2 g}{k_0} L \qquad \text{...(Eqn. 2.83)}$$

where, a_1, a_2 – respectively the coefficients of heat transfer from the surface of the work at $z = 0$ and $z = g$, W/cm^2°C

and L – Coefficient of linearisation of the boundary condition.

Considering specific cases of automatic welding of circular joints with a radius of 15 cm in 8 mm thick plates of $AlMg_6$ alloy at a speed of 36 m/hr (1 cm/sec) under three different heat transfer conditions, *viz.*,

(*i*) welding without any backing plate,

(*ii*) welding with a backing plate of steel,

(*iii*) welding with the lower surface of the plate water cooled.

The coefficient of heat transfer at the bottom of the plate for the above three conditions were taken respectively as 2.092×10^{-3}, 20.92×10^{-3} and 209.2×10^{-3} W/cm^2–°C.

Welding was done in a single pass with a 2 mm diameter wire using a welding current of 308 A with dcep polarity at an arc voltage of 25 V and a wire feed rate of 500 m/hr (8.33 m/min). The temperature distribution patterns obtained respectively for the three cases were reported to be as shown in *Figs. 2.9, 2.10 and 2.11.*

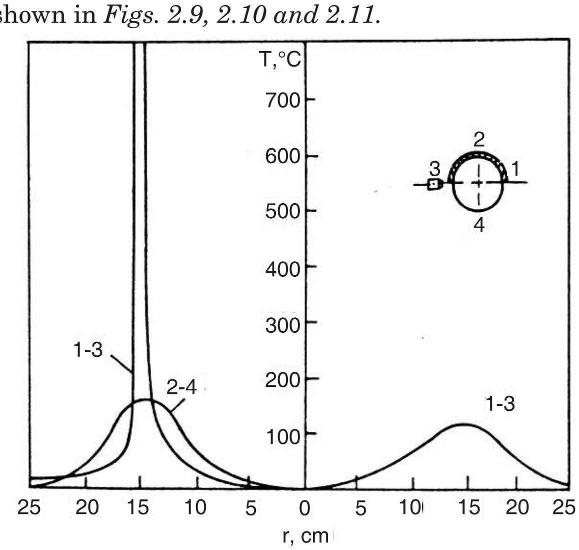

Fig. 2.9. Temperature distribution in sections 1–3 and 2–4 when the arc has travelled through half the circumference for welding a circular patch without any backing strip.

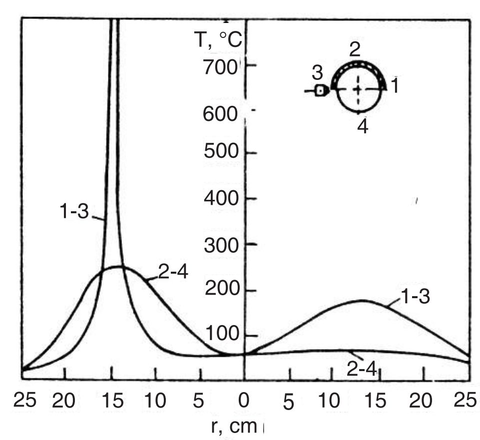

Fig. 2.10. Temperature distribution in sections 1–3 and 2–4 when the arc has travelled through half the circumference for welding a circular patch with a backing plate of steel.

*Fig. 2.*9 shows the temperature field in sections 1-3 and 2-4. It is seen that in the case of heat transfer from both sides of the plate to the ambient air central part of the plate is heated to high temperatures. In the course of welding, the heat source moves over the already heated zone resulting in increased dimensions of the weld pool and that displaces the pool towards the centre of the circle.

Fig. 2.10 shows the temperature distribution when Al-alloy plate is resting on a steel plate during welding. It is evident that the temperatures are all along reduced, as compared with the first case, indicating a higher heat sink effect provided by the steel backing plate.

Fig. 2.11 shows the temperature distribution when the $AlMg_6$ plate is water-cooled at the bottom. It is evident that in this case the source moving along a circle may be replaced by a circular source applied to the entire circumference of a circle with radius r_0, however this substitution cannot be applied to earlier two cases. In practice, the concept of a circular heat source may be used with success in calculation of temperature fields in certain specific cases. These cases include the heating of a sheet surface with a rapidly moving electron beam, with high frequency induction coils, the resistance welding of nipples, GMAW at speeds above 60 m/hr, etc.

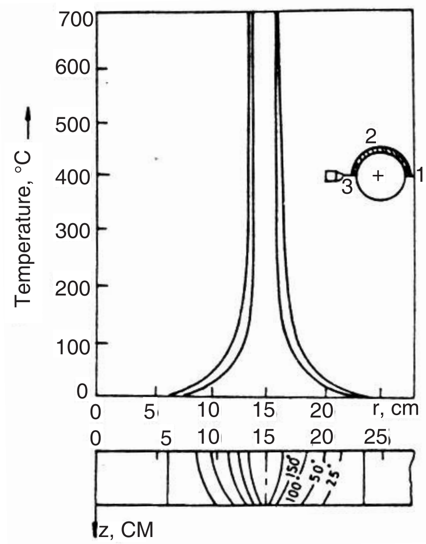

Fig. 2.11. Temperature distribution in a plate when the arc has travelled through half the circumference for welding a circular patch when the plate is water-cooled at the bottom.

Taking the above considerations into account temperature distribution under the effect of a circular source can be derived. The differential equation of heat conduction for this case has the following form :

$$\frac{\partial^2\theta}{\partial r^2}+\frac{1}{r}\frac{\partial\theta}{\partial r}+\frac{\partial^2\theta}{\partial z^2}=\frac{1}{\alpha}\frac{\partial\theta}{\partial t}-\frac{q}{2\pi kr}\,g\,(r-r_0)\cdot g\,(z-z_0)\,g\,(t) \qquad ...(2.84)$$

and the boundary conditions are,

$$\frac{\partial\theta}{\partial z}-a_1\theta=0 \qquad \text{at } z=0 \qquad ...(2.85)$$

$$\frac{\partial\theta}{\partial z}+a_2\theta=0 \qquad \text{at } z=g \qquad ...(2.86)$$

$$\theta\to 0 \text{ for } r\to\infty \qquad ...(2.87)$$

The initial conditions are : $\theta = 0$ at $t = 0$ ...(2.88)

Consequently, we obtain, $$\theta=\frac{q}{2\pi kgt}I_0\left(\frac{rr_0}{2\alpha t}\right)\sum_{n=1}^{\infty}B_n\,.\,A_n(z)e^{\left(-\frac{r^2+r_0^2}{4\alpha t}-\frac{\mu_n^2\alpha t}{g^2}\right)} \qquad ...(2.89)$$

where I_0 is the modified Bessel Function of the zero order.

If the circular source acts for a specific period of time t_0, the solution for the given problem may be written as follows.

$$\theta=\frac{q}{2\pi kg}\int_{t-t_0}^{t}I_0\left(\frac{rr_0}{2\alpha\tau}\right)\sum_{n=1}^{\infty}B_n\,.\,A_n(z)e^{\left(-\frac{r^2+r_0^2}{4\alpha\tau}-\frac{\mu_n^2\alpha\tau}{g^2}\right)}\frac{d\tau}{\tau} \qquad ...(2.90)$$

If the temperature field is observed from a steady circular heat source ($t_0\to\infty$), we obtain,

$$\theta=\frac{q}{2\pi kg}\sum_{n=1}^{\infty}B_n\,.\,A_n(z)\left\{I_0\left(\frac{r\mu_n}{g}\right)K_0\left(\frac{r_0\mu_n}{g}\right)S(r_0-r)+I_0\left(\frac{r_0\mu_n}{g}\right)K_0\left(\frac{r\mu_n}{g}\right)S(r-r_0)\right\} \qquad ..(2.91)$$

where K_0 is the Modified Bessel Function of the zero order, and S is the Heaviside Function:

$$S_x = \begin{cases} 1, & x > 0 \\ 1/2, & x = 0 \\ 0, & x < 0 \end{cases}$$

Fig. 2.12 shows the temperature field in the welding of 8 mm thick plate with the circular heat source and without any backing strip. The calculated results given in *Fig. 2.12* are based on equations (2.79) and (2.89). This figure indicates that at high temperatures the data calculated with and without the consideration of the effect of temperature on thermophysical properties have considerable differences.

For calculations in the above mentioned cases the $AlMg_6$ plates were considered with the values of different parameters as given below.

$$\zeta = 0.00068,\ \alpha = 0.5,\ k_0 \text{ (Th. cond.)} = 0.28,$$
$$L = 0.877,\quad g = 0.8, \text{ and } Z_0 = 0.$$

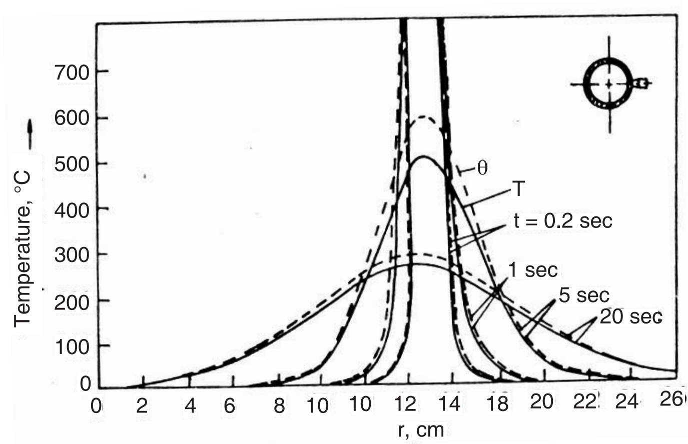

Fig. 2.12. Temperature field resulting from the use of a circular heat source on the surface of the plate of $AlMg_6$ alloy.

2.6. HEAT FLOW IN RESISTANCE WELDING

In this section two types of resisting welding processes *viz.*, *spot welding* and *zonal welding* are discussed. The discussion will be confined to resistance spot welding and upset butt welding to represent the two types of welding processes.

2.6.1. Heat Flow in Resistance Spot Welding

There are three important variables in resistance spot welding *viz.*, current, time, and pressure. In any resistance welding process the heat generated by the passage of current is given by either of the following two equations.

$$(i)\ Q = \int_0^t I^2 R\tau d\tau \qquad \text{...(2.92)}$$

$$(ii)\ Q = \int_0^t IVd\tau \qquad \text{...(2.93)}$$

where, Q = heat generated, watt–sec or joules,
I = welding current, amps.,
R = contact resistance between workpieces being welded, ohms,

V = voltage across the secondary, volts,

t = total time for which the current flows, sec.

Current, voltage, and resistance all vary with time.

Of the total heat generated *i.e.* Q, only a fraction is used to make the weld. The balance leaks into the work, and more so to the water-cooled copper alloy electrodes of high electrical and thermal conductivities. It is obvious that, for a given quantity of heat generated (Q), the longer the time of generation, the larger the fraction that leaks off. Further, it can be shown mathematically that the rate at which the heat leaks away from the weld is a maximum at the beginning of the weld period (because of cold workpiece) and that the amount of heat loss is proportional to the square root of the duration of the weld time.

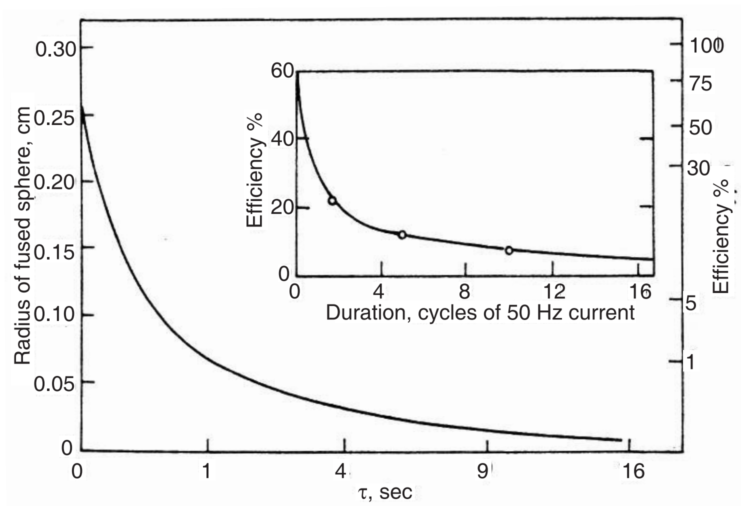

Fig. 2.13. Variation of melting efficiency with time, in resistance spot welding.

If heat transfer efficiency be taken as the ratio of the volume of steel actually melted by a fixed quantity of heat to the volume which could be melted if no heat were lost then the weld time versus efficiency curve for Q = 300 cals is shown in *Fig. 2.13*. This curve is plotted for a theoretical spot weld made by generating heat at a point source between two steel sheets in contact. It can be seen from this figure that the maximum possible efficiency obtained, when the heat is generated instantaneously, is 60%. For 300 calories generated in 1 sec, the efficiency is only 1%. For a typical spot welding operation, 3000 calories per second for 0.1 sec, the efficiency is about 10%. Thus, it is evident that for resistance spot welding as well as for other similar processes, for example, seam welding, projection welding, etc., these must be inherently short time, high current processes. Most of the features of these processes, and many of the industrial problems met with in their applications, are caused by this limitation.

Considering the case of resistance spot welding, let Q calories of heat be generated instantaneously at a point within an infinite body. The temperature distribution about the point, as a function of time and distance is given by,

$$T - T_0 = \frac{Q}{8c\rho\,(\pi\alpha t)^{3/2}}\,e^{-\frac{r^2}{4\alpha t}} \quad \text{...(2.94)}$$

This equation satisfies the following differential equation of radial heat flow,

$$\frac{\partial T}{\partial t} = \frac{\alpha}{r^2}\frac{\partial}{\partial r}\left(r\frac{\partial T}{\partial r}\right) \quad \text{...(2.95)}$$

for the boundary condition that all the heat remains within the body.

It is of interest to know the peak temperatures at various radii, especially in the radius of the sphere within which T_{max} = 1485°C, T, of course, equals T_{max} when $\frac{\partial T}{\partial r} = 0$. Differenting with time equation (2.94), we get,

$$\left(\frac{\partial T}{\partial r}\right)_r = \frac{Q}{8c\rho\,(\pi\alpha t)^{3/2}}\,e^{-\frac{r^2}{4\alpha t}} \times \left(\frac{r^2}{4\alpha t} - \frac{3}{2t}\right) \qquad ...(2.96)$$

At a finite time, and radius not equal to zero, the only term that can vanish in equation (2.96) is the one within the parentheses, and thus,

$$T = T_{\max} \qquad \text{when } \frac{r^2}{4\alpha t^2} - \frac{3}{2t} = 0$$

or

$$T = T_{\max} \qquad \text{when } t = \frac{r^2}{6\alpha} \qquad ...(2.97)$$

Substituting these values in equation (2.93), we get,

$$T_{max} = \frac{Q}{8c\rho r^3}\left(\frac{\pi e}{6}\right)^{-3/2} \qquad ...(2.98)$$

Thus, for a given amount of heat input, the peak temperature at any point is inversely proportional to the cube of the distance of this point from the point at which the heat is introduced.

Putting T = 1500°C, Q = 300 calories, C = 0.12 cal/gm.°C, ρ = 7.8 g/cm^3, we get, r = 0.25 cm.

This locates t = 0 point for the curve of *Fig 2.13*. Weld time versus efficiency of heat utilisation in spot, seam, and projection welding is given by the inset curve in *Fig. 2.13*. It is evident that the weld time duration should approach as low a value as possible. It is therefore imperative to use very high welding current in all these resistance welding processes.

2.6.2. Heat Flow in Upset Butt Welding

In general the welding processes require that a certain temperature be reached and maintained long enough for the weld to be completed. For example, in upset or resistance butt welding the aim is for an interface temperature of the order of the solidus temperature, T_s, of the work material. This temperature when reached needs to be held only until the oxide layer at the interface has been dislodged by fragmentation or diffusion, or until sufficient lengths of the workpieces have been heated to permit upsetting.

Let us consider upset butt welding of two round bars of steel, each of length l and cross-sectional area A. Assume that the interface is raised instantaneously to the solidus temperature, T_S, and that the opposite ends of bars are held at room temperature. To determine the temperature variation, along the length of the bar, with time let us consider an element of thickness dx of the bar centred x cm from the interface as shown in *Fig. 2.14.* Assume that the interface has been at temperature T_s long enough so that the element has a temperature above the room temperature, T_0, but has not attained as yet its steady-state temperature.

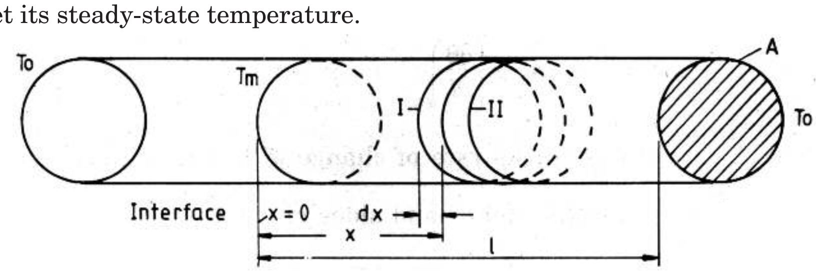

Fig. 2.14. Model for heat flow in resistance butt welding.

Applying Fourier's equation, the heat flow at section x is given by,

$$q = -kA\left(\frac{\partial \theta}{\partial x}\right)_\tau \qquad ...(2.99)$$

where, $\theta = T - T_0$,

k = thermal conductivity of bar material which is assumed to be independent of temperature, T.

The partial derivate indicates that the heat flow at a definite time t is being considered. At face I of the element, heat is flowing at the rate q_I as given by the following equation,

$$q_I = -kA\left[\frac{\partial \theta}{\partial x} - \frac{\partial}{\partial x}\left(\frac{\partial \theta}{\partial x}\right)\frac{dx}{2}\right]_\tau \qquad ...(2.100)$$

where the second derivative indicates that there may be a change in gradient as we move from plane x to the boundary plane I. Similarly at face II, we have,

$$q_{II} = -kA\left[\frac{\partial \theta}{\partial x} + \frac{\partial}{\partial x}\left(\frac{\partial \theta}{\partial x}\right)\frac{dx}{2}\right] \qquad ...(2.101)$$

If surface losses are neglected, the difference $q_I - q_{II} = q_n$ gives the rate at which the heat is accumulating in the element,

$$\therefore \qquad q_n = kA\left[\frac{\partial^2 \theta}{\partial x^2}\right]dx \qquad ...(2.102)$$

Now, if the heat is accumulating in the differential element, its temperature must be changing. Taking c as the specific heat of bar material and ρ its density, and assuming that these also do not change with temperature T, thus q_n can also be given by the following relationship,

$$q_n = c \cdot \rho \cdot A\, dx \left[\frac{\partial \theta}{\partial t}\right]_x \qquad ...(2.103)$$

where $\left(\frac{\partial \theta}{\partial t}\right)_x$ refers to the rate of change of temperature on the plane x. Equating the right hand sides of equations (2.103) and (2.102), we get,

$$c\rho\left(\frac{\partial \theta}{\partial t}\right) = k \cdot \frac{\partial^2 \theta}{\partial x^2}$$

or

$$\frac{\partial \theta}{\partial t} = \frac{k}{c\rho}.\frac{\partial^2 \theta}{\partial x^2} = \alpha\frac{\partial^2 \theta}{\partial x^2} \qquad ...(2.104)$$

where $\alpha = \frac{k}{c\rho}$, the thermal diffusivity of the bar material.

Equation (2.104) is a general equation for any case of unidirectional heat flow through a body containing no heat source(s) and no heat sink(s) other than its own heat capacity. When extended to three dimensional heat flow system it reads as

$$\frac{\partial \theta}{\partial t} = \alpha\left(\frac{\partial^2 \theta}{\partial x^2} + \frac{\partial^2 \theta}{\partial y^2} + \frac{\partial^2 \theta}{\partial z^2}\right) \qquad ...(2.105)$$

Now, to solve the differential equation (2.103) we must find a solution that satisfies the following boundary conditions.

$\theta = \theta_s$ at $x = 0$ $\qquad t \geq 0$,

$\theta = 0$, at $x = \pm l$ $\qquad$ for all values of t

$\theta = 0$ at $t = 0$ $\qquad$ for all values of x between $\pm l$ except at $x = 0$.

It is also known from steady-state heat conduction theory that when $t = \infty$ the solution of equation (2.104) must reduce to,

$$\frac{\theta}{\theta_s} = 1 - \frac{x}{l} \qquad \text{...(2.106)}$$

The most general solution to equation (2.105) for the period representing the interval before any heat has reached the ends of the bars is a temperature distribution given by,

$$\frac{\theta}{\theta_s} = 1 - \frac{2}{\pi}\int_o^u e^{-u^2} du \qquad \text{...(2.107)}$$

where $u = \dfrac{x}{\sqrt{\alpha t}}$.

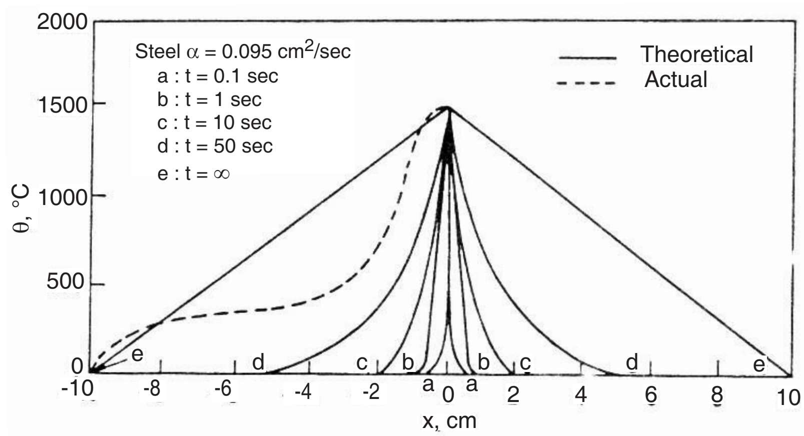

Fig. 2.15. Temperature distribution during resistance butt welding.

Values of $\frac{2}{\pi}\int_o^u e^{-u^2} du$ known as the *Gaussian error function* (erf u) can be obtained from standard mathematical tables. Equation (2.107) fails if it indicates that the temperature at ± l is increasing. Thus, to test the valadity of a temperature distribution obtained by its use, it is merely necessary to calculate θ at $x = l$ at the desired time. If θ_l is greater than 5 or 10 degrees (above the ambient), the distribution will be inaccurate. *Fig 2.15* illustrates the application of this equation for l = 10 cm for the aforementioned boundary conditions. The actual temperature distribution generally looks more like the dotted curve of Fig. 2.15.

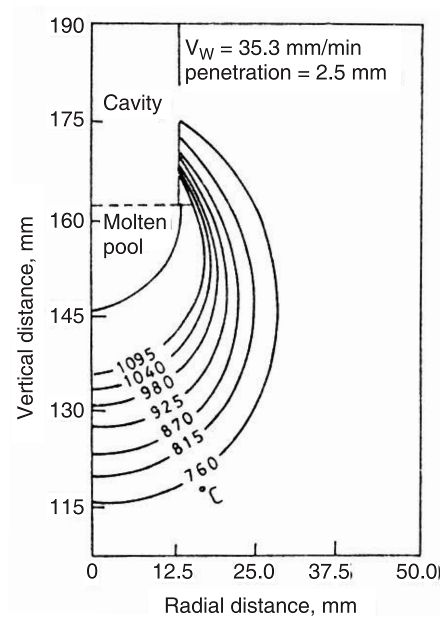

Fig. 2.16. Calculated isotherm shapes for electroslag welding.

2.7. HEAT FLOW IN ELECTROSLAG WELDING

In electroslag welding (ESW) the heat source is large and moves slowly. This implies that the material ahead of the moving heat source is preheated to a much higher degree than in normal arc welding so that the heat flow patterns associated with ESW are not likely to be well described by considering point heat source. Also, the important role of the slag in this process with its resistive heating effect should also be taken into account particularly with regard to its effects on the shape and size of the heat source. Because the slag volume is quite large in ESW thus the assumption of a point heat source is not representative of this process.

Attempts to simulate the heat flow of ESW have been made by different researchers. One such model based on symmetrical parabolic model to represent the moving molten-solid interface yielded fairly satisfactory results; typical isotherm shapes as calculated from such a model are shown in *Fig. 2.16*.

2.8. HEAT FLOW IN UNDERWATER WELDING

The process of underwater welding is broadly divided into two types *viz.*, Dry Underwater Welding, and Wet Underwater Welding. In *dry underwater welding* the spot to be welded is enclosed by a chamber from which water is excluded under pressure. The welding so done is very similar to that carried out in open air conditions except that the pressure varies with the water depth. Temperature distribution in the work therefore remains similar to that encountered in normal atmospheric welding.

Wet underwater welding is carried out in water without any chamber around the spot to be welded. The process basically remains same as used in normal open air welding but the change from air to water environment results in higher heat losses and the arc is constricted. In wet underwater welding, the heat losses from the surface of the workpiece are so high that the temperature at a short distance from the outer periphery of the weld pool remains unaltered which results in the establishment of very steep thermal gradients. Thus, the isotherms are confined to a very narrow zone which makes experimental measurements of temperature, at a point, quite difficult. The present discussion about heat flow in underwater welding is limited to wet underwater welding only.

2.8.1. Heat Flow in Wet Underwater Welding

In wet underwater welding, the heat flow takes place inside the workpiece by conduction while heat flow by convection accounts for most of the heat dissipation from the surface of the workpiece. The temperature distribution inside the solid body, away from the heat source, is very well accounted for by Fourier's 3-dimensional, heat flow equation (2.15) and by differential equation of the quasi-stationary state of welding, that is, by equation (2.26) ; however the heat transfer at the surface of the workpiece is by convection. At the two major bounding surfaces, since the heat is transferred through the laminar boundary layer of fluid only by conduction, thus at these surfaces equation (2.15) reduces to,

$$dQ = -k \cdot dA \cdot \frac{\partial T}{\partial z} \qquad \text{...(2.108)}$$

This transfer of heat from the surface of the workpiece could also be represented by *Newton's law of cooling* as,

$$dQ = h \cdot dA \cdot T \qquad \text{...(2.109)}$$

Equating the right hand sides of equations (2.108) and (2.109), we get,

$$\frac{\partial T}{\partial z} = -\frac{h}{k}\, T \qquad \text{...(2.110)}$$

Fig 2.17 shows that equation (2.110) is valid only for $z = 0$, whereas at $z = g$, expressions (2.108) and (2.109) lead to,

$$\frac{\partial T}{\partial z} = +\frac{h}{k}\, T \qquad \text{...(2.111)}$$

or, in general, the boundary conditions at the two major bounding surfaces could be expressed as,

$$\frac{\partial T}{\partial z} \pm \frac{h}{k}\, T = 0 \qquad \text{...(2.112)}$$

The quenching caused by the surrounding water in wet underwater welding results as, already discussed, in the setting up of steep temperature gradients in the body of the workpiece. Therefore, the temperature of the plate drops to ambient comparatively at a short distance from the weld pool.

Hence, it is logical to assume that the temperature at the periphery of the workpiece must be the same as that of the surrounding water.

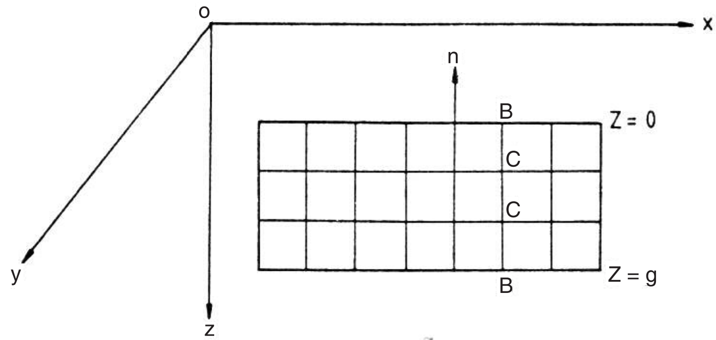

Fig. 2.17. Plate with equidistance grid spacing and the direction of outwardly drawn normal at one of the grid points.

A solution of temperature distribution problem for wet underwater welding would be one that satisfies simultaneously equations (2.26) and (2.112). To achieve this the values of α (thermal diffusivity), k (thermal conductivity), and h (surface heat transfer coefficient) must be known. Though it is possible to use some average values for α and k without any serious effects on the final results but the change in the value of h with temperature is so large, over the temperature range encountered in welding, that to assume any single value for it is out of question. To arrive at any conclusion about the value(s) of h to be used a thorough insight into the effects of different situations developed in wet underwater welding on this parameter is required and the same is done in the following sections.

2.8.1.1. Surface Heat Transfer Coefficient

In underwater SMAW the arc is surrounded by a very active vapour pocket which dissociates 12 to 16 times per second from around the arc. This keeps the water in the vicinity of the arc always in an agitated state. Thus, it is not the case of what is termed as 'pool boiling' in which the whole volume of the water involved boils and thus stirs without agitation due to any external source.

The value of the surface heat transfer coefficient, h, depends upon the temperature difference between the workpiece and that of the surrounding water as has been expressed by equation (2.109) and the temperature of the work (steel) may vary from around 2500°C to the ambient water temperature. Moreover due to the very high temperature of the arc the water immediately around the vapour pocket boils. Owing to the agitation of water and convection currents the boiling water moves up, comes in contact with the bulk and gets condensed. Thus, the heat transfer around the arc and consequently the weld pool is high and a very complex phenomenon involving heat transfer by conduction, convection and radiation. The convective heat transfer is further complicated because it involves simultaneously the phenomenon of *boiling* and *condensation*. Boiling heat transfer is itself quite complex because apart from the phase change it involves a large number of variables such as the geometry of the work, the viscosity, density, thermal conductivity, expansion coefficient, specific heat of the fluid, the surface characteristics, surface tension, latent heat of evaporation, liquid pressure, etc. Moreover, in underwater welding it is not a case of pool boiling but instead it is a case of what is known as 'Local Boiling', or 'Surface Boiling', or more comprehensively termed as 'Surface Boiling of Subcooled Liquid'. Before discussing 'Local Boiling' a note on the mechanism of 'Pool Boiling' is imperative as that forms the basis to which all deviations will be referred to.

2.8.1.2. Pool Boiling

Consider a heated plate submerged in a pool of water at saturation temperature (T_{sat}). As the temperature of the work (T_w) is raised the value of the heat transfer coefficient, h, goes on increasing. *Fig. 2.18* represents the type of heat transfer data obtained as the work temperature is increased above ambient. In this figure heat flux $\left(\frac{q}{A}\right)$ and surface heat transfer coefficient, h, are plotted against the excess temperature ΔT, where $\Delta T = T_w - T_{sat}$.

As the temperature T_w is raised, ΔT is increased, convection currents cause the liquid to circulate and the steam is produced by evaporation at the liquid surface. This is represented as regime 1 and is called 'Interface Evaporation'. Here, only the liquid is in contact with the heated surface and the heat transfer is due only to free convection.

With further increase in ΔT the energy level of the liquid adjacent to the work surface becomes high at a number of favoured spots where vapour bubbles are formed. They rise above the plate surface but condense before reaching the liquid surface. This is known as regime 2. As the temperature of the work is raised further, up to point A in the figure, the bubbles become more numerous. The liquid is so hot as not to allow any condensation of the bubbles which rise to the free liquid surface and help rapid evaporation. This is known as regime 3. Both the regimes 2 and 3 fall in the category of 'Nucleate Boiling'.

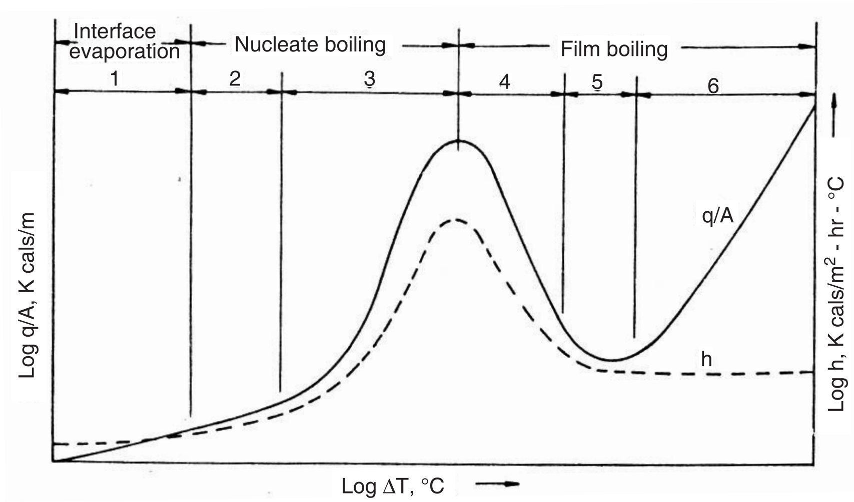

Fig. 2.18. Heat flux and heat transfer coefficient vs. temperature difference in boiling water at atmospheric pressure.

Beyond the point A, representing the critical heat flux, the number of bubbles formed is so high that they form patches of vapour film which form and break regularly. This constitutes regime 4 and is often termed as 'Unstable Film Boiling'. Any further increase in heat input to the work results in the formation of continuous vapour film over the whole body of the workpiece. This is termed as regime 5 and is called 'Stable Film Boiling'. The regimes 4 and 5 are also often simply termed as 'Film Boiling'. Here the number of bubbles formed is so large that they almost cover the whole of the work surface and provide insulating effect. This counteracts the beneficial effects of agitation by bubbles and results in decrease in the heat flux. The vapour film is unstable in regime 4, as under the action of circulating currents it collapses but reforms rapidly. In regime 5 the vapour film is stable and the heat flow is the lowest. For values of ΔT beyond 550°C (regime 6) the temperature of the work surface is quite high and heat transfer occurs predominantly by radiation, thereby increasing the heat flux.

2.8.1.3. Local or Surface Boiling

The boiling process in a liquid whose bulk temperature is below the saturation temperature but whose boundary layer is sufficiently superheated that vapours form next to the heated surface is usually called 'Local Boiling'. These vapour bubbles break off and begin to rise through the cooler liquid and get condensed to the liquid phase again. Thus boiling at the heated surface is combined with convection at a distance from it and condensation of vapour at the interface between the boiling boundary layer and mass of cold liquid. The intensity of vapourisation on the wall depends on the degree of superheat of the liquid, the process of condensation is determined by difference between saturation temperature and the bulk temperature, that is by the degree of subcooling of the liquid.

Subcooling from the saturation temperature to the bulk temperature is a reference parameter that distinguishes surface boiling from pool boiling. If superheating determines the intensity of vapourisation, subcooling determines the size of the region that is affected by the disturbing action of vapourisation. The greater the subcooling of the liquid, the narrower is the region where boiling takes place. Also, the bubbles increase in number while their sizes and average life time decreases with decreasing bulk temperature at a given heat flux. As a result of increase in the bubble population, the agitation of the liquid caused by the motion of the bubbles is more intense in a subcooled liquid than in a pool of saturated liquid and thus much higher heat flux is attained before any vapour film is formed.

To appreciate the effect of subcooling on critical heat flux reference may be made to Kutateladze's equation given below.

$$\frac{(q_{cr})_\theta}{(q_{cr})_0} = \left[1+0.065\left(\frac{\gamma'}{\gamma''}\right)^{0.8} \cdot \frac{c\theta}{r}\right] \quad ...(2.113)$$

where, $(q_{cr})_\theta$ = critical heat flux at θ° subcooling,

$(q_{cr})_0$ = critical heat flux at 0° subcooling,

γ' = specific weight of water at bulk temperature and operating pressure,

γ'' = specific weight of saturated steam at the operating pressure,

c = specific heat of water,

θ = degree of subcooling, °C,

r = latent heat of vapourisation.

Putting the values of different variables for the actual condition of operation, with bulk water temperature of 30°C it was found that,

$$\frac{(\ _{cr})_{\theta=70°C}}{(\ _{cr})_{\theta=\ °C}} = 2.565$$

which means that the critical heat flux increased 2.565 times for 70°C of subcooling.

Apart from subcooling other major factors that affect heat flux, and consequently the surface heat transfer coefficient are the ambient pressure, position of heated surface and the motion of the fluid. The effects of these factors are discussed as follows.

2.8.1.4. The Effect of Pressure

The effect of pressure on the heat transfer coefficient in well developed nucleate boiling is more or less the same for all liquids. According to test data reported by Mikheyev the peak heat flux (q_{peak}) first sharply increases, reaches a certain maximum with rising pressure, then drops to zero at critical pressure. If a graph is drawn between $\frac{}{_{cr}}$ and $\frac{q_{peak,\,P}}{q_{peak,\,1}}$ then the curve is at its maximum for $\frac{q_{peak,\,P}}{q_{peak,\,1}}$ = 3.2 and $\frac{P}{P_{cr}}$ = 0.35. If this data is applied to water (P_{cr} = 225 ata.) it will be seen that the peak occurs at a pressure equal to 80 atmosphere. Further, it has been recommended, from the charts plotted for pressures ranging from P = 0.2 to P = 100 ata., that the coefficient of heat transfer of water in nucleate boiling may be calculated from the following relationship,

$$h = 39\,(\Delta T)^{2.33} \text{ kcals/m}^2\text{–hr–°C} \quad ...(2.114)$$

The relationship suggested by Jackob and Hawkins for finding the effect of pressure on heat transfer coefficient is given by the equation,

$$h_p = h_{ps} \left(\frac{P}{P_s}\right)^{0.4} \qquad \text{...(2.115)}$$

where, P = pressure of water at the point under consideration,

P_s = pressure of standard atmosphere,

h_p = boiling heat transfer coefficient at pressure, P,

h_{ps} = boiling heat transfer coefficient at atmospheric pressure, P_s.

2.8.1.5. The Effect of Position of Heated Surface

The heat transfer coefficient, h, and the heat flux $\left(\frac{q}{A}\right)$ depend, to a great extent, upon the conditions in which the generated vapours separate from the heated surface. These conditions are most favourable in the case of horizontal heated surfaces, the heated side of the surface facing upwards. The aforementioned equations [(2.113) to (2.115)] hold good for such conditions. If the heated side of the work faces downwards, the conditions in which vapours separate from the surface deteriorate sharply and the peak heat flux diminishes by as much as 40%. This is because the motion of the fluid is only in a thin layer underneath the work, the rest of the fluid below that layer remains stationary.

Fig. 2.19 represents the commonly accepted nature of convection currents above and below a horizontally placed heated flat plate.

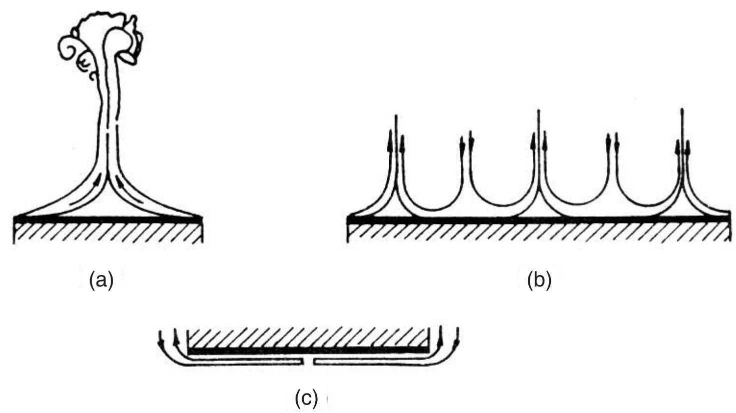

Fig. 2.19. Free flow of fluid near heated horizontal flat plates : (*a* and *b*) heated surface upwards, (*c*) heated surface downwards.

2.8.1.6. The Effect of Motion of Fluid

Apart from the aforementioned factors, heat transfer coefficient is considerably influenced by the rate of forced circulation of the fluid. If there be no forced circulation of the liquid the steam bubbles which are generated on the heated surface grow to a specific size before detachment thus the heat transfer coefficient is governed by the intensity of vaporisation. If the liquid is made to circulate then the steam bubbles are detached before they attain critical size. As the fluid density is increased further the effect of intensity of vapourisation is gradually reduced till it reaches a value that of free convection in a single phase liquid. Thus it can be said that at low circulation velocity (w) the intensity of vapourisation (q_v) is predominant and at higher circulation velocity the effect of w is predominant or in other words the coefficient of heat transfer can be expressed as,

$$h = f(w, q_v) \qquad \text{...(2.116)}$$

In the case of underwater SMAW, when an arc is struck between the electrode and the workpiece a bubble or a vapour pocket is formed with the arc at its centre. Next to the arc would probably be a mixture of incandescent gases emitted by the arc and superheated steam around this an envelope of saturated steam in contact with ambient water. The vapour bubble fluctuates, as stated earlier, 12 to 16 times per second releasing about 200 cm^3 of combustion gases and steam per second. This leads to enormous disturbance of liquid in a sufficiently big volume around the arc.

From the factors discussed above and also because of the wide variations in the results of many researchers in the field of boiling heat transfer it is rather difficult to arrive at any standard relation for predicting boiling heat transfer coefficient for the conditions under consideration. However, from the above considerations the different values of heat transfer coefficient, for different ranges of temperatures, can be based on the careful study and weightage given to different factors discussed as follows.

The peak value of 'h' for pool boiling given by Mikheyev is 5×10^4 Kcals/m^2hr°C and that by Kutateladze is about 2.55×10^4 Kcals/m^2-hr-°C. Kutateladze has also recommended equation (2.113) for finding the effect of subcooling on the value of h. Using this equation with 70°C of subcooling (*i.e.* for a room temperature of 30°C) h increases, as already stated, by a factor of 2.565 thus giving peak value of h as 6.3×10^4 Kcals/m^2-hr-°C. Taking into consideration these two values and the agitational effect of the detaching bubbles around the arc it is considered best to use Mikheyev's expression and the subcooling factor found by equation (2.113) to get peak value of h of the order of 12.8×10^4 Kcals/m^2 -hr-°C.

The different values of 'h' for work temperature up to 121.5°C could be decided on the basis of results given by different researchers. However, for work temperature higher than 121.5°C, h can be taken as equivalent to peak value mentioned above because it is not a case of pool boiling and there being considerable disturbance around the arc the application of the formula of continuous film to the work being welded appears to be impractical. Moreover, the use of peak value of h for higher temperatures also takes care of heat transfer by radiation above 550°C.

Thus, from the above mentioned considerations the values of surface heat transfer coefficient, h, for different ranges of temperature, encountered in wet underwater welding may be taken as follows.

(*i*) Heat transfer coefficient can be taken as directly proportional to the temperature difference between the work and the bulk of water for and up to $T_w = T_{sat} = 100$°C.

(*ii*) For interface evaporation, *i.e.*, for the work temperature between 100.1 and 104.7°C,

$$h = 896\,(\Delta T)^{1/3} \times \text{subcooling factor}^*,\ \text{Kcals}/\text{m}^2 - \text{hr} - {}^\circ\text{C}$$

(*iii*) For nucleate boiling, *i.e.,* for work temperature between 104.8 and 121.5°C,

$$h = 39\,(\Delta T)^{2.33} \times \text{subcooling factor, Kcals/m}^2 - \text{hr} - {}^\circ\text{C}$$

(*iv*) For work temperature above 121.5°C,

$$h = 39\,(21.5)^{2.33} \times \text{subcooling factor, Kcals/m}^2 - \text{hr} - {}^\circ\text{C}.$$

The values of heat transfer coefficient on the bottom side of the work may be taken as 60% that of the value of h on the upper side of the work.

Having developed the model for determining the value of surface heat transfer coefficient, it is possible to determine the temperature distribution in wet underwater welding provided it satisfies certain boundary conditions.

2.8.1.7. Boundary Conditions

It is required to satisfy the condition that the heat entered the work at a uniform rate through the arc and that the same is also conducted away at a uniform rate partly into the body of the workpiece and partly dissipated to the surroundings. The size of the arc being finite the area over which it supplies the heat is also finite. That means arc supplies heat into the heat input zone of the work from where it flows by conduction into the body of the work; the molten weld pool zone can be taken as the heat input zone. The shape of the weld pool can be determined practically by studying the crater shapes obtained by sudden interruption of welding process.

* Subcooling factor = 2.565 for undercooling of 70°C *i.e.* for bulk temperature of 30°C.

Since the work and with that the heat input zone is continuously moving thus heat is transferred to the work not only by conduction from the lower and side bounding surfaces of the molten metal zone but also by the movement of the work. Thus, the heat balance at the source may be expressed by the following equation,

$$Q = -k\iint_s \frac{\partial T}{\partial n}\, ds + c\rho \iint_s TV_n\, ds \qquad \text{...(2.117)}$$

where $\frac{\partial T}{\partial n}$ is the temperature gradient along the outward drawn normal to the surface element ds, and V_n is the component of welding velocity in that direction.

In equation (2.117), the first term *i.e.* $-k\iint_s \frac{\partial T}{\partial n} ds$, accounts for the heat going out of the heat input zone by conduction and the second term, *i.e.,* $c\rho \iint_s TV_n\, ds$ represents the heat carried away by that portion of the plate which directly passes through the arc zone. The sum of these two terms is equated to the heat input per unit time, *i.e.,* Q, which is equal to ηVI, where η is the percentage of heat going into the heat input zone — the total heat generated being the product of arc voltage (V) and the welding current (I).

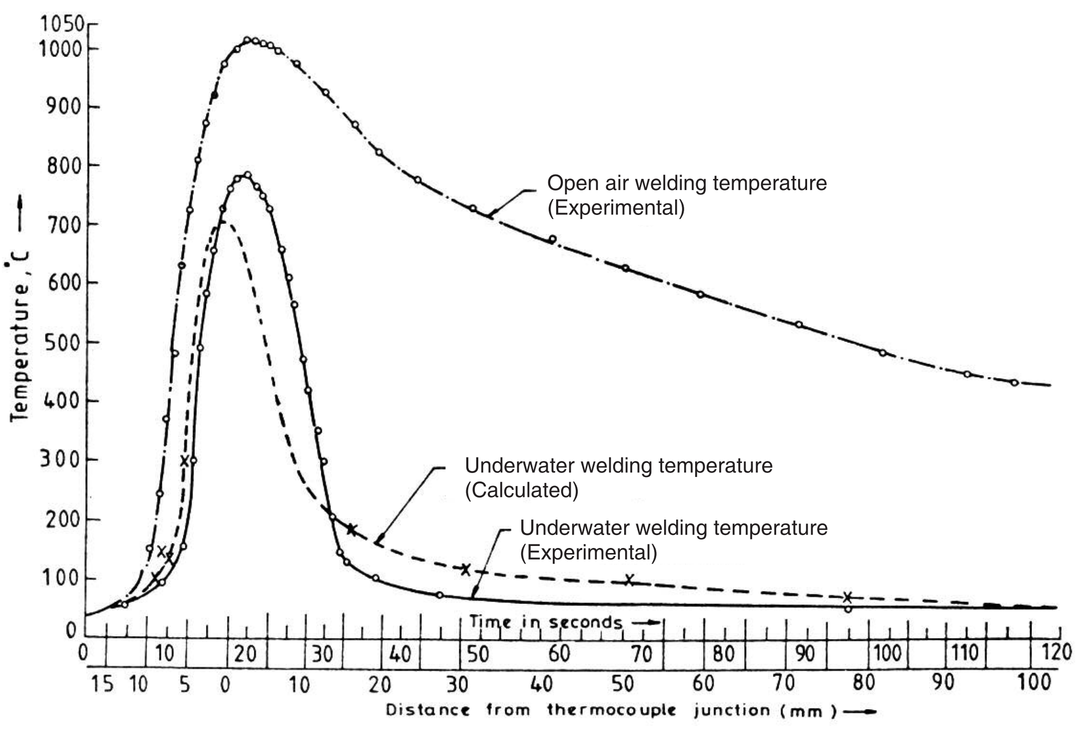

Fig. 2.20. Temperature histories of backsides of 7 mm thick plates at 6 mm from the weld centre line—both for underwater and open air conditions.

The heat taken away by water from the electrode and by way of steam formation, etc. is generally considered to be about 15% that of the total heat input. Thus, for calculating the temperature histories in wet underwater welding the heat input into the molten metal zone is taken as 50% of the observed value of the power input into the arc. The corresponding value for open air conditions are generally taken as 65%.

Thus, the final solution of the heat transfer model must not only satisfy the equation representing the heat conduction in the quasi-stationary state, *i.e.* equation (2.26) but also the boundary conditions expressed by equations (2.112) and (2.117). This can be done by using the numerical tools like finite difference and finite element methods. The results obtained by solving the problem by finite difference is shown in *Fig. 2.20* which also shows the temperature histories practically obtained for welding underwater and the normal open air conditions. These graphs represent the quasi-stationary temperature distributions along a line parallel and 6 mm away from the weld centreline; $x = 0$ being the centre of the arc.

Fig. 2.21 shows the quasi-stationary temperature distribution, for the bottom side of the plate type work, along the transverse section at 4 mm from the centre of the arc, and perpendicular to the weld centreline.

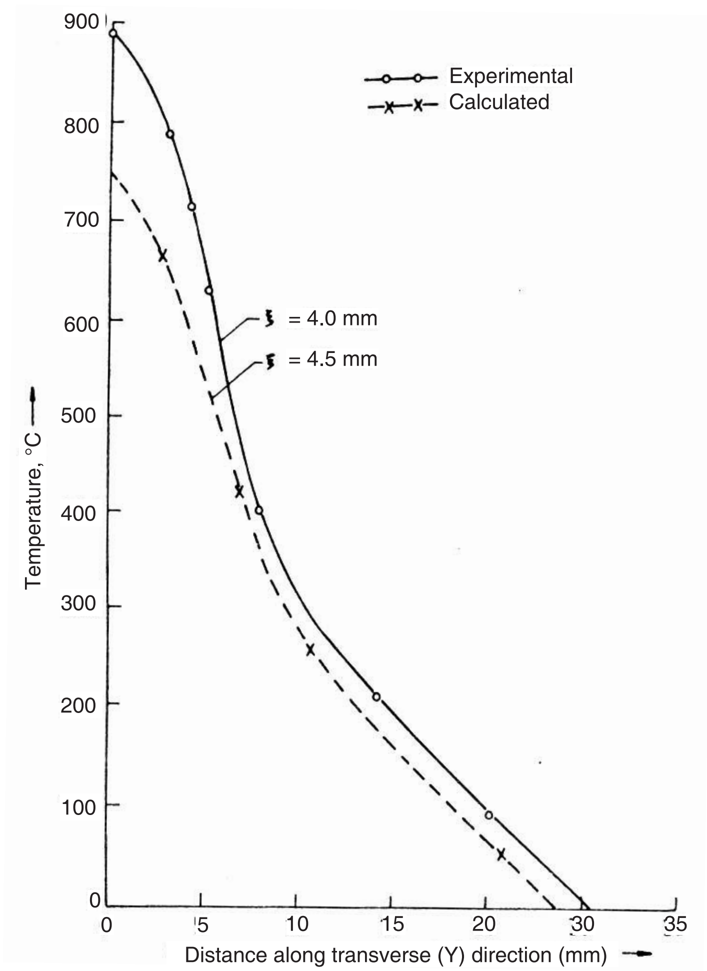

Fig. 2.21. Quasi-stationary temperature distribution at the bottom of the plate in underwater welding—along-*y*-axis.

Fig. 2.22(a) shows experimental quasi-stationary temperature distribution on the backside of the work (plate) along the weld centreline and along different parallel lines at 3, 4, 5, 6.5, 7.5, 8, 9.5 and 14 mm away from the weld centreline. In *Fig. 2.22(b)* are shown the isotherms for the temperature distribution of *Fig. 2.22(a)*. The isotherms plotted are for temperature range of 100 to 1000°C at an interval of 100°C.

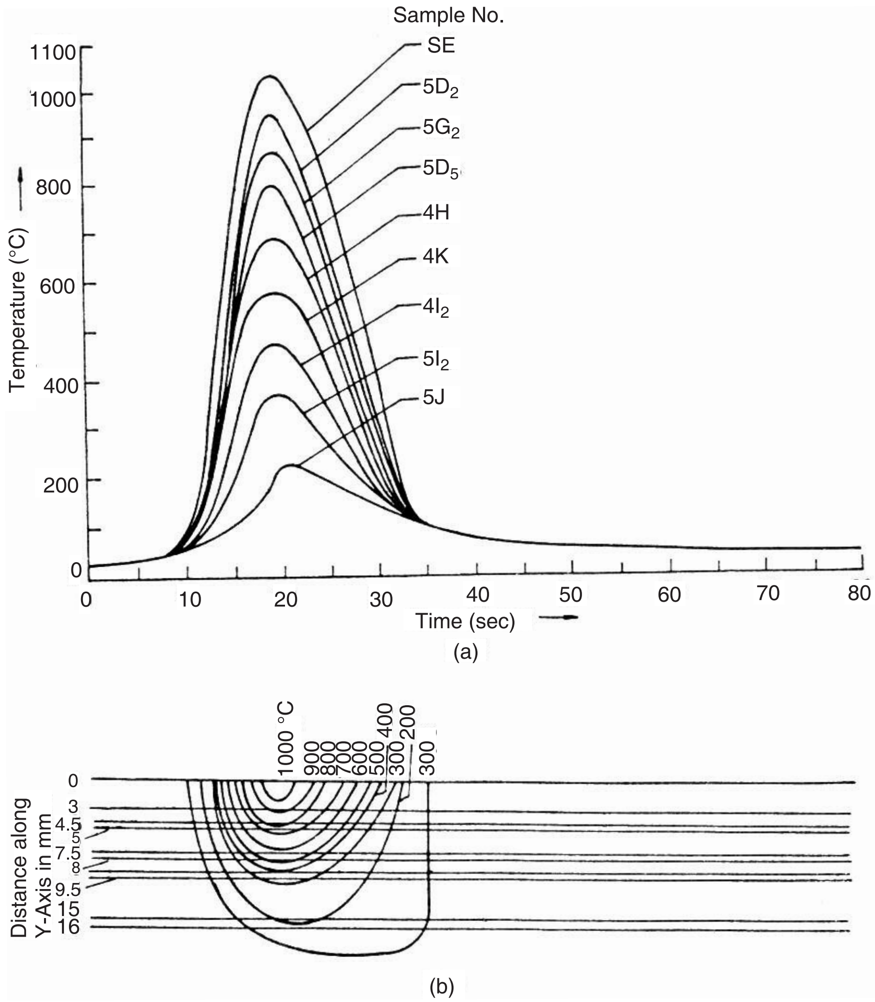

Fig. 2.22. (*a*) Experimental quasi-static temperature distribution at the back side of the plate at different points along a transverse section, (*b*) the corresponding isotherms in °C.

2.9. METALLURGICAL EFFECTS OF HEAT FLOW IN WELDING

Using equations given in the earlier sections it is possible to determine temperature at any given point during quasi-stationary state of welding and from such a data it is possible to draw thermal histories for any point of interest. If sufficient number of such thermal histories are known for different points along a transverse section with respect to the weld centreline then such thermal histories can be utilised to draw isotherms for different temperatures keeping the weld pool as the innermost isotherm representing the solidus temperature of the material being welded as shown for slow and fast welding in *Fig. 2.23*.

From these isotherms it is possible to determine the cooling rate in any desired direction such as *A*, *B*, *C*, *D*, *E*, etc. If such a cooling rate is superimposed on time-temperature-transformation curves or on continuous cooling transformation curves of the material under consideration, then it is possible to predict the micro-structure of the heat affected zone along that direction; from which it may be possible to determine the mechanical strength of the weldment. Thus, it is possible to predict the probable service behaviour of the welded fabrication.

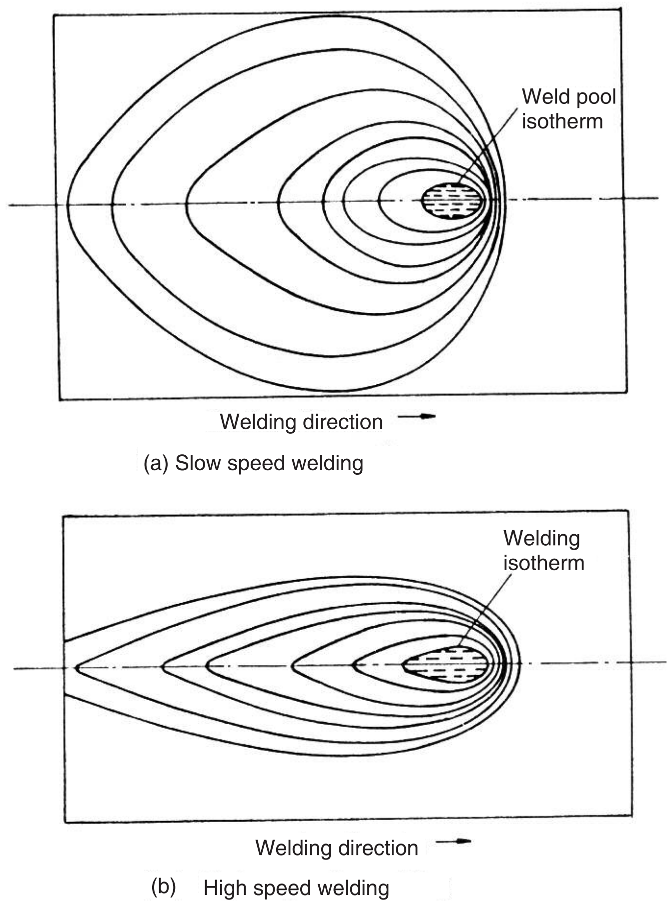

Fig. 2.23. Isotherms in quasi-stationary state welding:
(*a*) slow welding, (*b*) fast welding.

Thus, the first step to predict the metallurgical effects of heat flow in welding is to determine the cooling rate for a given set of welding conditions. The experimental method of doing so is described in the following section.

2.9.1. Experimental Determination of Cooling Rates in Welding

Take a 6 mm thick steel plate of sufficient width and length (say 200 mm × 300 mm) so that quasi-stationary state will be established after welding has proceeded through a length of 50 mm. Mark it on the bottom side as shown in *Fig. 2.24(a)*. Drill 3–4 mm deep holes with 1 mm diameter drill bit at points 1, 2, 3, ..., 6. Imbed the hot junctions of Alumel-chromel thermocouples in these holes which are filled up with high temperature brazing material—using oxy-acetylene brazing torch. The other ends of these thermocouples are connected to temperature recorders for recording thermal histories of these points during welding on the top side.

When welding is carried out with the required heat input and at the desired welding speed then the recorded thermal histories will resemble the records shown in *Fig. 2.24(b).* From these temperature histories isotherms for temperature T_1, T_2, T_3, ..., T_6, etc. can be drawn as shown in *Fig. 2.24(c).* The procedure for doing so is shown for isotherm T_6 and the same may be followed for all other isotherm; employ interpolation, where required. From these isotherms cooling rates can be determined in any desired direction like *K, L, M, N*, etc. For steels, cooling times from 800°C to 500°C is highly significant since this is the critical temperature range in which phase transformations and, therefore, the microstructure and properties of the heat affected zone (HAZ) are characterised. Cooling rate is expressed by the parameter of cooling time for example $t_{8/5}$ represents the cooling time between 800 and 500°C, $t\ T_{max/100}$ stands for the cooling time between the maximum temperature of the thermal cycle and 100°C. On the other hand v_{300} stands for cooling rate at 300°C.

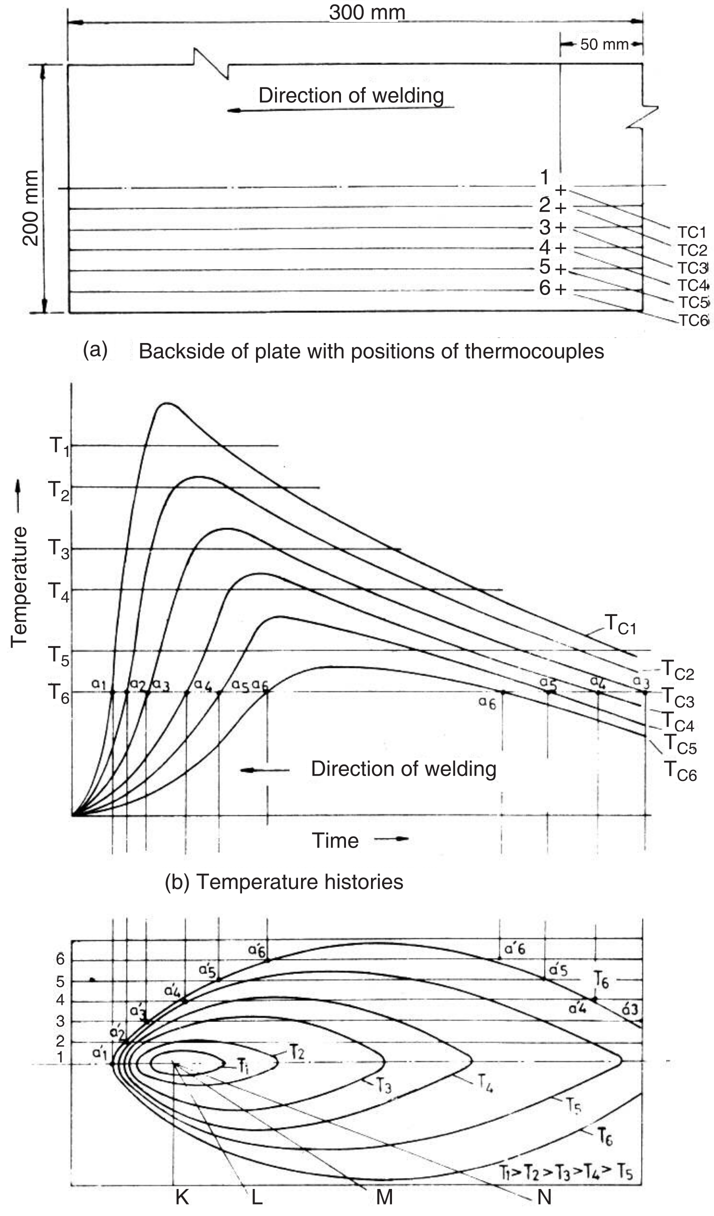

Fig. 2.24. Experimental determination of cooling rates in welding,
(*a*) Backside of steel plate with positions of thermocouples marked on it,
(*b*) Thermal histories for point along transverse section to welding direction,
(*c*) Different isotherms obtained from thermal histories of (*b*).

Fig. 2.25 shows the temperature histories for SMAW, SAW and ESW with cooling times marked for the range of 800 to 500°C. It is evident that the cooling rate in SMAW is much higher than the cooling rates of SAW and ESW. For each steel, there is a critical cooling rate which decides the final hardness of weldment particularly in its heat affected zone.

2.9.1.1. Critical Cooling Rate

It is the fastest rate at which steel can be cooled without the appearance of martensite, or stated conversely, it is the slowest rate at which the steel can be cooled that will still produce martensite. Also, it can be said that any rate of cooling faster than critical cooling rate produces a structure containing pearlite.

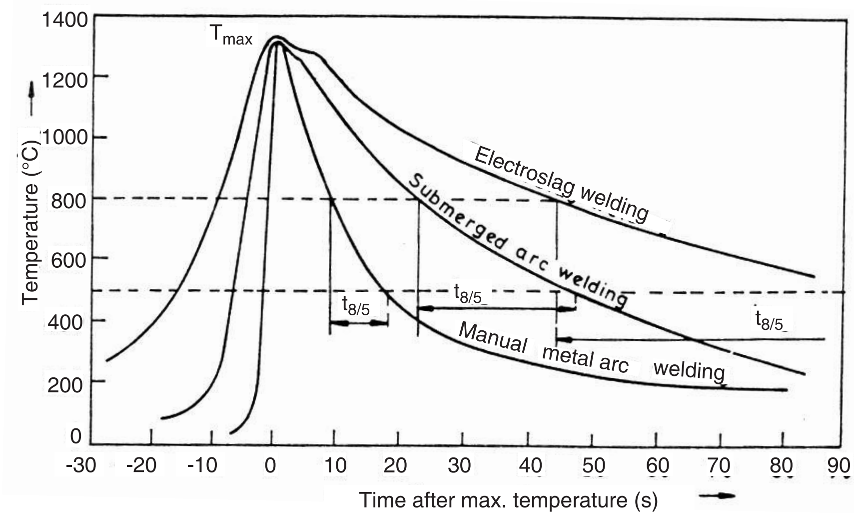

Fig. 2.25. Typical shapes of thermal histories of the underbead zone with different welding processes. (After Hrivnak).

Steels of low hardenability have a high critical cooling rate and *vice versa*. Increase in carbon content reduces the cooling rate *i.e.* raises the hardenability. The majority of alloying elements, with the exception of cobalt, have a similar effect. The so-called air-hardening steels have such a low critical cooling rate that even slow cooling from the austenitic range produces martensite. Water-hardening steels on the other hand, because of their high critical cooling rates, must be rapidly cooled to produce desired hardening.

Apart from the standard critical cooling rate for a steel there are other critical rates related to the formation of different transformation products, for example, *p*, *f*, and *z* cooling rates represent the cooling rates for the formation of pearlite, ferrite, and bainite respectively.

2.9.1.2. Transformation Products

Three major constituents formed on cooling steel from its austenitic state are pearlite, bainite and martensite. Both pearlite and bainite are formed by processes depending on the diffusion rate of various alloying elements. Thus, both these structures require a certain period of time for formation, a period which varies with temperature. In other words the transformation rate of austenite depends on the temperature of transformation. Both processes are preceded by a certain incubation period which must elapse before any transformation takes place. The martensitic transformation, on the other hand, is practically independent of time, occurring instantaneously when a certain temperature is reached.

Thus, each composition of steel has its own characteristic way of transforming when it is cooled at a given rate from the austenitic state, and there are only two ways to summarise the effects of differing conditions *viz*., isothermal transformation tests and continuous cooling tests. Curves derived from the former are called *Time-Temperature-Transformation* (TTT) diagrams and from the latter, *Continuous-Cooling-Transformation* (CCT) diagrams. Brief description of these two types of diagrams follows.

2.10. TIME-TEMPERATURE-TRANSFORMATION DIAGRAMS (TTT CURVES)

A TTT diagram shows in graphical form the time required, at various temperatures, for steel in the austenitic state to transform to ferrite, pearlite, bainite, and/or martensite. Which of these transformation products are actually formed depends on the transformation temperature? Thus, for example, the austenite in a medium carbon steel breaks down to ferrite and pearlite in the temperature range of 700 to 500°C, whereas if the cooling rate is somewhat higher, pearlite formation can be partly or wholly suppressed, and bainite will form at a lower temperature. At extreme cooling rates, even bainite formation can be suppressed, and martensite will form at a still lower temperature.

TTT diagrams are constructed from the data obtained on small specimens of the steel under investigation, which are heated to slightly above A_3 temperature*, and cooled to the temperature at which transformation rate is to be studied. The specimen can, for example, be quenched in a lead or salt bath, and since it is very small it very quickly reaches the bath temperature. The specimen is held at this temperature for a certain accurately determined time and finally water-quenched. The testing procedure is similar to the heat treatment method of *austempering*. Subsequent microscopic examination shows the percentage of austenite which has transformed within the test period and the structure of transformation product(s) typical of the test temperature. By making a sufficient number of these tests TTT diagrams can be constructed. This usually contains curves showing when the amount of austenite transformed is 10%, and when it is 99% or 100% complete; curves for 30, 50, 70%, etc. transformation are also often included.

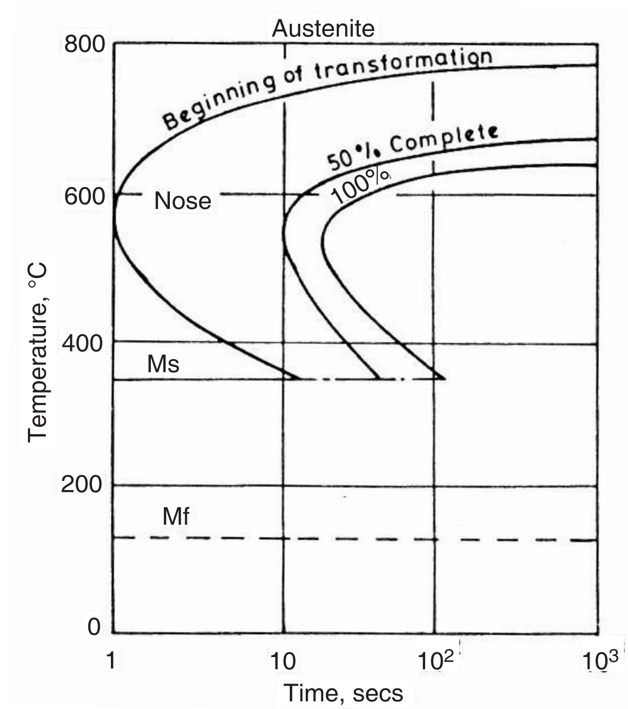

Fig. 2.26. Approximate form of TTT diagram for a 0.35% plain carbon steel.

*A_3 temperature is the upper recrystallisation temperature for low and medium carbon steels. Refer to *Fig. 3.1* or *3.27*.

The complete transformation of austenite requires long test periods within certain temperature ranges and for this reason the time axis of TTT diagrams is usually plotted on a logarithmic scale. A typical simple TTT diagram for 0.35% plain carbon steel is shown in *Fig. 2.26* while *Fig. 2.27* shows the TTT diagram for an eutectoid commercial steel AISI 1080 which contains 0.79% carbon and 0.76% manganese. Note that while for 0.35% plain carbon steel the nose of the starting curve touches the Y-axis indicating no possibility of getting 100% martensitic transformation even if the cooling rate is extremely high; while for the eutectoid steel the nose is shifted towards right indicating that 100% martensitic transformation is a possibility.

All the alloying elements used in alloy steel production influence the eutectoid condition of steel, each one lowering the eutectoid composition, but the influence varies from element to element, for example, some like Cr and Mo raise the eutectoid temperature while others like Mn and Ni lower it. The relative effects of different amounts of some additions are illustrated in *Fig. 2.28*. Also, these alloying elements may either retard or accelerate the decomposition of austenite. If it retards the decomposition then the critical cooling rate is reduced and it results in shifting the TTT curves to right or a 'bay' on the nose of the diagram appears as is shown in *Fig. 2.29*. However, if the decomposition rate of austenite is accelerated the TTT diagram tends to bulge more towards left, indicating that the steel is more difficult to harden; this effect is rare and is caused only by cobalt in certain circumstances.

Although TTT diagram is useful for comparing steels, it does not predict accurately the results of welding conditions or heat-treatment because they involve continuous cooling. The CCT diagrams can therefore be used more effectively for these purposes.

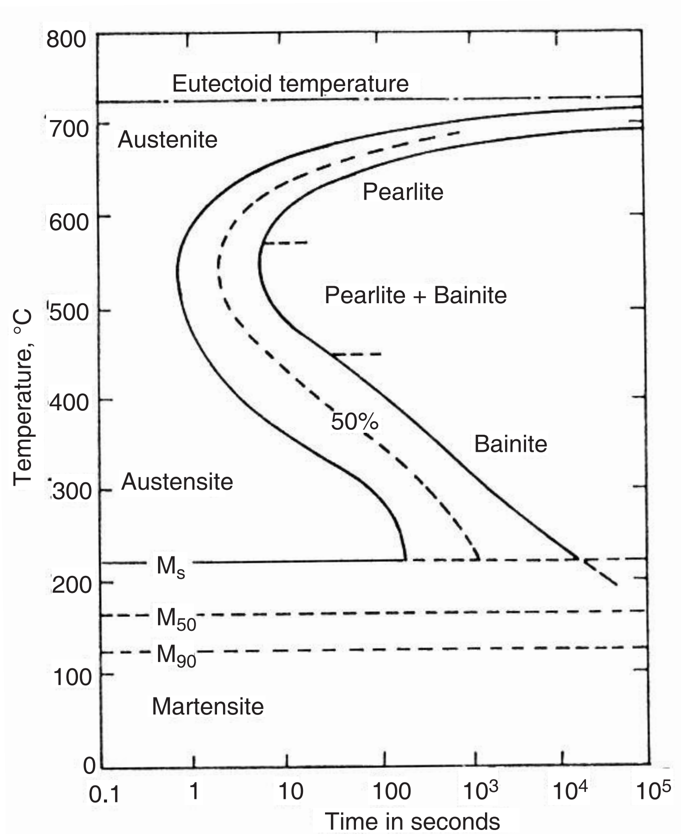

Fig. 2.27. Complete TTT diagram for
eutectoid steel AISI 1080 containing 0.79% C and 0.76% Mn.

2.11. CONTINUOUS COOLING TRANSFORMATION DIAGRAMS (CCT CURVES)

A CCT diagram is a record of the transformation behaviour of that steel under continuous cooling conditions which can be correlated fairly closely with the kind of continuous cooling occurring in the vicinity of a weld. From such a diagram it is possible to determine whether or not martensite or brittle structure is likely to form under given welding conditions. The farther to the right and lower the curves on the diagram the more hardenable the steel and more difficult the welding.

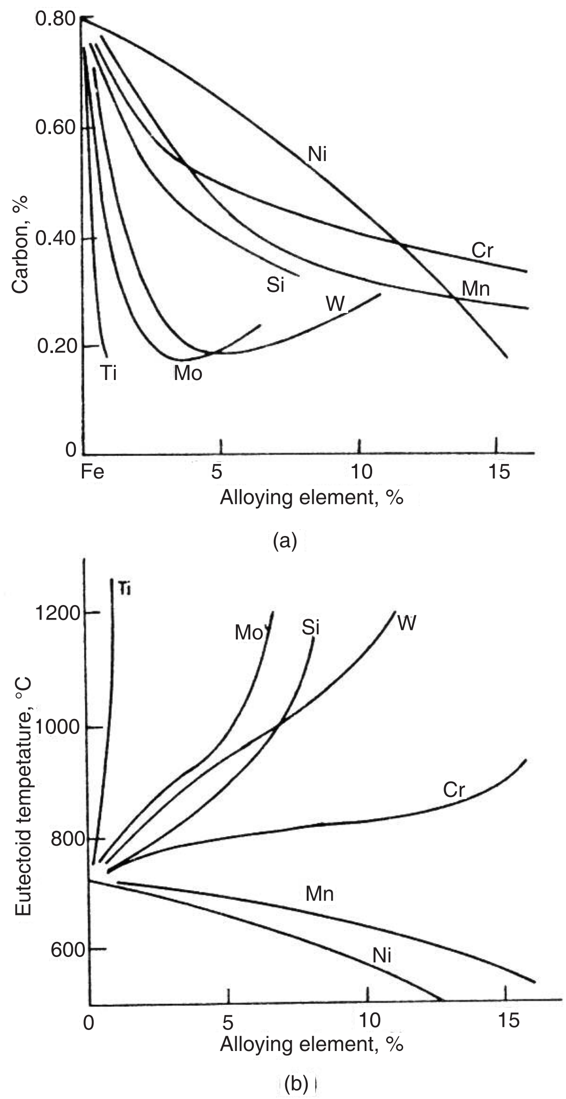

Fig. 2.28. The relative effects of alloying elements on the eutectoid relationships of steel : (*a*) effect on eutectoid composition (*b*) effect on eutectoid temperature.

Tests used for constructing CCT diagrams utilise differing sizes of round bar to derive cooling conditions equivalent to oil quenching conditions on round bar. From these tests the effects on structure at the middle, surface, and half radius respectively, of the bar are studied and recorded on a graph. Bar diameter is represented on the x-axis and temperature on the Y-axis as shown in *Fig. 2.30*. The general form of CCT diagram is similar to that of TTT diagram as shown by comparison of two sets of curves in *Fig. 2.30*.

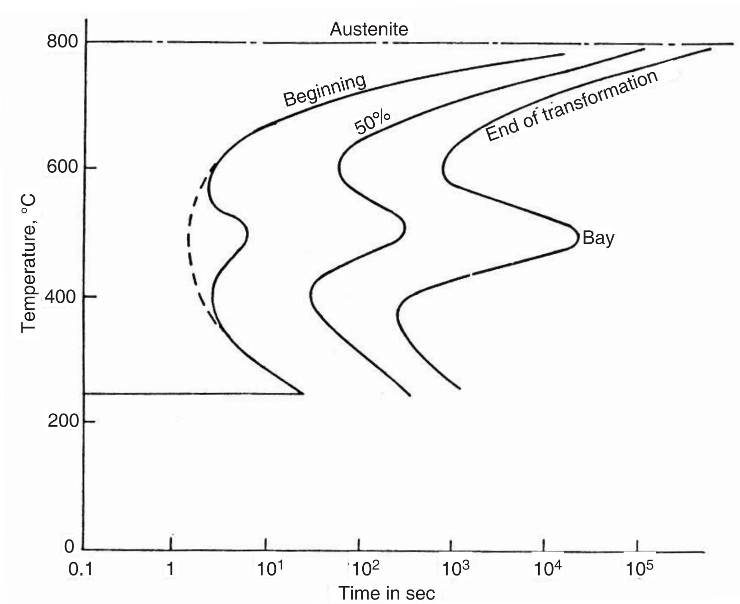

Fig. 2.29. Effect of alloying elements like Ni and Cr in changing the shape of TTT diagram by developing a bay on the nose.

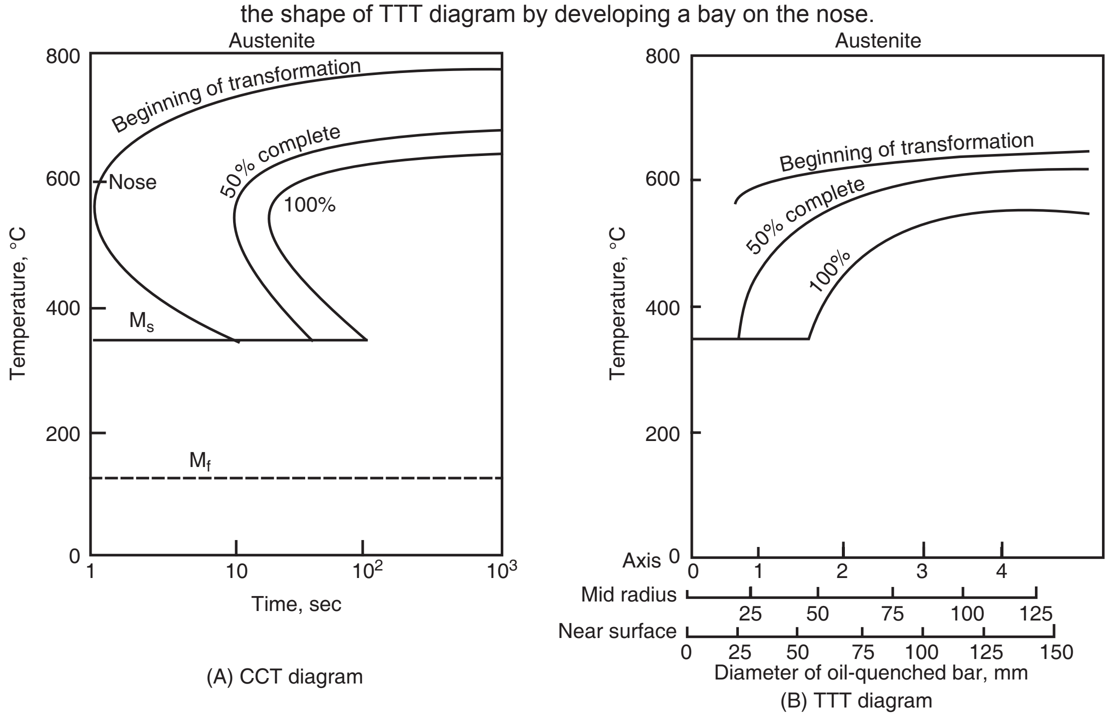

Fig. 2.30. CCT and TTT diagrams for a 0.35% plain carbon steel.

The difference between TTT diagrams and CCT diagrams are perhaps most easily understood by comparing these two forms for a steel of eutectoid composition as shown in *Fig. 2.31*. The cooling curves, corresponding to different rates of continuous cooling, superimposed on TTT and CCT diagrams are also shown in Fig. 2.31. In each case the cooling curves start above the eutectoid temperature and fall in temperature with increasing times.

Considering the curve marked 1, it crosses the line representing the beginning of the pearlite transformation, at the point marked '*a*', at the end of approximately 6 second. The significance of point '*a*' is that it represents the time required to nucleate pearlite isothermally at 650°C. A specimen cooled at the rate represented by line 1, however, reached the 650°C isothermal at the end of 6 second and was at temperatures above 650°C for the entire 6 second interval. Because the time required to start the pearlite transformation is longer at temperatures above 650°C than it is at 650°C, the continuously cooled specimen is not ready to form pearlite at the end of 6 second. In other words, more time is needed before transformation can begin under continuous cooling condition compared with isothermal transformation. Since in continuous cooling an increase in time is associated with a drop in temperature, the point at which transformation actually starts is '*b*' which lies to the right and below point '*a*'. In the same way it can be shown that the finish of the pearlite transformation, point *d*, is depressed downward and to the right of point *c*, the point where the continuous cooling curve (Curve 1) crosses the line representing the finish of isothermal transformation.

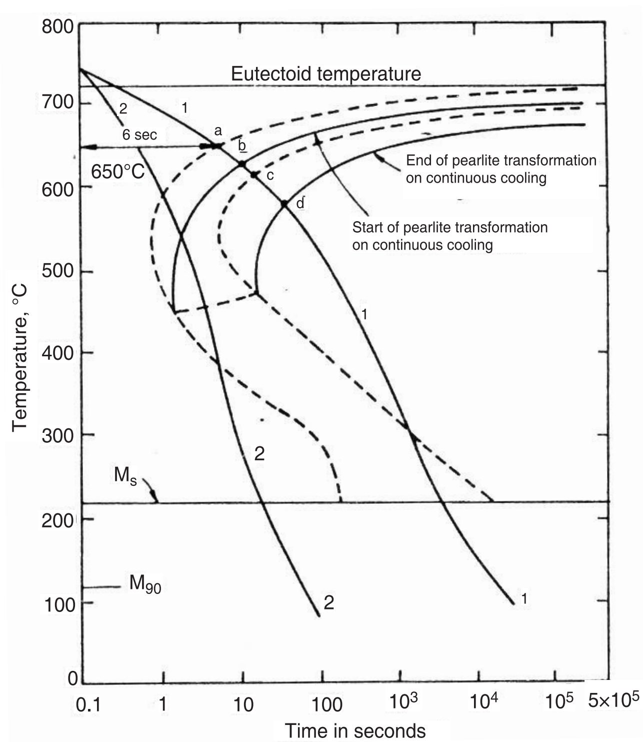

Fig. 2.31. Schematic representation of relationships between CCT and TTT curves for an eutectoid steel. (After Reed-Hill).

Fig. 2.31 also shows that the bainite reaction does not appear on the continuous cooling diagram because the pearlite reaction lines extend over and beyond the bainite transformation lines. Thus, on slow or moderate rate of cooling (represented by cooling rate curve 1), austenite in the specimens is converted completely to pearlite before the cooling curve reaches the bainite transformation range. Because the austenite has already been completely transformed to pearlite, thus no bainite can form. Alternatively, as shown by cooling rate curve 2, the specimen is in the bainite-transformation region for too short a period of time to allow any appreciable amount of bainite to form. In the second case it is also to be kept in mind that the rate at which bainite forms rapidly decreases with falling temperatures. It is generally assumed, as a first approximation, in drawing a CCT diagram for an eutectoid steel, that the transformation, along a path such as curve 2, stops in the region where the bainite and pearlite transformations overlap on the isothermal diagram. Thus, the microstructure corresponding to path 2 should consist of a mixture of pearlite and martensite, with possibly a small amount of bainite which may be ignored. The martensite forms from the austenite which did not transform to pearlite at higher temperatures.

Different transformation products obtained by cooling an eutectoid steel under different continuous cooling rates are represented in *Fig. 2.32.* The curve marked 'full anneal' represents very slow cooling and is obtained by cooling, suitably austenitized specimen, in a furnace which has its power supply switched off. Under this rate of cooling the specimen is brought to room temperature in about a day. Here the transformation of the austenite takes place at a temperature close to the eutectoid temperature and thus the final structure is coarse pearlite and similar to that predicted for an isothermal transformation.

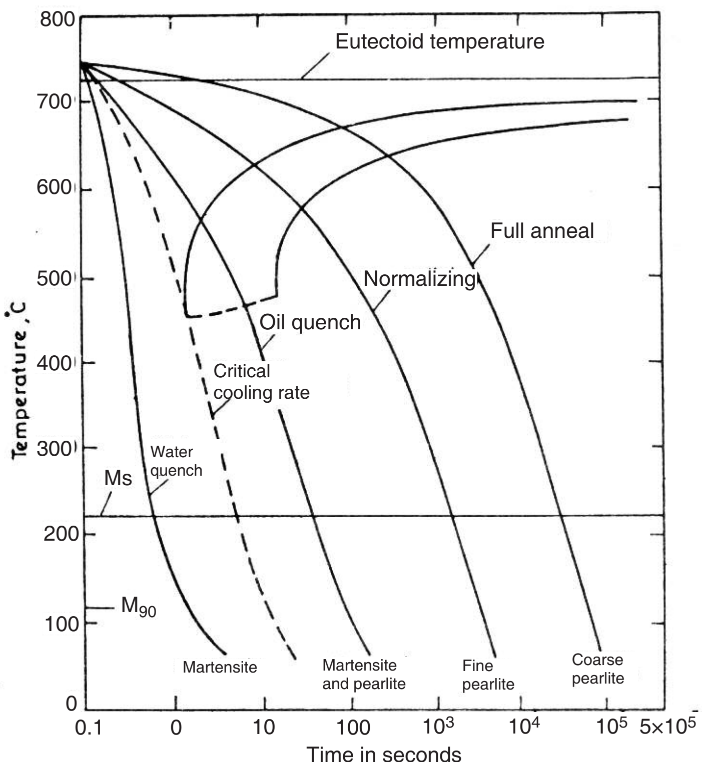

Fig. 2.32. Transformation products produced by different continuous rates in an eutectoid steel. (After Reed-Hill)

The second curve, marked normalizing represents a heat treatment in which specimens are cooled at an intermediate rate by pulling them out of the austenitizing furnace and allowing them to cool in air. In this case, cooling is accomplished in a matter of minutes and the specimen transforms in the range of temperatures between 550°C and 600°C. The structure obtained under this rate of continuous cooling is again pearlite but much finer in texture than obtained in the full annealing treatment.

The continuous cooling curve marked as 'oil quench' represents a still faster rate of cooling, such as might be obtained when a red-hot specimen is quenched by immersion in an oil bath. Cooling at this rate produces a microstructure which is a mixture of pearlite and martensite.

Finally, the continuous cooling rate curve farthest to the left and marked 'water-quench' represents a rate of cooling so rapid that no pearlite is able to form and the structure is entirely martensitic.

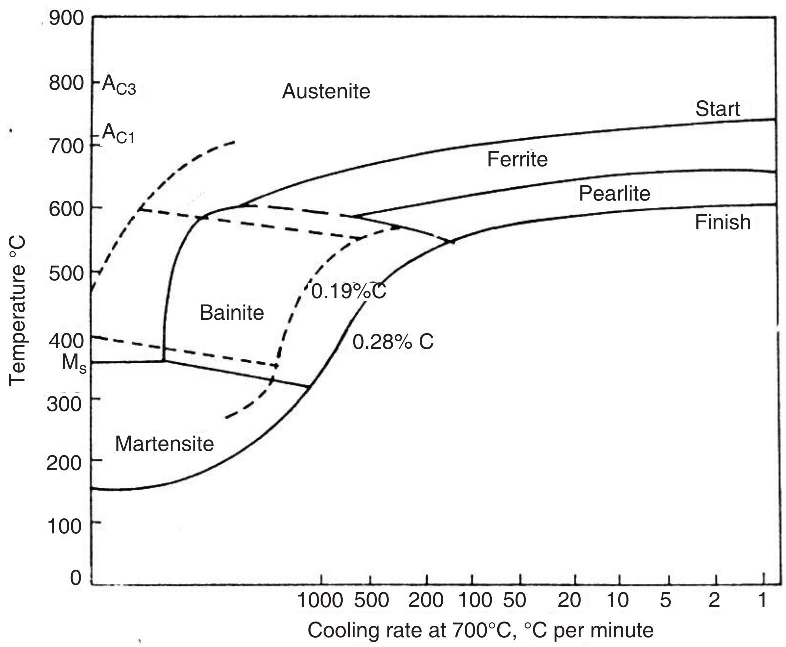

Fig. 2.33. CCT curves of plain C-Mn steel with 0.19% C (dotted) and 0.28% C (full lines). (After Easterling)

The dashed continuous cooling rate curve between the oil-quench curve and water-quench curve represents the critical cooling rate curve; any rate of cooling faster than this produces a martensitic structure while any slower rate than that (dashed line) produces a structure containing some pearlite.

While *Figs. 2.31* and *2.32* show schematic representation of CCT curves for an eutectoid steel; *Fig. 2.33* shows the actual CCT curves of two plain C-Mn steels with 0.19% C (dotted lines) and 0.28% C (full lines). This figure (Fig. 2.33) shows the effect of relatively small increase in carbon content on the position of the martensite and bainite fields.

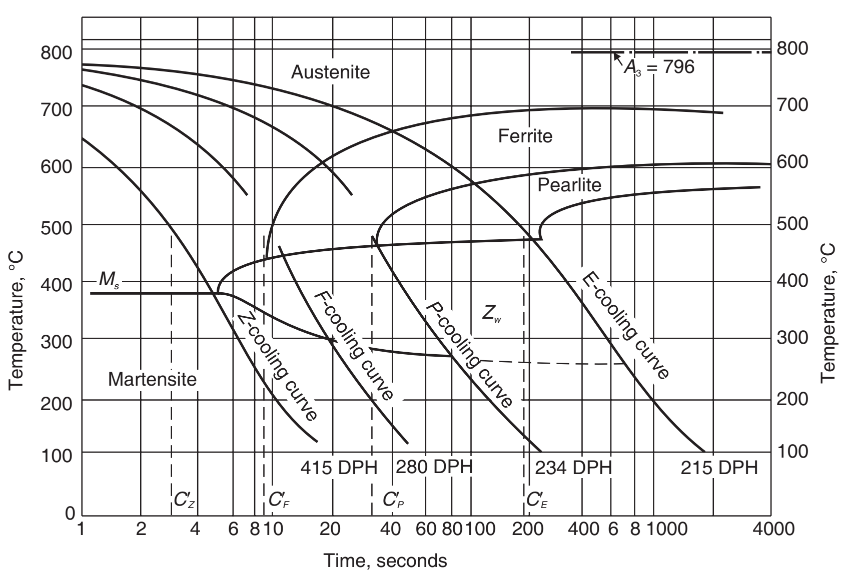

Fig. 2.34. CCT diagram for a C-Mn steel with different continuous cooling rates marked on it.

Fig. 2.34 shows the CCT curves for a C-Mn steel with different critical cooling rates like *Z*, *F*, *P* and *E* marked on it; the corresponding CCT curves for AISI 4340 (C = 0.4%, Mn = 0.70%,

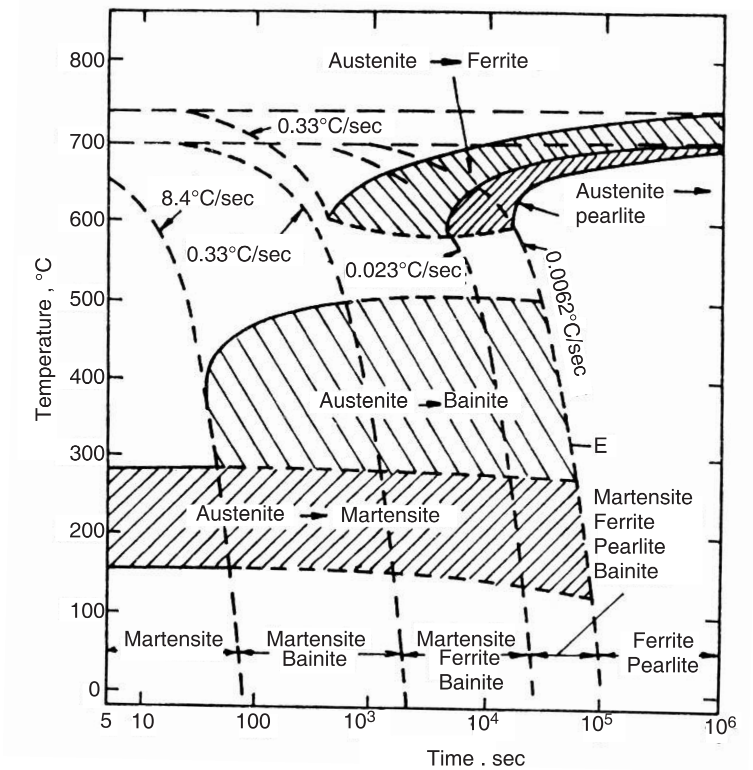

Fig. 2.35. CCT diagram for AISI 4340 steel showing transformation products obtained with different continuous cooling rates. (After Reed-Hill).

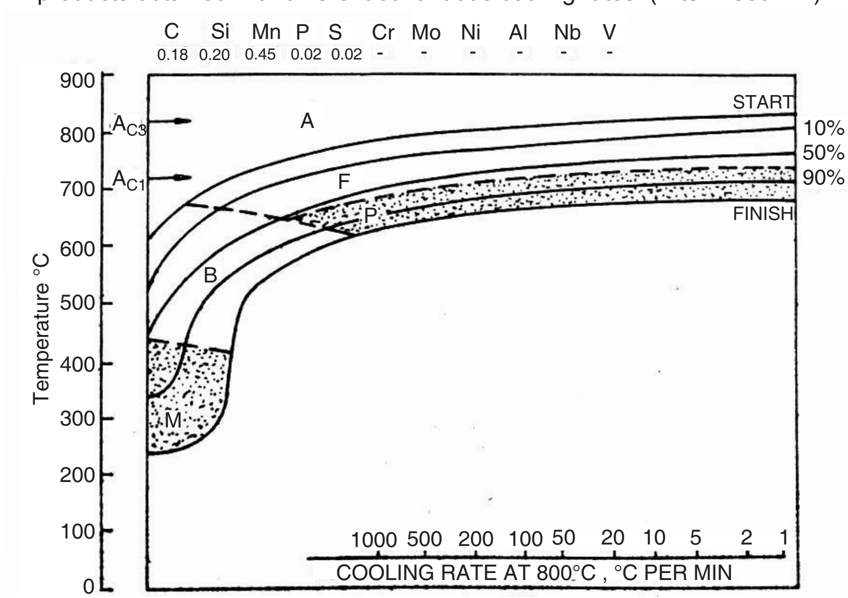

Fig. 2.36. CCT diagram for AISI 1018 steel.

S and P = 0.040% (each), Si = 0.30%, Ni = 1.80%, Cr = 0.80% and Mo = 0.25%) is shown in *Fig. 2.35*. It is evident from *Fig. 2.35* that cooling rate slower than *E* produces microstructure consisting of only ferrite and pearlite while cooling rates faster than that represented by *E* produce a microstructure consisting of martensite, ferrite, pearlite and bainite.

The detailed CCT diagram for AISI 1018 steel containing 0.18% C, 0.20% Si and 0.45% Mn is shown in *Fig. 2.36*, which also shows the lines for 10%, 50%, and 90% transformation of austenite.

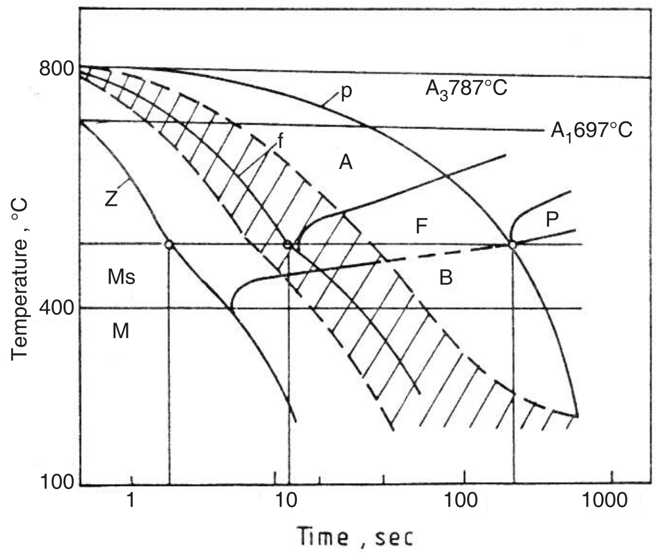

Fig. 2.37. CCT curves for T-1 Q and T steel. The hatched area represents the region of optimum cooling rates. (After Sindo Kou).

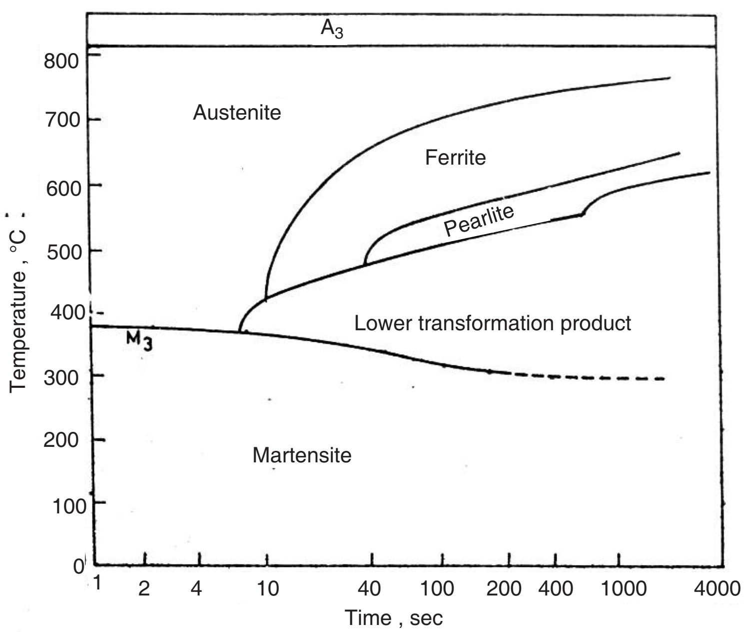

Fig. 2.38. A weld CCT diagram for a medium strength C-Mn steel, using an austenizing temperature of 1400°C. (After Easterling).

Lastly *Fig. 2.37* shows CCT curves for T-1 Q&T steel (C = 0.15%, Mn = 0.80%, Si = 0.25%, Cr = 0.5%, Ni = 0.85%, Mo = 0.5 %, V = 0.05%, Cu = 0.30%, and B = 0.004%) having a tensile strength of about 900 N/mm^2 and yield strength of 700 N/mm^2. Cooling rates marked as p, f, and z represent the critical cooling rates for the formation of pearlite (P), ferrite (F), and bainite (B) respectively. The hatched area represents the region of optimum cooling rates.

Although a CCT diagram for a given material gives fairly accurate prediction about its microstructure but the microstructure in the HAZ of a weldment is most accurately obtained from *Weld CCT* diagrams which are based on much higher austenizing temperature, usually 1350–1400°C, that correspond to grain growth zone. Such diagrams are plotted using a weld simulator to produce the appropriate thermal cycle. An example of such a diagram is shown in *Fig. 2.38*. However, weld CCT diagrams are quite expensive to produce and are, therefore, available for much less number of steels and other industrially important materials.

The best guide to the weldability of a particular alloy steel is thus its weld CCT diagram but if a weld CCT diagram is not available a CCT diagram will suffice but even if that is not available a TTT diagram will give a good guide though not so accurate as CCT diagrams. In case TTT diagram is used, the welding becomes more difficult with the shifting of curve to right and/or lowering of any nose on the diagram (See Fig. 2.30), since these features indicate that the transformation is likely to be delayed under continuous cooling conditions, to a lower temperature at which the metal will be relatively brittle. Most severe weld cracking tends to occur when transformation takes place below 300°C.

No doubt it is not possible to assess the basic weldability for a given welding situation from either CCT or TTT diagrams, without knowledge of the equivalent weld cooling condition, however it is possible to compare the relative weldability of two different alloys for similar welding purposes by comparing the relative position and sizes of their respective curves.